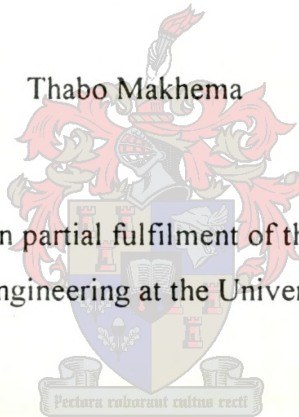


PERFORMANCE EVALUATION OF AIR-COOLED HEAT EXCHANGERS

by

Thabo Makhema

This thesis is prepared in partial fulfilment of the requirement for the degree of Masters of Engineering at the University of Stellenbosch.



Thesis supervisor: Prof. D.G. Kröger

Department of Mechanical Engineering
University of Stellenbosch

June 2000

DECLARATION

I, Thabo Makhema, the undersigned, hereby declare that the work contained in this thesis is my own original work and has not previously, in its entirety or in part, been submitted at any other university for a degree.

Signature :

Date:

ABSTRACT

The main objective of this study to determine the air-side heat transfer and pressure drop performance characteristics of commercially available round and elliptical finned tubes. A computer code to compare the performance of industrial forced and induced draught air-cooled heat exchangers (henceforth referred to as ACHE's) commonly found in the petrochemical industry is also developed. The comparison is extended to include both round and elliptical finned tubes.

From the tests conducted, it is found that there is generally an increase in the heat transfer parameter with a decrease in the fin pitch. The decrease in the fin pitch however also results in an increase in the pressure drop across the tube bundle. The performance of the tubes is compared with round reference tubes having circular or plate fins for which performance correlations are available in the literature. The fan power required by an induced draught air-cooled heat exchanger is found to be higher than that required by a forced draught heat exchanger rejecting the same amount of heat.

OPSOMMING

Die hoofdoel van hierdie studie is om die werksverrigting van industriële geforseerde trek en geinduseerde trek lugverkoelde warmteruilers (LVWR) soos algemeen aangetref in die petrochemiese nywerheid te vergelyk. Warmteruiler bundels word gewoonlik opgebou uit ronde vinbuis. Die werksverrigting van laasgenoemde word vergelyk met die werksverrigting van warmteruiler bundels wat gebruik maak van elliptiese vinbuis.

Die werksverrigting van 'n reeks kommersieël verkrygbare ronde en elliptiese vinbuis word deur middel van toetsing bepaal. In die algemeen word 'n toename in die warmteoordrag-parameter waargeneem met 'n afname in die vinsteek. 'n Toename in die vinsteek gaan egter gepaard met 'n toename in die drukverlies oor die bundel. Die werksverrigting van hierdie buis word vergelyk met bestaande korrelasies vir die werksverrigting van ronde verwysingsbuis wat gebruik maak van ronde of plaatvinne. Daar is bevind dat die drywing wat benodig word deur 'n waaier vir 'n geinduseerde trek lugverkoelde warmteruiler, heelwat hoër is as in die geval van 'n geforseerde trek lugverkoelde warmteruiler, vir dieselfde hoeveelheid hitte verwydering.

ACKNOWLEDGEMENTS

I would like to express my gratitude to the following:

1. SASOL for their financial assistance in the form of a bursary and grant to the university.
2. Prof. D.G. Kröger, my study supervisor, for his encouragement, guidance and motivation in difficult times. The practical insight into engineering and his constant insistence on working hard in this study is greatly appreciated.
3. All co-workers for their contributions, especially Kobus Zietsman for his generally helpful nature and for his help with the assembly of the test apparatus.
4. Finally, to my family, especially Basetsana Makhema, for their constant patience and love.

CONTENTS

Declaration	i
Abstract	ii
Opsomming	iii
Acknowledgements	iv
Contents	v
List of symbols	viii
1. Introduction	1-1
2. Air-cooled heat exchangers	
2.1 Introduction	2-1
2.2 Energy and draught equations for a forced and an induced draught ACHE's	2-3
2.2.1 The energy equations for a forced draught ACHE	2-3
2.2.2 The draught equation for a forced draught ACHE	2-4
2.2.3 The energy and draught equations for an induced draught ACHE	2-7
3. Heat transfer surfaces	
3.1 Introduction	3-1
3.2 Finned surfaces	3-1
3.3 Test facilities and procedure	3-3
3.3.1 Evaluation of air mass flow rate	3-5
3.4 Presentation of data	3-6
4. Presentation of experimental data and results	
4.1 Introduction	4-1
4.2 Effect of fin pitch and the water mass flow rate on the thermal-flow	

performance of a heat exchanger bundle	4-1
4.3 Thermal-flow performance of the C-2.5 and C-4.3 elliptical finned tubes	4-2
4.4 Thermal-flow performance of the AE elliptical finned tubes (type AE)	4-3
4.5 Thermal-flow performance of the ED-, F- and R-finned tubes	4-5
5. Performance comparison of different finned tube bundles	
5.1 Introduction	5-1
5.2 Determine the thermal-flow performance of the reference extruded finned tube	5-1
5.2.1 Evaluating the pressure drop across the reference tubes	5-3
5.3 Heat transfer results	5-5
5.3.1 Theoretical and experimental comparison of the heat transfer for staggered circular finned tubes	5-5
5.3.2 Determining the thermal contact resistance for a R-2.3D finned round tube	5-6
5.3.3 Theoretical and experimental comparison of the isothermal pressure drop for staggered circular finned tubes	5-12
5.4 McQuiston heat transfer correlation for staggered plate-finned round tubes	5-14
5.4.1 Evaluating the heat transfer parameter	5-16
5.4.2 Evaluating the pressure drop parameter	5-18
5.5 Performance comparison of different finned tubes in a forced draught ACHE	5-20
6. Conclusion	6-1
References	
References	R-1

APPENDICES

A. Effect of fin pitch and water mass flowrate on the thermal-flow performance of a heat exchanger bundle	A.1
B. Sample calculation for determining the heat transfer characteristics for a single pass air-cooled heat exchanger bundle	B.1
C. Thermal-flow performance of C-2.5 and C-4.3 elliptical finned tubes	C.1
D. Thermal-flow performance of AE elliptical finned tubes	D.1
E. Thermal-flow performance of ED-, F- and R-finned tubes	E.1
F. Sample calculation for a forced-draught air-cooled heat exchanger bay	F.1

LIST OF SYMBOLS

A	Area, m^2
a	Constant
b	Coefficient, or constant, or as defined by equation (5.3.3)
C	Heat capacity rate mc_p , W/K, or C_{min} / C_{max}
c_p	Specific heat at constant pressure, J/kgK
c_v	Specific heat at constant volume, J/kgK
DALR	Dry adiabatic lapse rate, K/m
d	Diameter, m
d_e	Equivalent or hydraulic diameter, m
E_y	Characteristic pressure drop parameter, m^{-2}
e	Effectiveness
F	Fan, or correction factor
f	Friction factor, or f_{in}
G	Mass velocity, kg / sm^2
g	Gravitational acceleration, m/s^2
H	Height, m
h	Heat transfer coefficient, W/m^2K
K	Loss coefficient
k	Thermal conductivity, W/mK
L	Length, m or mm
LMTD	Logarithmic mean temperature difference, $^{\circ}C$
m	Mass flow rate, kg/s
N	Revolutions per minute, $minute^{-1}$, or NTU
NTU	Number of transfer units, UA/C_{min}
N_y	Characteristic heat transfer parameter, m^{-1}
P	Pitch, mm, or power, W
p	Pressure, N/m^2 or Pa
Q	Heat transfer rate, W
R	Gas constant, J/kgK, or thermal resistance, m^2K/W
R_y	Characteristic flow parameter, m^{-1}
T	Temperature, $^{\circ}C$ or K
t	Thickness, mm

U	Overall heat transfer coefficient, $\text{W/m}^2\text{K}$
V	Volume flow rate, m^3/s or volume, m^3
v	Velocity, m/s
Y	Defined by equation (3.3.4)
z	Elevation, m

Greek Symbols

α_c	Kinetic energy coefficient
γ	c_p/c_v
Δ	Differential
μ	Dynamic viscosity, kg/ms
ν	Kinematic viscosity, m^2/s
ξ	Temperature lapse rate, K/m
ρ	Density, kg/m^3
σ	Area ratio
ϕ	Expansion factor defined by equation (3.3.3), or as defined by equation (5.3.4)

Dimensionless Groups

Eu	Euler number, $\Delta p/(\rho v^2)$
Nu	Nusselt number, hL/k for a plate, or hd/k for a tube
Pr	Prandtl number, $\mu c_p/k$
Re	Reynolds number, $\rho vL/\mu$ for a plate, or $\rho v d/\mu$ for a tube

Subscripts

a	Air, or based on air side area
atm	Atmospheric
av	Mixture of dry air and water vapour
c	Casing, or contraction, or contact
do	Downstream
db	Drybulb
e	Energy, or effective, or equivalent, or expansion
F	Fan

Fr	Fan reference
Fs	Fan static
f	Fin, or fluid
fr	Frontal or face
g	Ground
he	Heat exchanger
i	Inlet, or inside
iso	Isothermal
lm	Logarithmic mean
m	Mean, or mixture
max	Maximum
min	Minimum
n	Nozzle
o	Outlet, or outside
p	Process fluid, or passes
pl	Plenum chamber
r	Root, or reference
rec	Recovery
s	Support
si	Inlet shroud
ΔT	Constant temperature difference
T	Temperature
t	Total, or tube, or blade tip
tr	Tube row
ts	Tube cross-section, or tower support
tus	Windtunnel upstream cross-section
up	Upstream
w	Water
wb	Wetbulb

Abbreviation

ACHE	Air-cooled heat exchanger
no.	Number

Chapter 1

INTRODUCTION

SASOL is at present updating the SASOL Specification on Air-Cooled Heat Exchangers and is considering the possibility of including elliptical finned tubes as a design option in its specification. In order to achieve this, more information regarding the performance characteristics of these types of finned tubes is required.

The present study is involved with the evaluation of the thermal-flow performance characteristics of commercially available round and elliptical finned tubes, with a view to comparing their performance in an air-cooled heat exchanger.

The main aims and objectives of this report are to:

- Determine the characteristics of the different finned tubes. This includes the thermal as well as the pressure drop characteristics on the air side.
- Compare the performance of forced and induced draught ACHE's incorporating the different finned tubes tested.

In order to obtain the performance characteristics contained in this report, use was made of an existing code test tunnel at the University of Stellenbosch. Published correlations on heat transfer and pressure drop applicable to finned tubes are also used to extend the scope of this study.

This report begins by firstly describing typical air-cooled heat exchangers commonly used in the petro-chemical industry; namely the forced draught as well as the induced draught air-cooled heat exchangers. The governing energy and draught equations are then derived. The performance comparison of the two types of air-cooled heat exchangers incorporating round finned tubes for which performance correlations are available from the literature is also presented. The report then goes on to describe the different types of finned surfaces that are tested

as well as the test facility used. A description of the test procedure used as well as the format for the presentation of data is given.

The thermal-flow performance characteristics are evaluated for different finned tubes and the results are presented. The effect of fin pitch on the heat transfer as well as the pressure drop is investigated. The effect of varying the water flowrates in the tube on the heat transfer is also examined. For proprietary reasons, geometric and material details of certain tubes are not specified and their characteristics are referred to by a code.

The thermal-flow performance of round reference tubes having circular or plate fins and for which performance correlations are available in the literature are compared with the thermal performance of the commercial tubes tested.

Subsequently, the performance of forced and induced draught air-cooled heat exchangers incorporating the different finned tube bundles is compared. This is achieved by simultaneously solving the two governing equations, namely the energy and draught equations. Results are compared and conclusions are drawn.

Chapter 2

AIR-COOLED HEAT EXCHANGERS

2.1 Introduction

In view of rising water costs and due to an increased consciousness of environmental problems, power stations and petro-chemical plants are increasingly using water-independent air-cooled cooling systems.

In the petro-chemical industry, two types of mechanical draught air-cooled heat exchangers (henceforth referred to as ACHE's) are commonly found. These are of the **forced draught** type as shown in figure 2.1 where the air is blown through the bundles and the **induced draught** configuration as shown in figure 2.2 whereby the air is drawn through the bundles. The basic design of such a system consists of the heat exchanger (made up of bundles of finned tubes) supported in a metal and/or concrete structure with an axial flow fan creating an air flow through the bundles. The structure supports the heat exchanger at a sufficient elevation above ground level to allow the necessary volume of air to enter at a reasonable approach velocity.

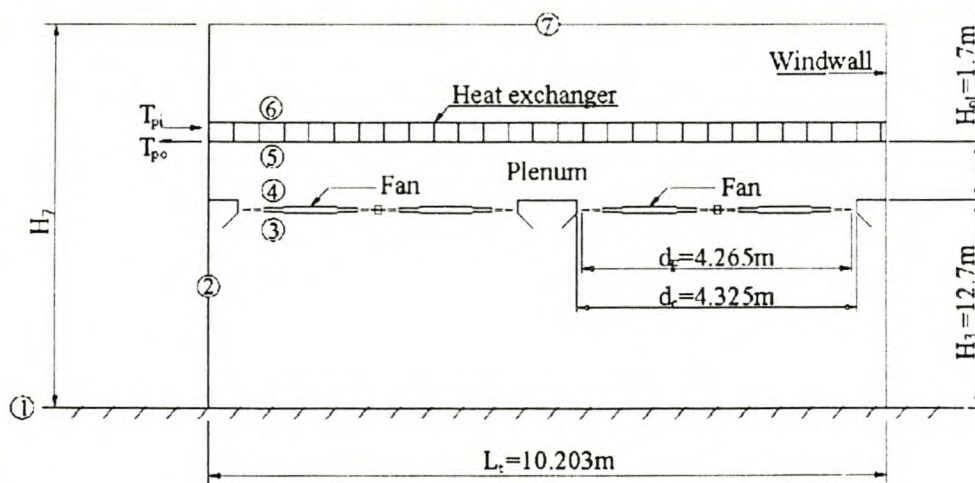


Figure 2.1: Forced draught air-cooled heat exchanger bay.

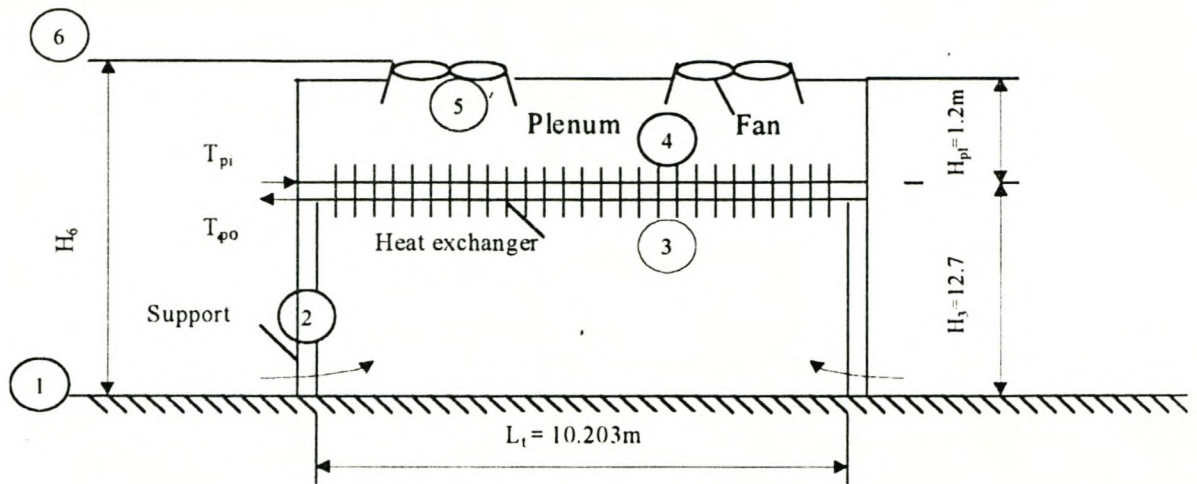


Figure 2.2: Induced draught air-cooled heat exchanger bay.

A brief summary of the main advantages and disadvantages of the two types of layouts follows [91BE1]:

Forced draught

Advantages:

- a) Lower fan shaft power consumption
- b) Location of fan drives offers better accessibility for maintenance work
- c) Fan drives not exposed to high temperatures making the choice of construction material less critical

Induced draught

- a) Better distribution of air across the bundle
- b) Relatively high escape of the air from the fan reduces plume recirculation and makes system less susceptible to crosswinds
- c) Bundle is protected in part by plenum from weather conditions

Disadvantages:

- | | |
|--|---|
| a) Poor air distribution across bundle | a) High fan shaft power consumption |
| b) Low discharge velocity increases the risk of plume recirculation | b) Low accessibility of fan components for maintenance work |
| c) Exposure of the finned surfaces to the atmosphere can affect performance due to wind, rain, hail or solar radiation | c) Fan and drive system exposed to the warm air stream making the choice of construction material more critical |

2.2 Energy and draught equations for a forced and an induced draught ACHE's.

Energy and draught equations for both a forced as well as an induced draught ACHEs will be discussed. These two equations need to be satisfied simultaneously to evaluate the correct air mass flow rate and heat transfer rate. They take into account all flow obstacles and the heat exchanger layout.

2.2.1 The energy equations for a forced draught ACHE

The energy equation represents the amount of heat that is transferred to the air stream flowing across the tube bundles from the process fluid flowing inside the tubes. This can be expressed as

$$Q_a = m_a c_{pa} (T_{a6} - T_{a5}) = m_p c_{pp} (T_{pi} - T_{po}) \quad (2.2.1)$$

where the subscript, p, refers to the process fluid.

The heat transfer rate may also be expressed in terms of the effectiveness of the heat exchanger i.e.

$$Q = eC_{\min}(T_{pi} - T_{as}) \quad (2.2.2)$$

where C_{\min} is the smaller of $m_a c_{pa}$ and $m_p c_{pp}$ and the effectiveness, e , depends on the geometry and flow patterns of the fluids through the heat exchanger.

Where the air and process fluid mass flow rates are known, it is customary to employ the NTU-effectiveness method in evaluating heat exchanger performance. The effectiveness is defined as

$$e = \frac{Q}{Q_{\max}} = \frac{C_{\min} \Delta T_{\min}}{C_{\min} \Delta T_{\max}} = \frac{\Delta T_{\min}}{\Delta T_{\max}} \quad (2.2.3)$$

where

ΔT_{\min} = the temperature difference of fluid having a C_{\min}

ΔT_{\max} = the maximum temperature difference in the heat exchanger

The effectiveness of numerous practical arrangements is found in various sources in the literature [84KA1], [81SH1] and [91AS1].

2.2.2 The draught equation for a forced draught ACHE

In practice the draught for an ACHE is sometimes obtained by simply matching the fan performance curve and the flow characteristics through the heat exchanger bundles only, and evaluating the thermophysical properties of the air at ambient ground level conditions. In some cases, this may give useful approximate values but because of increased competitiveness and high system costs, a more detailed analysis is adopted.

The fan chosen must be able to overcome a series of flow resistances and hence deliver a cooling air flow rate that will guarantee the desired heat transfer rate.

Considering figure 2.1, stagnant ambient air at 1 far from the heat exchanger accelerates and flows across the heat exchanger supports at 2 before reaching the fan at section 3, where upstream obstacles such as structural supports or a screen or mesh guard may be located. After leaving the fan at 4 where further downstream obstacles may be located, the flow experiences losses in the plenum before entering the heat exchanger bundle at 5 and exiting at 6. A windwall of height, H_w , is installed to reduce the recirculation of hot plume air exiting at 7.

External to the heat exchanger there is however also a decrease in the ambient pressure with the height of the ACHE. In a 24-hour cycle, the temperature near the surface of the earth may vary significantly. This is due to temperature inversions at night at certain locations and a dry adiabatic lapse rate (DALR) of approximately 0.00975 K/m during the day [98KR1].

Using the DALR, the temperature at any elevation, z , can be written as:

$$T_{az} = T_{a1} - 0.00975z \quad (2.2.4)$$

The pressure gradient in a gravity field is given by

$$dp / dz = - \rho_a g \quad (2.2.5)$$

The air density may be expressed through the perfect gas law as

$$\rho_a = p_a / RT_a \quad (2.2.6)$$

where $R = 287.08 \text{ J/kgK}$

Substitute equation (2.2.4) and (2.2.6) into equation (2.2.5) and integrate between points 1 and 7 to obtain the following pressure difference far from the ACHE

$$(p_{a1} - p_{a7}) = (p_{a1} - p_{a6}) + (p_{a6} - p_{a7})$$

$$\begin{aligned} &\approx p_{a1}[1 - (1 - 0.00975 H_6 / T_{a1})^{3.5}] \\ &+ p_{a6}\{1 - \{1 - 0.00975 (H_7 - H_6) / T_{a1}\}^{3.5}\} \end{aligned} \quad (2.2.7)$$

where the ambient air temperature at elevation 6 is assumed to be approximately equal to T_{a1} . Although the air temperature distribution near ground level generally deviates considerably from the DALR, the error introduced by this assumption in equation (2.2.7) is small for relatively high heat exchangers.

The pressure change across a flow obstacle can be expressed in terms of the loss coefficient of the particular obstacle

$$\Delta p = K\rho_a / 2v_a^2 = K\rho_a / 2(m_a / A)^2 \quad (2.2.8)$$

The difference in pressure between 1 at ground level and 7 at the outlet of the ACHE may be expressed in terms of the losses experienced by the air stream as it flows through the various obstacles in the ACHE as follows

$$\begin{aligned} (p_{a1} - p_{a7}) = &p_{a1}[1 - (1 - 0.00975H_6/T_{a1})^{3.5}] + K_{ts}(m_a / A_2)^2 / (2\rho_{a1}) + K_{Fsi}(m_a / \\ &A_c)^2 / (2\rho_{a3}) + K_{up}(m_a / A_e)^2 / (2\rho_{a3}) - (K_{Fs} + K_{rec})(m_a / A_c)^2 / (2\rho_{a3}) + K_{do}(m_a / \\ &A_e)^2 / (2\rho_{a3}) + K_{he}(m_a / A_{fr})^2 / (2\rho_{a56}) + p_{a6}[1 - (1 - 0.00975(H_7 - H_6)/T_{a6})^{3.5}] \\ &+ \alpha_{c6}(m_a / A_{fr})^2 / (2\rho_{a6}) \end{aligned} \quad (2.2.9)$$

With the aid of equation (2.2.7), equation (2.2.9) can be written as follows:

$$\begin{aligned} &p_{a6}\{[1 - 0.00975(H_7 - H_6) / T_{a6}]^{3.5} - [1 - 0.00975(H_7 - H_6) / T_{a1}]^{3.5}\} \\ &\approx p_{a1}\{[1 - 0.00975(H_7 - H_6) / T_{a6}]^{3.5} - [1 - 0.00975(H_7 - H_6) / T_{a1}]^{3.5}\} \end{aligned}$$

$$\begin{aligned}
 & \text{(a)} & \text{(b)} & \text{(c)} \\
 & = K_{ts}(m_a / A_2)^2 / (2\rho_{a1}) + K_{Fsi}(m_a / A_c)^2 / (2\rho_{a3}) + K_{up}(m_a / A_e)^2 / (2\rho_{a3}) \\
 & \text{(d)} & \text{(e)} & \text{(f)} \\
 & - (K_{Fs} + K_{rec})(m_a / A_c)^2 / (2\rho_{a3}) + K_{do}(m_a / A_e)^2 / (2\rho_{a3}) + K_{he}(m_a / A_{fr})^2 / (2\rho_{a56}) \\
 & \text{(g)} \\
 & + \alpha_{e6}(m_a / A_{fr})^2 / (2\rho_{a3}) \tag{2.2.10}
 \end{aligned}$$

This is known as the draught equation for the forced draught air-cooled heat exchanger.

It is assumed on the left-hand side of equation (2.2.10) that $p_{a6} \approx p_{a1}$ and $\rho_{a2} \approx \rho_{a1}$, $\rho_{a4} \approx \rho_{a3}$, $\rho_{a7} \approx \rho_{a6}$. It is further assumed that frictional losses between 6 and 7 are negligible and that the kinetic energy factor $\alpha_{e6} \approx \alpha_{e7}$.

The harmonic mean density through the heat exchanger is given by

$$\rho_{a56} = 2p_{a1} / [R(T_{a5} + T_{a6})] \tag{2.2.11}$$

The different pressure loss coefficients in equation (2.2.10) are:

- (a) Heat exchanger support loss support (K_{ts})
- (b) Fan shroud inlet loss coefficient (K_{Fsi})
- (c) Pressure loss coefficient due to obstacles on the fan suction (upstream) side (K_{up})
- (d) The fan static and plenum recovery pressure rise coefficients respectively (K_{Fs} , K_{rec})
- (e) Pressure loss coefficient due to flow obstacles on the fan discharge (downstream) side (K_{do})
- (f) Heat exchanger bundle loss coefficient (K_{he})
- (g) Kinetic energy velocity distribution correction factor (α_{e6})

2.2.3 The energy and draught equations for an induced draught ACHE.

By following the above procedure, the energy and draught equations can be deduced for the induced draught ACHE shown in figure 2.2

The heat transfer rate is

$$Q = m_a c_{pa} (T_{a4} - T_{a3}) = m_p c_{pp} (T_{pi} - T_{po}) \quad (2.2.12)$$

or

$$Q = e C_{\min} (T_{pi} - T_{a3}) \quad (2.2.13)$$

where

$$T_{a3} = T_{a1} - 0.00975 H_3 - v_{a3}^2 / (2c_{pa}) \approx T_{a1} - 0.00975 H_3 \quad (2.2.14)$$

In an induced draught heat exchanger the air flow through the heat exchanger is usually relatively uniform and upstream turbulence is low.

The draught equation is given by

$$\begin{aligned} & p_{a1} [\{ 1 - 0.00975 (H_6 - H_4) / T_{a4} \}^{3.5} - \{ 1 - 0.00975 (H_6 - H_4) / T_{a1} \}^{3.5}] \\ &= K_{ts} (m_a / A_2)^2 / (2\rho_{a1}) + K_{he} (m_a / A_{fr})^2 / (2\rho_{a34}) + K_{pl} (m_a / A_c)^2 / (2\rho_{a4}) + \\ & \alpha_{e6} (m_a / A_c)^2 / (2\rho_{a6}) - K_{Fs} (m_a / A_c)^2 / (2\rho_{a4}) + K_{up} (m_a / A_c)^2 / (2\rho_{a4}) + K_{do} \\ & (m_a / A_c)^2 / (2\rho_{a4}) \end{aligned} \quad (2.2.15)$$

A performance evaluation of a forced draught ACHE is done in appendix F and a comparison is made with an induced draught ACHE. The results are presented in table F.1 (appendix F).

Chapter 3

HEAT TRANSFER SURFACES

3.1 Introduction

The most expensive and most critical component of any air-cooled heat exchanger is the heat transfer surface area. The heat exchanger may consist of bundles of one or more rows of finned tubes. The heat transfer from the inside process fluid to the air is influenced by, among others, the following variables

- (a) The temperature difference between the fluid and the air.
- (b) The design and surface arrangement of the heat exchanger.
- (c) The thermophysical properties of the fluid both inside and outside of the tubes.

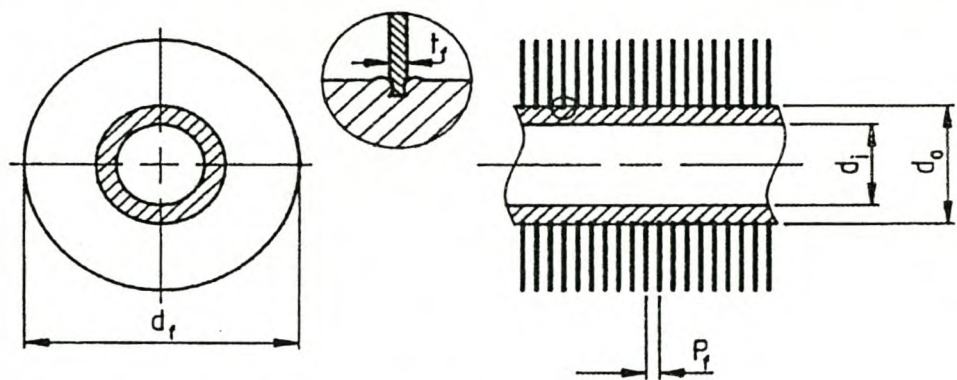
According to M. Abu Madi et al. [98AB1], the heat transfer and pressure loss correlations used on the internal tube surfaces (process fluid side) in most cases provide adequate accuracy. Since the air-side thermal resistance is usually significantly higher than that on the inside of the tube, small errors in predicting the air-side heat transfer performance lead to corresponding errors in predicting the overall thermal performance of heat exchangers. The accuracy of a heat exchanger model may, therefore, be judged by the availability of reliable air-side heat transfers and pressure loss data.

3.2 Finned surfaces

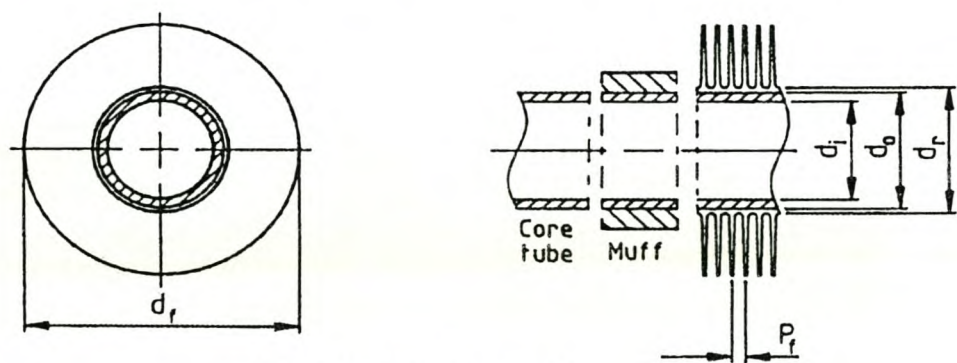
Finned tubes may be round, elliptical, flattened or otherwise streamlined to reduce the flow resistance on the air-side. Kröger [98KR1] illustrates different types and shapes of fins commonly used.

This report is restricted only to the performance evaluation of round and elliptical finned tubes.

Figure 3.1(a) shows a helically wound aluminium G-finned tube. The core tube is provided with a groove into which the fin is rolled, whereafter the groove is peened back against the sides of the fin material. Where corrosion is a major consideration, an extruded bimetallic E-fin tube as shown in figure 3.1(b) is recommended. The finned surface is obtained by plastically deforming an outer aluminium muff onto an internal steel tube during a rolling process. The fins can also be extruded from materials other than aluminium.



(a) Type G-fin.



(b) Extruded fin, Type E.

Figure 3.1: Grooved and extruded finned tubes

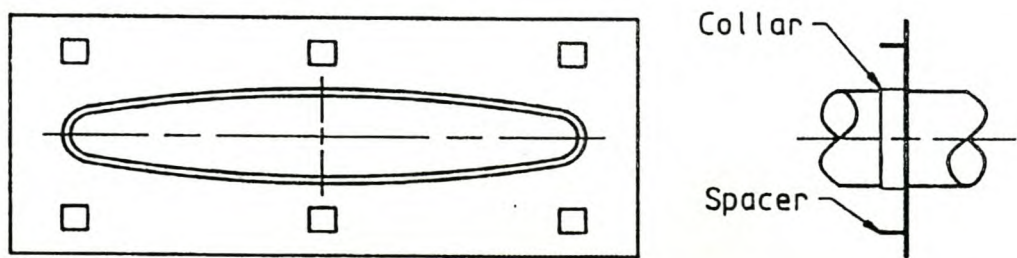


Figure 3.2: Elliptical tube with rectangular plate fin.

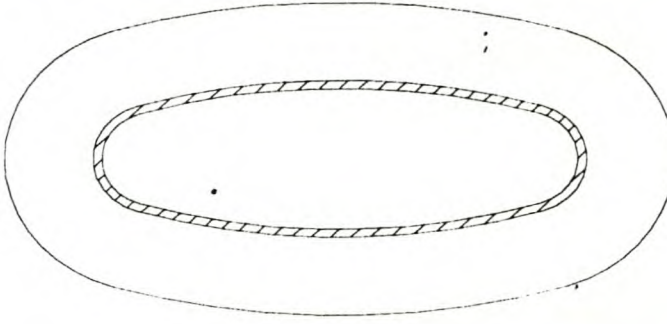


Figure 3.3: Elliptical tube with wrap-on fin (Galvanised).

An elliptical steel tube with a rectangular steel-plate fin and wrap-on fin is shown in figures 3.2 and 3.3 respectively. The finned tube is galvanised after assembly to ensure good thermal contact between fin and tube.

3.3 Test facilities and procedure

The Stellenbosch University's code test windtunnel is used to determine the performance characteristics of the extended surfaces. A windtunnel designed specifically for this purpose is shown in figure 3.4.

A radial fan 8 draws air uniformly through the rounded inlet section, where its wet- and drybulb temperature is measured, and then across the heat exchanger bundle 1 which is heated by a fluid flowing inside the tubes. The static pressure difference is measured across the bundle at points located in the duct wall 3. Depending on the type of bundle to be tested, care should be taken that the outlet pressure tap is in a position where it will not be influenced by flow distortions immediately after the bundle. After the heat exchanger, the air passes through an insulated connecting section 2 and two sets of air mixers 4, followed by a venturi in which a sampling tube is located.

The air discharged from the heat exchanger may have a non-uniform temperature distribution together with a non-uniform velocity distribution. The most accurate means of measuring the mean temperature of the air stream under these conditions, is to introduce air mixers and then to sample the

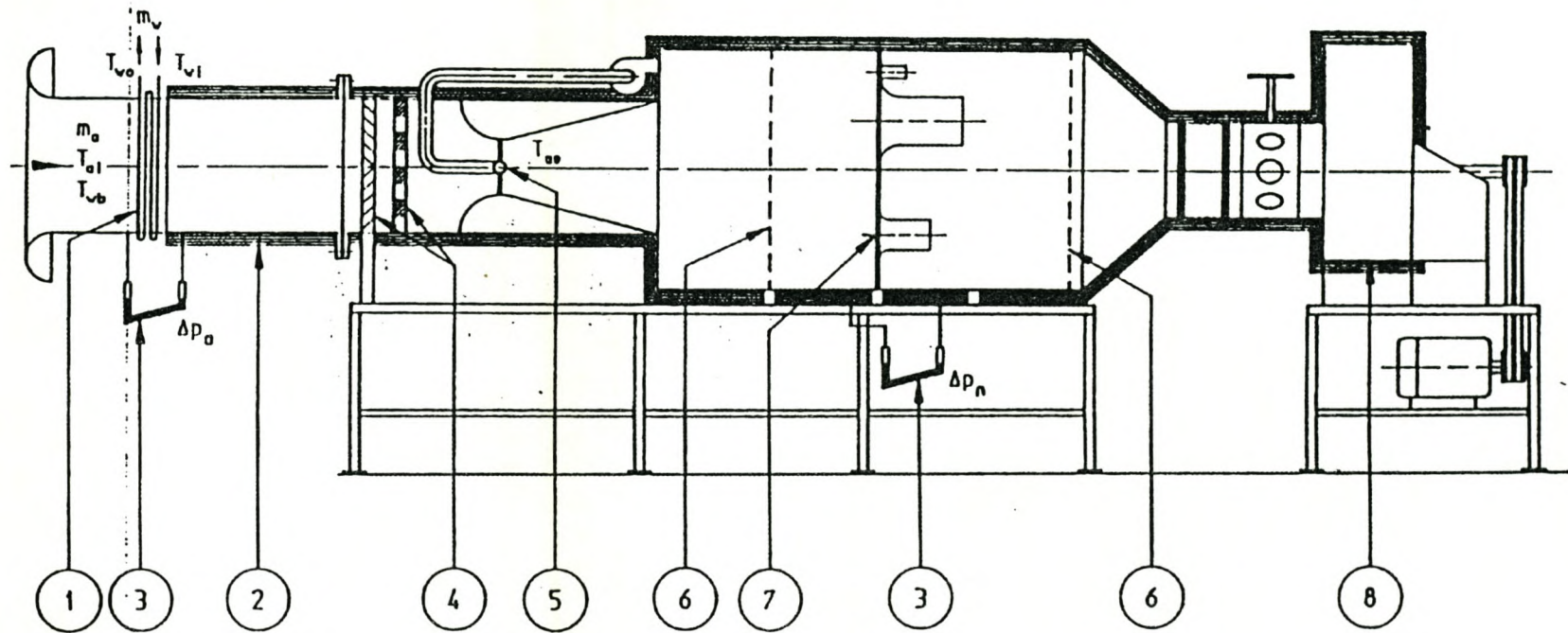


Figure 3.4: Code test windtunnel.

stream at a number of points. Air mixers may consist of a series of vanes arranged to divide the air flow into many small streams that are diverted across each other. The venturi arrangement after the mixers tends to minimize the non-uniformity of the air-stream velocity. The sampling tube 5 permits the withdrawal of air from numerous points across the venturi throat and conveys it to a convenient location where the mean dry- and wetbulb temperature may be measured.

Warm water, steam or some other heated fluid is passed through the tubes. Where warm water is employed, a uniform distribution of flow must be ensured through each of the tube passes. This can be achieved by the correct design of the manifolds. Air-water counterflow conditions are normally preferred.

3.3.1 Evaluation of air mass flow rate

The air flow rate is determined by measuring the pressure drop across one or more elliptical nozzles mounted in a plate 7 between perforated plates 6. The corresponding mass flow rate is given by

$$m_a = C_n \phi_g Y A_n (2\rho_n \Delta p_n)^{0.5} \quad (3.3.1)$$

The nozzle coefficient of discharge, C_n , is a function of the nozzle Reynolds number. For $30000 < Re_n < 100000$,

$$C_n = 0.954803 + 6.37817 \times 10^{-7} Re_n - 4.65394 \times 10^{-12} Re_n^2 + 1.33514 \times 10^{-17} Re_n^3 \quad (3.3.2a)$$

For $100000 < Re_n < 350000$

$$C_n = 0.9758 + 1.08 \times 10^{-7} Re_n - 1.6 \times 10^{-13} Re_n^2 \quad (3.3.2b)$$

and for $Re_n > 350000$, $C_n = 0.944$

The gas expansion factor ϕ_g may be approximated by the following relation:

$$\phi_g = 1 - 3 \Delta p_n / (4 p_{up} c_p / c_v) \quad (3.3.3)$$

where $c_p / c_v = 1.4$ for air and p_{up} is the upstream pressure.

For a compressible fluid, it can be shown that the approach velocity factor is approximately

$$Y = 1 + 0.5 (A_n / A_{tus})^2 + 2 (A_n / A_{tus})^2 \Delta p_n / (p_{up} c_p / c_v) \quad (3.3.4)$$

Equation (3.3.1) neglects thermal expansion or contraction of the nozzle.

3.4 Presentation of data

Different methods for presenting the heat transfer and pressure drop characteristics of finned tubes are found in the literature. Generally the heat transfer is presented in the form of the dimensionless Nusselt number, i.e.

$$Nu = h d_e / k = a_1 Re^{b_1} Pr^{0.333} \quad (3.4.1)$$

where d_e is some equivalent diameter. Similarly, the pressure differential may be represented by the dimensionless Euler number

$$Eu = \Delta p / \rho v^2 = \rho \Delta p / G^2 \quad (3.4.2)$$

or a loss coefficient

$$K = 2 \Delta p_t / \rho v^2 = 2 \Delta p_t / G^2 \quad (3.4.3)$$

where Δp_t is the change in the total pressure across the heat exchanger. The mass velocity may be based on the minimum flow area through the heat exchanger, or the frontal area of the heat exchanger.

A method for presenting the experimentally obtained performance data of finned tubes which has particular merit in the case of industrial finned-tube heat exchangers adopted for the thesis is the one evaluated by Kern [80KE1] and presented by Kröger [86KR1] in a modified form. This method is used to present the performance characteristics of the evaluated tube bundles.

Both the Nusselt number and the Reynolds number contain an equivalent or hydraulic diameter. Because of the relatively arbitrary nature or the definition of this quantity for finned surfaces, different definitions are found in the literature. This may often lead to confusion and makes any comparison of performance characteristics of different types of finned surfaces meaningless. In the absence of the equivalent diameter, equation (3.4.1) may be written as

$$h/k = a_2 Ry^{b_2} Pr^{0.333} \quad (3.4.4)$$

where

$$Ry = G_{fr} / \mu = m / (\mu A_{fr}) \quad (3.4.5)$$

is known as the characteristic flow parameter.

The effective finned surface area and the heat exchanger frontal area play a significant role in comparing and optimising heat exchangers. These parameters are introduced into equation (3.4.4) to give the following relation:

$$Ny_h = he_f A / (k A_{fr} Pr^{0.333}) = a_{Ny_h} Ry^{b_{Ny_h}} \quad (3.4.6)$$

where Ny_h is known as the characteristic heat transfer parameter.

For most cases of industrial finned surfaces that have been performance tested, the actual fin-side heat transfer coefficient, h , and the finned surface effectiveness, e_f , is of no particular interest. Henceforth the use of an effec-

tive heat transfer coefficient based on the air-side surface area is preferred to define a corresponding heat transfer parameter

$$h_{ae}A_a = \left(\frac{1}{h_a e_f A_a} + \sum_n \frac{R_n}{A_n} \right)^{-1} = \left(\frac{F_T \Delta T_{lm}}{Q} - \frac{1}{h_w A_w} \right)^{-1} \quad (3.4.7)$$

where h_{ae} is the effective air-side heat transfer coefficient.

The logarithmic mean temperature difference is given by

$$\Delta T_{lm} = \frac{(T_{wo} - T_{ai}) - (T_{wi} - T_{ao})}{\ln[(T_{wo} - T_{ai})/(T_{wi} - T_{ao})]} \quad (3.4.8)$$

The experimentally determined value of the heat transfer rate, Q_a , is determined by calculating the heat transfer on the air-side of the heat exchanger bundle as follows

$$Q_a = m_a c_{pam} (T_{ao} - T_{ai}) \quad (3.4.9)$$

According to Roetzel [84RO1], a temperature correction factor can in general be expressed as

$$F_T = 1 - \sum_{i=1}^4 \sum_{k=1}^4 a_{i,k} (1 - \phi_{cf})^k \sin \left(2i \arctan \frac{\phi_h}{\phi_c} \right) \quad (3.4.10)$$

where the dimensionless temperature changes of the two streams may be respectively defined as

$$\phi_h = \frac{T_{hi} - T_{ho}}{T_{hi} - T_{ci}} \quad (3.4.11)$$

and

$$\phi_c = \frac{T_{co} - T_{ci}}{T_{hi} - T_{ci}} \quad (3.4.12)$$

For a counterflow case, a dimensionless mean temperature difference can be expressed in terms of the logarithmic mean temperature difference as follows

$$\phi_{cf} = \frac{\Delta T_{lm}}{T_{hi} - T_{ci}} \quad (3.4.13)$$

Kröger [98KR1] gives values of $a_{i,k}$ for ten different heat exchanger geometries.

The water-side heat transfer coefficient is determined by the following equation as proposed by Gnielinski [75GN1]

$$h_w = \frac{Nu_w d_e}{k_w} = \frac{(f_D / 8)(Re_w - 1000) Pr [1 + (d_e / L)^{0.67}]}{1 + 12.7(f_D / 8)^{0.5} (Pr^{0.67} - 1)} \left(\frac{d_e}{k_w} \right) \quad (3.4.14)$$

For turbulent flow inside smooth tubes, the Darcy friction factor, f_D , is determined by the following equation as proposed by Filonenko [54FI1]

$$f_D = (1.82 \log_{10} Re_w - 1.64)^{-2} \quad (3.4.15)$$

The pressure loss coefficient based on the total pressure difference across the heat exchanger and the mean density can be defined as

$$K_{heiso} = \frac{\Delta p_t}{\frac{1}{2} \rho_m v_m^2} = a_k Ry^{b_k} \quad (3.4.16)$$

For non-isothermal flow conditions [98KR1], the resultant loss coefficient is

$$K_{he} = K_{heiso} + \frac{2}{\sigma^2} \left(\frac{\rho_i - \rho_o}{\rho_i + \rho_o} \right) = a_k Ry^{b_k} + \frac{2}{\sigma^2} \left(\frac{\rho_i - \rho_o}{\rho_i + \rho_o} \right) \quad (3.4.17)$$

where σ is the ratio of the minimum air-side flow area between tubes and the corresponding frontal area. Thermophysical properties are evaluated at the arithmetic mean temperature $T_m = (T_i + T_o) / 2$.

As mentioned previously this method of data presentation enables one to readily compare the performance of different heat exchangers.

Chapter 4

PRESENTATION OF EXPERIMENTAL DATA AND RESULTS

4.1 Introduction

In order to effectively design a finned tube air-cooled heat exchanger (ACHE) knowledge of the heat transfer as well as the pressure drop characteristics of the finned tubes to be used is required. These performance characteristics enable the designer to predict the heat transfer and pressure drop across a particular heat exchanger bundle. The performance characteristic results presented in this chapter are determined using the code test windtunnel described in section 3.3. A method for the presentation of the experimental heat exchanger data as presented in section 3.4 is employed. Tubes of different geometries and from different manufactures are tested and results are presented and subsequently discussed.

4.2 Effect of fin pitch and the water mass flowrate on the thermal-flow performance of a heat exchanger bundle.

Four different elliptical finned tube bundles (AE-type) having fin pitches of 2.2, 2.3, 2.4 and 2.5 mm are evaluated. The aim of the investigation is to determine the effect of fin pitch on the air-side performance characteristics of the tubes.

The tube specifications, test data and thermal-flow performance results are tabulated and presented in appendix A from table A.1.1 through to table A.4.5. These results are further presented graphically from figure A.1.1 through to figure A.4.2. The effects of fin pitch on the heat transfer parameter and pressure coefficient is graphically shown from figure A.5 through to figure A.7.

As expected, there is an increase in the heat transfer parameter with a decrease in the fin pitch, as shown in figure A.5. The decrease in fin pitch however also results in a higher pressure drop across the bundle as is shown in figures A.6 and A.7. The non-isothermal

pressure loss coefficient conditions, which the tube is likely to experience under normal operation, is always higher than for a corresponding isothermal case.

The effect of varying the water mass flowrate on the heat transfer parameter, everything else being held constant, is also determined and the results are tabulated and presented in tables A.5.1 (a) through to A.5.2 (b) for tubes AE-2.4. The results are further presented graphically in figure A.8. From the results presented, it is shown that varying the water mass flowrate has essentially no effect on the heat transfer parameter, Ny . This result is to be expected and confirms the reliability of the test results for Ny which are shown to be independent of the water flow rate.

A sample calculation for determining the heat transfer characteristics for a single pass air-cooled heat exchanger bundle with elliptical finned tubes is presented in appendix B.

4.3 Thermal-flow performance of the C-2.5 and C-4.3 elliptical finned tubes.

The heat transfer and pressure drop characteristics of the C-2.5 and C-4.3 elliptical finned tubes (AE-type) are determined experimentally. The following configurations are considered.

- (a) The performance characteristics of a heat exchanger bundle consisting of one row of elliptical finned tubes having a 2.5 mm fin pitch (C-2.5) and a heat exchanger consisting of one row of elliptical finned tubes having a 4.3 mm fin pitch (C-4.3) respectively, are determined experimentally. The tube specifications, data and results of these tests are tabulated and presented in appendix C from tables C.1.1 through to C.2.5
- (b) A heat exchanger bundle consisting of two elliptical finned tube rows (upstream fin pitch 4.3 mm, i.e. C-4.3, downstream fin pitch 2.5 mm, i.e. C-2.5) is tested. The resultant data and test results are tabulated and presented in appendix C from tables C.3.1 (a) through to C.3.4

The results of both (a) and (b) are further presented graphically from figures C.1 through to C.3. It is observed that there is a consistent behaviour where the two-row heat exchanger has the highest heat transfer parameter as well as the pressure drop coefficient (isothermal

and non-isothermal). The C-4.3 tube bundle exhibits the lowest heat transfer parameter as well as the lowest pressure drop coefficient (isothermal and non-isothermal). This is consistent with the findings observed in appendix A concerning the effect of fin pitch on the heat transfer characteristics.

4.4 Thermal-flow performance of elliptical finned tubes (type AE).

The heat transfer and pressure drop characteristics of different type AE elliptical finned tubes are determined experimentally and the following configurations are considered.

- (a) The performance characteristics of a heat exchanger bundle consisting of two elliptical finned tube rows having type DE turbulators and a 2.5 mm fin pitch (AE-2.5 DE) upstream and downstream respectively are determined experimentally. This is called a double row test. The tube specifications, data and results of this test are tabulated and presented in appendix D from tables D.1.1 through to D.1.5. The results are further presented graphically in figures D.1.1 and D.1.2
- (b) The performance characteristics of a heat exchanger bundle consisting of two elliptical finned tube rows having type DE turbulators and a 4 mm fin pitch (AE-4.0 DE) upstream and downstream respectively are determined experimentally. The tube specifications, data and results of this double row test are tabulated and presented in appendix D from tables D.2.1 through to D.2.5. The results are further presented graphically in figures D.2.1 and D.2.2.
- (c) The performance characteristics of a heat exchanger bundle consisting of two elliptical finned tube rows having type DA turbulators and a 4.3 mm fin pitch (AE-4.3 DA) upstream and downstream respectively are determined experimentally. The tube specifications, data and results of this double row test are tabulated and presented in appendix D from tables D.3.1 through to D.3.5. The results are further presented graphically in figures D.3.1 and D.3.2.
- (d) The performance characteristics of a heat exchanger bundle consisting of two elliptical finned tube rows having type DA turbulators and a 4.5 mm fin pitch (AE-4.5 DA) upstream and downstream respectively are determined experimentally. The tube specifications, data and results of this double row test are tabulated and presented in

appendix D from tables D.4.1 through to D.4.5. The results are further presented graphically in figures D.4.1 and D.4.2.

- (e) The performance characteristics of a heat exchanger bundle of two elliptical finned tube rows (upstream fin pitch 4 mm, i.e. type DE turbulator AE-4.0 DE tube, downstream fin pitch 2.5 mm, i.e. type DE turbulator AE-2.5DE tube) are determined experimentally. The resultant data and test results are tabulated and presented in appendix D from tables D.5.1 (a) through to D.5.4. The results are further represented graphically in figures D.5.1 and D.5.2.
- (f) The performance characteristics of a heat exchanger bundle of two elliptical finned tube rows (upstream fin pitch 4.3 mm, i.e. type DA turbulator AE-4.3 DA tube, downstream fin pitch 2.5 mm, i.e. type DE turbulator AE-2.5DE tube) are determined experimentally. The resultant data and test results are tabulated and presented in appendix D from tables D.6.1 (a) through to D.6.4. The results are further represented graphically in figures D.6.1 and D.6.2.
- (g) The performance characteristics of a heat exchanger bundle of two elliptical finned tube rows (upstream fin pitch 4.5 mm, i.e. type DA turbulator AE-4.5 DA tube, downstream fin pitch 2.5 mm, i.e. type DE turbulator AE-2.5DE tube) are determined experimentally. The resultant data and test results are tabulated and presented in appendix D from tables D.7.1 (a) through to D.7.4. The results are further represented graphically in figures D.6.1 and D.6.2.

Comparison of the performance characteristics of the different double row as well as the combination tests for the elliptical finned tubes are shown graphically from figures D.8 through to D.13. For the double row test the tube bundle having the 2.5 mm fin pitch (AE-2.5 DE) has the highest heat transfer parameter as well as the highest pressure drop coefficient whereas the 4.5 mm fin pitch (AE-4.5 DA) tube bundle has the lowest performance characteristics. It is observed that though the AE-4.3 DA) tube bundle has a smaller pitch than the 4.3 mm fin pitch (AE-4.3 DA) tube bundle, hence more available fin area for heat transfer, it has lower performance characteristics. This could be attributed to the fact that the fins have different turbulators, which affect their performance differently.

4.5 Thermal-flow performance of the ED-, F- and R-finned tubes.

The heat transfer and pressure drop characteristics of the elliptical ED- and F-type finned tubes as well as the round G- and E-type (see figure 3.1) finned tubes are determined experimentally and the following configurations are considered.

- (a) The performance characteristics of a heat exchanger bundle consisting of four tube rows having four tube passes, made up of the elliptical ED-2.5L and ED-2.5S finned tubes (similar to one shown in figure 3.3) are determined experimentally. The tube specifications, data and results of these tests are tabulated and presented in appendix E from tables E.1.1 through to E.1.5 and from table E.2.1 through to E.2.5 respectively. These results are further shown graphically in figures E.1 to E.4.
- (b) The performance characteristics of a heat exchanger bundle consisting of six tube rows having a three row and three tube passes, made up of the elliptical F-3.0 finned tubes are determined experimentally. The tube specifications, data and results of these tests are tabulated and presented in appendix E from tables E.3.1 through to E.3.5. These results are further shown graphically in figures E.5 and E.6.
- (c) The performance characteristics of a heat exchanger bundle consisting of four tube rows having four tube passes, made up of round R-2.4G (G-fin) and R-2.3D (Extruded fin) (19.6mm and 20.86mm inside tube diameters respectively) finned tubes are determined experimentally. The tube specifications, data and results of these tests are tabulated and presented in appendix E from tables E.4.1 through to E.4.5 and from table E.5.1 through to E.5.5 respectively. These results are further shown graphically in figures E.7 to E.10.

Comparison of the heat transfer parameter as well as the pressure drop coefficient of the above-mentioned finned tubes is shown graphically in figures E.11 and E.12 respectively. In figure E.11, it is shown that the tube bundle having the ED-2.5L finned tubes has the highest heat transfer parameter whilst the one for the R-2.4G has the lowest. Scattering of data is seen for the latter from figure E.7. Furthermore, it has lower performance characteristics than for a similar tube, the R-2.3D finned tube.

Chapter 5

PERFORMANCE COMPARISON OF DIFFERENT FINNED TUBE BUNDLES

5.1 Introduction

Heat exchanger bundles having different finned tubes are installed in a forced draught ACHE (similar to figure 2.1) with the view to comparing their respective thermal-flow performance. The heat exchanger that performs best will be the one requiring the least amount of fan and process fluid pumping power for a given heat rejection rate. The specified heat to be rejected is 5.022 MW at a water flowrate of 100 kg/s given a water velocity of $v_w \approx 2.5$ m/s through the tubes. This water velocity through the reference extruded bimetallic finned tube bundle (see section 5.2), which forms a basis for comparing the thermal-flow performance of the different finned tubes, ensures that no cavitation occurs through the tubes. Reasonably low noise levels need to be maintained and a recommended fan blade tip speed of $v_t = 60$ m/s or less is prescribed.

5.2 Determine the thermal-flow performance of a reference extruded finned tube.

To illustrate the procedure for performance evaluation of heat exchanger bundles having different finned tubes, an existing extruded finned round tube (to be referred to as reference tube and shown in figure 5.1) heat exchanger bundle is considered. The thermal-flow performance characteristics of a heat exchanger having such tubes are determined by Kröger [98KR1] and the results obtained are used as a reference value to enable comparison between different heat exchanger bundles.

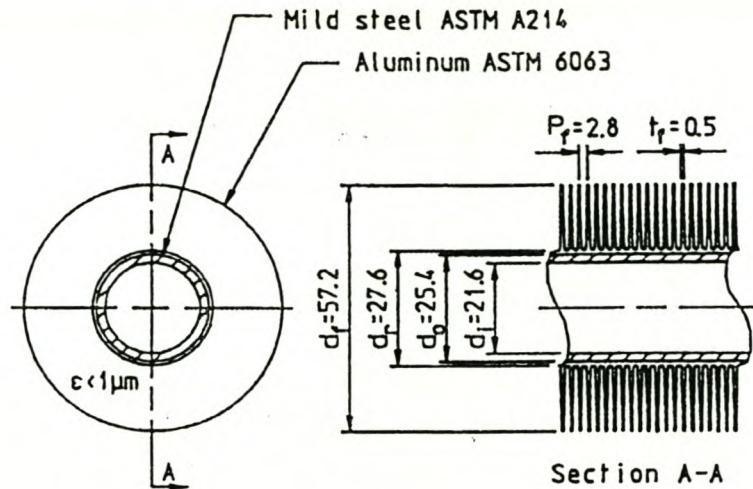


Figure 5.1: Extruded bimetallic round finned tube.

Details of the extruded reference finned tube shown in figure 5.1 are as follows:

Fin material	ASTM 6063 aluminium
Thermal conductivity	$k_f = 204 \text{ W/mK}$
Fin diameter	$d_f = 57.2 \text{ mm}$
Fin root diameter	$d_r = 27.6 \text{ mm}$
Fin shape	Tapered
Fin tip thickness	$t_{ft} = 0.25 \text{ mm}$
Fin thickness (mean)	$t_f = 0.5 \text{ mm}$
Fin root thickness	$t_{fr} = 0.75 \text{ mm}$
Fin pitch	$P_f = 2.80 \text{ mm}$
Fin surface roughness	$\epsilon_f < 1 \mu m$
Tube material	ASTM A214 mild steel
Thermal conductivity	$k_t = 50 \text{ W/mK}$
Tube outside diameter	$d_o = 25.4 \text{ mm}$
Tube inside diameter	$d_i = 21.6 \text{ mm}$
Mean thermal contact resistance	$R_c = 4 \times 10^{-5} \text{ m}^2\text{K/W}$
Tube arrangement	Staggered
Effective length of finned tube	$L_t = 10.203 \text{ m}$
Transversal tube pitch	$P_t = 58 \text{ mm}$
Longitudinal tube pitch	$P_l = 50.22 \text{ mm}$

Number of tube rows $n_r = 4$

Number of tubes per row $n_{tr} = 55$

Number tube passes $n_p = 2$

The experimentally determined characteristic heat transfer parameter for the bundle is given by

$$N_y = 383.617313 R_y^{0.523761}$$

The isothermal loss coefficient through the bundle is

$$K_{heiso} = 1383.94795 R_y^{-0.332458}$$

A 4.265-m diameter fan is used in this application. The fan blade tip speed is given by

$$v_t = N_F d_F (\pi/60) \quad (5.2.1)$$

where

N_F = fan rotational speed, rpm

d_F = fan diameter, m

The maximum allowable fan rotational speed is found using equation (5.2.1)

$$N_F = 60 v_t / (\pi d_F) = 60 \times (60/\pi) \times 1 / 4.265 = 268.68 \text{ rpm}$$

5.2.1 Evaluating the pressure drop across (inside) the reference tubes.

In order to be able to determine the required process fluid pumping power, the pressure drop between the inlet to and outlet of a tube is evaluated.

The Reynolds number for the water flowing in the tube is

$$Re_w = \frac{4m_w}{\pi d_i \mu_w n_{tr}} = \frac{4 \times 100}{\pi \times 0.0216 \times 4.631 \times 10^{-4} \times 55 \times 2} = 115713.9$$

The flow in the tube is turbulent. The water mass velocity through the tubes is thus

$$G_w = \frac{m_w}{n_t A_{ts}} = \frac{100 \times 4}{55 \times 2 \times \pi \times 0.0216^2} = 2480.9 \text{ kg/m}^2 \cdot \text{s}$$

The frictional pressure drop may be determined according to the following equation

$$\Delta p_f = f_D \left(\frac{L_t}{d_i} \right) \frac{G_{wi}^2}{2 \rho_{wi}} \quad (5.2.2)$$

For a smooth tube, the friction factor according to equation (3.4.15) is

$$f_D = (1.82 \log_{10} \text{Re}_w - 1.64)^{-2} = (1.82 \log_{10} 115713.9 - 1.64)^{-2} = 0.017426$$

The frictional pressure drop is thus according to equation (5.2.2)

$$\Delta p_f = 0.017426 \left(\frac{10.203}{0.0216} \right) \frac{2480.9^2}{2 \times 983.22} = 25763.5 \text{ Pa}$$

For the particular tube layout, the area ratio for the entering water stream is

$$\sigma = A_c / A_{fr} = \pi \times 21.6^2 / (4 \times 58 \times 50.22) = 0.125803$$

The jet contraction ratio for round tubes [98KR1] is

$$\begin{aligned} \sigma_c &= 0.61375 + 0.13318\sigma - 0.26095\sigma^2 + 0.51146\sigma^3 \\ &= 0.61375 + 0.13318 \times 0.125803 - 0.26095 \times 0.125803^2 + 0.51146 \times 0.125803^3 \\ &= 0.62739 \end{aligned}$$

For turbulent flow, the inlet contraction loss coefficient may be approximated [50KA1] by

$$K_c = 1 - 2 / \sigma_c + 1 / \sigma_c^2 = 1 - 2 / 0.62739 + 1 / 0.62739^2 = 0.3527$$

The corresponding static pressure drop at the inlet to the tube is

$$\Delta p_i = 0.5 \rho_w v_w^2 [(1 - \sigma^2) + K_e] = 0.5 \times 983.22 \times 2.5^2 [(1 - 0.125803^2) + 0.3527] = 4107.63 \text{ Pa}$$

The outlet expansion coefficient is approximated by

$$K_e = (1 - \sigma^2) = (1 - 0.125803)^2 = 0.7642$$

The corresponding static pressure drop (recovery) at the outlet of the tube is

$$\Delta p_e = 0.5 \rho_w v_w^2 [K_e - (1 - \sigma^2)] = 0.5 \times 983.22 \times 2.5^2 [0.7642 - (1 - 0.125803^2)] = -675.88 \text{ Pa}$$

Because the inlet (Δp_i) and outlet (Δp_e) pressure drops are relatively small, they will be neglected in all further process fluid pressure drop evaluation.

5.3 Heat transfer results

Numerous heat transfer and pressure drop correlations for flow through bundles of round finned tubes have been reported in the literature [78MC1],[98AB1]. In the following section, a theoretical prediction of the heat transfer and pressure drop for staggered circular and plate finned tubes will be presented. These results will be compared with corresponding experimental results.

5.3.1 Theoretical and experimental comparison of the heat transfer for staggered circular finned tubes.

Ganguli et al. [85GA1] proposed the following heat transfer correlation for three or more rows of staggered circular finned tubes:

$$Nu = h d_r / K = 0.38 Re^{0.6} Pr^{0.333} (A/A_r)^{-0.15} \quad (5.3.1)$$

Figure 5.2 below shows the experimentally determined heat transfer parameter for the reference extruded finned round tube and this is compared with the Ganguli correlation [98KR1]. The experimentally determined values for the R-2.3D finned tube (see table E.5.4b, appendix E) is also plotted. The reference tube is compared to the R-2.3D finned tube as the two are similar and thus should have similar performance characteristics.

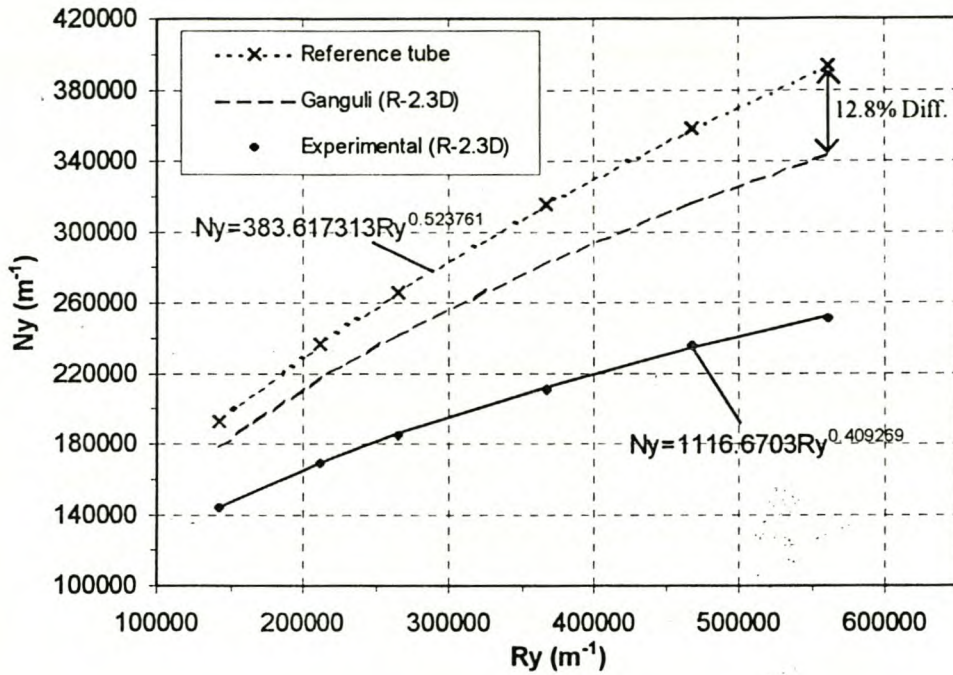


Figure 5.2: Experimental and theoretical prediction of the heat transfer parameter.

It is shown from figure 5.2 that the heat transfer parameter for the tested R-2.3D finned tube bundle (experimental) is well below that predicted by the Ganguli correlation and that of the reference extruded finned tube. Visual inspection of the R-2.3D finned tube showed that the fin made poor contact with the tube resulting in a possible significant thermal contact resistance.

5.3.2 Determining the thermal contact resistance for a R-2.3D finned round tube.

The following section evaluates the approximate thermal contact resistance between the fin and tube of the R-2.3D finned round tube assuming the correlation of Ganguli et al. [85GA1] to be applicable.

Details of the R-2.3D finned tube are as follows:

Fin material	Aluminium
Thermal conductivity	$k_f = 204 \text{ W/mK}$
Fin diameter	$d_f = 57.85 \text{ mm}$
Fin thickness	$t_f = 0.3 \text{ mm}$

Fin pitch	$P_f = 2.35 \text{ mm}$
Tube material	mild steel
Thermal conductivity of tube	$k_t = 50 \text{ W/mK}$
Tube outside diameter	$d_o = 25.4 \text{ mm}$
Tube inside diameter	$d_i = 20.86 \text{ mm}$
Tube arrangement	Staggered
Number of tube rows	$n_r = 4$
Number of tubes per row:	
effective	$n_{tr} = 7.5$
actual	$n_{tr} = 8$
Transversal tube pitch	$P_t = 64 \text{ mm}$
Longitudinal pitch	$P_l = 60 \text{ mm}$
Length of finned tube (effective)	$L_t = 0.47 \text{ m}$
Frontal area	$A_{fr} = 0.2256 \text{ m}^2$

The total effective airside fin surface area is given by

$$\begin{aligned}
 A_f &= [2(\pi d_f^2/4 - \pi d_o^2/4)] L_t n_r n_{tr} / P_f \\
 &= (\pi/2) (d_f^2 - d_o^2) L_t n_r n_{tr} / P_f \\
 &= \pi/2 \times [(57.85 \times 10^{-3})^2 - (25.4 \times 10^{-3})^2] \times 0.47 \times 4 \times 7.5 / 2.35 \times 10^{-3} \\
 &= 25.461 \text{ m}^2
 \end{aligned}$$

By adding the exposed root area to this value the total airside surface area is found

$$\begin{aligned}
 A_a &= A_f + \pi d_o (P_f - t_f) L_t n_r n_{tr} / P_f \\
 &= 25.461 + \pi \times 25.4 \times 10^{-3} (2.35 \times 10^{-3} - 0.3 \times 10^{-3}) \times 0.47 \times 4 \times 7.5 / 2.35 \times 10^{-3} \\
 &= 26.442 \text{ m}^2
 \end{aligned}$$

The minimum free flow area through the heat exchanger is given by

$$A_c = A_{fr} - n_{tr} L_t [d_i t_f + (P_f - t_f) / d_o] / P_f$$

$$= 0.2256 - 7.5 \times 0.47 [57.85 \times 0.3 \times 10^{-6} + (2.35 - 0.3) \times 25.4 \times 10^{-6}] / 2.35 \times 10^{-3}$$

$$= 0.12146 \text{ m}^2$$

The total effective water-side surface area is given by

$$A_w = n_r n_{tr} \pi d_i L_t = 4 \times 7.5 \times \pi \times 0.02086 \times 0.47 = 0.92402 \text{ m}^2$$

Solution

The following sample calculation is done for test run no.1 (see appendix E, tables 4.1 through to E.4.5) where the following properties are measured/calculated.

Dynamic viscosity of air	μ_a	= $1.864 \times 10^{-5} \text{ kg/ms}$
Thermal conductivity of air	k_a	= $2.66 \times 10^{-2} \text{ W/mK}$
Prandtl number of air	Pr_a	= 0.713087
Air inlet temperature	T_{ai}	= 27.0579°C
Air outlet temperature	T_{ao}	= 39.8052°C
Water inlet temperature	T_{wi}	= 59.2123°C
Water outlet temperature	T_{wo}	= 55.8337°C
Temperature correction factor	F_T	= 0.9984551
Heat transfer rate	Q_a	= 30598 W

Properties of water stream evaluated at the arithmetic mean temperature,

$$T_{wm} = (T_{wi} + T_{wo}) / 2 = (332.3623 + 328.9837) / 2 = 330.673 \text{ K}$$

Specific heat of water is

$$\begin{aligned} c_{pw} &= 8.15599 \times 10^3 - 2.80627 \times 10^4 T + 5.11283 \times 10^{-2} T^2 - 2.17582 \times 10^{-13} T^6 \\ &= 8.15599 \times 10^3 - 2.80627 \times 10^4 (330.673) + 5.11283 \times 10^{-2} (330.673)^2 - 2.17582 \times 10^{-13} (330.673)^6 \\ &= 4182.562 \text{ J/kgK} \end{aligned}$$

Dynamic viscosity of water is

$$\mu_w = 2.414 \times 10^{-5} \times 10^{\frac{247.8}{T-140}} = 2.414 \times 10^{-5} \times 10^{\frac{247.8}{(330.673-140)}} = 4.8122 \times 10^{-4} \text{ kg/ms}$$

Thermal conductivity of water is found from

$$\begin{aligned} k_w &= -6.14255 \times 10^{-1} + 6.9962 \times 10^{-3} T - 1.01075 \times 10^{-5} T^2 + 4.74737 \times 10^{-12} T^4 \\ &= -6.14255 \times 10^{-1} + 6.9962 \times 10^{-3} (330.673) - 1.01075 \times 10^{-5} (330.673)^2 \\ &\quad + 4.74737 \times 10^{-12} (330.673)^4 = 0.65076 \text{ W/mK} \end{aligned}$$

The Prandtl number of water is then found to be

$$Pr_w = \frac{\mu_w C_{p_w}}{k_w} = \frac{4.8122 \times 10^{-4} \times 4182.562}{0.65076} = 3.0929$$

We now determine the waterside heat transfer coefficient. Firstly, calculating the waterside Reynolds number.

$$Re_w = \frac{4m_w}{\pi d_i \mu_w} = \frac{4 \times 2.1877}{\pi \times 0.02086 \times 4.8122 \times 10^{-4}} = 277485.256$$

It follows for smooth tubes that the friction factor is

$$f_w = (1.82 \log_{10} Re_w - 1.64)^{-2} = (1.82 \log_{10} (277485.256) - 1.64)^{-2} = 0.0146331$$

From the Gnielinski equation, with $L_1 = 4 \times 0.47 = 1.88 \text{ m}$, the water-side heat transfer coefficient is,

$$h_w = \frac{k_w f_w (Re_w - 1000) Pr_w \left[1 + \left(\frac{d_e}{L_t} \right)^{0.67} \right]}{d_e \times 8 \left[1 + 12.7 \left(\frac{f_w}{8} \right)^{0.5} (Pr_w^{0.67} - 1) \right]}$$

$$= \frac{0.65076 \times 0.0146331 (277485.256 - 1000) \times 3.0929 \left[1 + \left(\frac{20.86}{1880} \right)^{0.67} \right]}{0.02086 \times 8 \left[1 + 12.7 \left(\frac{0.0146331}{8} \right)^{0.5} (3.0929^{0.67} - 1) \right]}$$

$$= 31710.92 \text{ W/m}^2 \text{ K}$$

Furthermore, the logarithmic mean temperature difference (LMTD) is given by

$$\Delta T_{lm} = \frac{(T_{wo} - T_{ai}) - (T_{wi} - T_{ao})}{\ln \left[\frac{(T_{wo} - T_{ai})}{(T_{wi} - T_{ao})} \right]}$$

$$= \frac{(55.8337 - 27.05794) - (59.2123 - 39.8052)}{\ln \left[\frac{(55.8337 - 27.05794)}{(59.2123 - 39.8052)} \right]} = 23.7847 \text{ K}$$

According to equation (5.3.1);

$$h_a d_r / k = 0.38 \text{ Re}^{0.6} \text{ Pr}^{0.333} (A_a / A_r)^{-0.15}$$

where

$$\text{Re} = G_c d_r / \mu_a = m_a d_r / (A_c \mu_a) = 2.35856 \times 0.0254 / (0.12146 \times 1.864 \times 10^{-5}) = 26460.71$$

therefore

$$h_a = (2.66 \times 10^{-2} / 0.0254) \times 0.38 \times 26460.71^{0.6} \times 0.713087^{0.333} \times (26.442 / 0.9815)^{-0.15}$$

$$= 97.7076 \text{ W/m}^2 \text{ K}$$

For a radial fin of uniform thickness, Schmidt [46SC1] proposes the following equation for determining the fin efficiency

$$\eta_f = \tanh (b d_o \phi / 2) / (b d_o \phi / 2) \quad (5.3.2)$$

where

$$b = (2h_a / k_{ftf})^{0.5} = (2 \times 97.7076 / 204 \times 0.3 \times 10^{-3})^{0.5} = 56.50715 \quad (5.3.3)$$

and

$$\phi = (d_f/d_o - 1)[1 + 0.35\ln(d_f/d_o)] \quad (5.3.4)$$

$$= (57.85/25.4 - 1)[1 + 0.35\ln(57.85/25.4)] = 1.64561$$

therefore

$$\begin{aligned} \eta_f &= \tanh(56.50715 \times 0.0254 \times 1.64561 \times 0.5) / (56.50715 \times 0.0254 \times 1.64561 \times 0.5) \\ &= 0.70092 \end{aligned}$$

Surface effectiveness is given as

$$e_f = 1 - A_f(1 - \eta_f) / A_a = 1 - 25.461(1 - 0.70092) / 26.442 = 0.712 \quad (5.3.5)$$

A characteristic flow parameter, R_y is found using equation (3.4.5)

$$R_y = m_a / (A_{fr} \times \mu_a) = 2.35856 / (0.2256 \times 1.864 \times 10^{-5}) = 560869.63 \text{ m}^{-1}$$

Similarly, a characteristic heat transfer parameter follows from equation (3.4.6)

$$\begin{aligned} N_y &= h_a e_f A_a / k_a A_{fr} Pr^{0.333} \\ &= 97.7076 \times 0.712 \times 26.442 / (2.66 \times 10^{-2} \times 0.2256 \times 0.713087^{0.333}) = 343078.537 \text{ m}^{-1} \end{aligned}$$

Using equation (3.4.7);

$$\left[\frac{1}{h_a e_f A_f} + \sum_n \frac{R_n}{A_n} \right] = \left[\frac{F_T \Delta T_{lm}}{Q} - \frac{1}{h_w A_w} \right]$$

Assuming negligible resistance due to the fin root, the R_n/A_n term includes resistances due to the tube wall as well as the thermal contact resistance at the steel-aluminium interface.

From the above equation,

$$\begin{aligned}\sum_n \frac{R_n}{A_n} &= \left[\frac{F_T \Delta T_{lm}}{Q} - \frac{1}{h_w A_w} - \frac{1}{h_a e_f A_a} \right] \\ &= \left[\frac{0.9984551 \times 23.7847}{30598} - \frac{1}{31710.92 \times 0.92402} - \frac{1}{97.7076 \times 0.712 \times 26.442} \right] \\ &= 0.000198377 \text{ K/W} \\ &= \frac{1}{n_r n_u L_t} \left[\frac{\ln(d_o/d_i)}{2\pi k_t} + \frac{R_c}{\pi d_o} \right]\end{aligned}$$

The mean thermal contact resistance is therefore given by

$$\begin{aligned}R_c &= [0.000198377 \times 4 \times 7.5 \times 0.47 - \ln(25.5/20.86) / (2\pi \times 50)] \pi \times 0.0254 \\ &= 1.7219 \times 10^{-4} \text{ m}^2 \text{ K/W}\end{aligned}$$

This value is more than four times higher than the specified thermal contact resistance of the reference extruded finned tube which has a value of $R_c = 4 \times 10^{-5} \text{ m}^2 \text{ K/W}$.

5.3.3 Theoretical and experimental comparison of the isothermal pressure drop for staggered circular finned tubes.

Considering the R-2.3D fin tube, Ganguli et al. [85GA1] propose the following equation for the pressure drop through bundles for staggered circular finned tube:

$$\begin{aligned}Eu = \rho \Delta p / G_c^2 &= 2n_r [1 + 2 \exp\{-(P_t - d_f) / (4d_r)\} / \{1 + (P_t - d_f) / d_r\}] \\ &[0.021 + 13.6 (d_f - d_r) / \text{Re} (P_f - t_f) + 0.25246 \{(d_f - d_r) / \text{Re} (P_f - t_f)\}^{0.2}]\end{aligned}$$

This equation is applicable since $2.5 < (d_f - d_r) / [2(P_f - t_f)] = (57.85 - 25.4) / [2(2.35 - 0.3)]$

$$= 7.9146 < 12.5$$

For the four-row bundle

$$\Delta p = 2 \times 4 \times 19.41845^2 / (1.1276) \times [1 + 2 \exp\{-(64 - 57.85) / (4 \times 25.4)\} / \{1 + (64 - 57.85) / 25.4\}] [0.021 + 13.6(57.85 - 25.4) / (26457.1545 \times (2.35 - 0.3))] + 0.25246\{(57.85 - 25.4) / (26457.1545 \times (2.35 - 0.3))\}^{0.2}] = 581.187 \text{ N/m}^2$$

This value compares with the measured experimental pressure differential of 582 N/m² (Appendix E, table E.5.3, test run no.1).

The pressure drop was also determined at other flow rates and the results are plotted in figure 5.3 below.

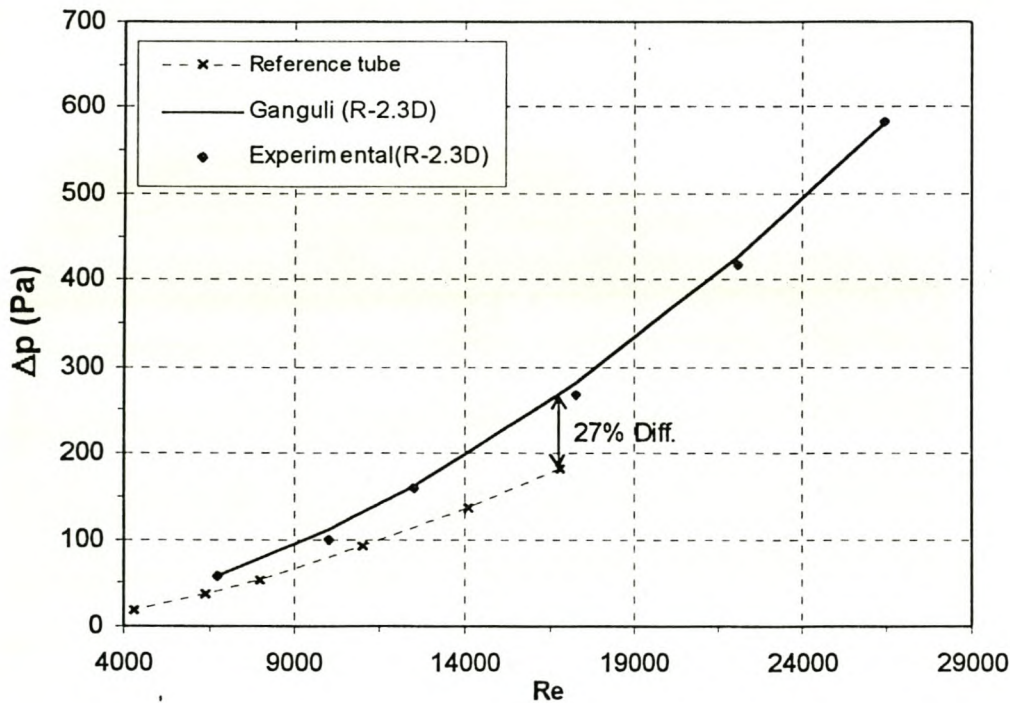


Figure 5.3: Experimental and theoretical prediction of the airside pressure drop.

5.4 McQuiston heat transfer correlation for staggered plate-finned round tubes.

In addition to correlations for round tubes with radial fins, correlations are also available for round tubes with plate fins. In the following analysis, the performance of an industrial plate finned heat exchanger will be determined. The application of this type of finned tube in an ACHE will also be compared with the performance of the other finned tubes being studied.

McQuiston [78MC1] presents heat transfer data for staggered plate-finned round tubes in dimensionless form according to a method originally proposed by Colburn [33CO1],

$$j = \frac{hPr^{0.67}}{G_c c_p} = \text{function of Re} \quad (5.4.1)$$

where j is known as the Colburn j -factor.

Details of the heat exchanger whose thermal-flow performance characteristics are to be evaluated using the McQuiston correlation are as follows:

Tube arrangement	Staggered
Number of tube rows	$n_r = 8$
Number of tubes per row	$n_{tr} = 40$
Transversal tube pitch	$P_t = 20$
Longitudinal tube pitch	$P_l = 20$
Frontal area	$A_{fr} = 0.5808 \text{ m}^2$
Tube material	Copper
Thermal conductivity of tube	$k_t = 364 \text{ W/mK}$
Tube outside diameter	$d_o = 10 \text{ mm}$
Tube inside diameter	$d_i = 8 \text{ mm}$
Fin material	ASTM 6063 aluminium
Thermal conductivity of fin	$k_f = 204 \text{ W/mK}$
Fin thickness	$t_f = 0.24 \text{ mm}$
Fin pitch	$P_f = 3 \text{ mm}$
Flow length through the bundle parallel to the air flow	$L = 160 \text{ mm}$
Width of bundle perpendicular to air flow	$W = 800 \text{ mm}$

The total effective airside fin surface area is given by

$$\begin{aligned}
 A_f &= [2 t_f(L + W) + 2 (L \times W - n_{tr} n_r \pi d_o^2 / 4)] L_t / P_f \\
 &= [2 \times 0.00024(0.16 + 0.8) + 2(0.8 \times 0.16 - 40 \times 8 \times \pi \times 0.01^2 / 4)] 726 / 3 \\
 &= 49.899 \text{ m}^2
 \end{aligned}$$

By adding the exposed root area to this value the total airside surface area is found

$$\begin{aligned}
 A_a &= A_f + A_r = A_f + \pi d_o (P_f - t_f) L_t n_r n_{tr} / P_f \\
 &= 49.899 + \pi \times 0.01(3 \times 10^{-3} - 0.24 \times 10^{-3}) \times 40 \times 8 \times 0.726 / (3 \times 10^{-3}) = 56.614 \text{ m}^2
 \end{aligned}$$

The minimum free flow area through the heat exchanger is given by

$$\begin{aligned}
 A_c &= n_{tr} L_t [P_t P_f - (d_f - d_r) t_f - P_f d_r] / P_f \\
 &= 40 \times 726 [20 \times 3 \times 10^{-6} - (20 - 10) \times 0.24 \times 10^{-6} - 3 \times 10 \times 10^{-6}] / 3 \\
 &= 0.26717 \text{ m}^2
 \end{aligned}$$

The area ratio is then

$$\sigma = A_c / A_{fr} = 0.26717 / 0.5808 = 0.46$$

The hydraulic diameter is defined by

$$D_h = 4 L A_c / A_a = 4 \times 160 \times 0.26717 / 56.614 = 3.02 \text{ mm}$$

During the particular performance test to evaluate the heat transfer coefficient, h_a , the following thermophysical properties at an air mean temperature of $T_{am} = 33.4316^\circ\text{C}$ (306.5816 K) are

Density	$\rho_a = 1.12759 \text{ kg/m}^3$
Specific density	$c_{pa} = 1017.717 \text{ J/kgK}$
Dynamic viscosity	$\mu_a = 1.864 \times 10^{-5} \text{ kg/ms}$
Thermal conductivity	$k_a = 2.6606 \times 10^{-2} \text{ J/kgK}$
Prandtl number	$Pr_a = 0.713$

For this particular test, an air mass flowrate of $m_a = 2.35857 \text{ kg/s}$ is used.

5.4.1 Evaluating the heat transfer parameter.

Two particular parameters in addition to the j factors feature predominantly in heat transfer correlations [78MC1]. The first is the Reynolds number based on the outside tube diameter [73RI1].

$$\begin{aligned} Re_D &= G_c d_o / \mu_a = m_a d_o / (A_c \mu_a) \\ &= 2.35857 \times 0.01 / (0.26717 \times 1.864 \times 10^{-5}) = 4736.04 \end{aligned} \quad (5.4.2)$$

The second is the ratio of total surface area to the outside surface area of the tubes without fins, A/A_t , which is expressed by McQuiston as

$$\begin{aligned} \frac{A}{A_t} &= \frac{4}{\pi} \frac{P_l}{D_h} \frac{P_t}{D} \sigma \\ &= 4/\pi \times (20/3.02) \times (20/10) \times 0.46 = 7.7575 \end{aligned} \quad (5.4.3)$$

The following correlating parameter for use with the j factors is obtained

$$\begin{aligned} JP &= Re_D^{-0.4} (A/A_t)^{-0.15} \\ &= 4736.04^{-0.4} (7.7575)^{-0.15} = 0.02491 \end{aligned} \quad (5.4.4)$$

Rich [75RI1] shows that the Reynolds number based on longitudinal tube spacing is important in expressing row effect.

$$\begin{aligned} Re_b &= G_c P_l / \mu_a \\ &= 2.35857 \times 0.02 / (0.26717 \times 1.864 \times 10^{-5}) = 9472.08 \end{aligned} \quad (5.4.5)$$

The j factor for an eight-row tube bundle is given by

$$j_8 = \left[\frac{1 - 1280n_r \text{Re}_b^{-1.2}}{1 - 5120\text{Re}_b^{-1.2}} \right] [0.0014 + 0.2618(JP)] \quad (5.4.6)$$

$$= \left[\frac{1 - 1280 \times 8 \times 9472.08^{-1.2}}{1 - 5120 \times 9472.08^{-1.2}} \right] [0.0014 + 0.2618 \times 0.02491] = 0.0071704$$

From equation (5.4.1), the heat transfer coefficient is

$$h_a = j_8 G_c c_{pa} \text{Pr}_a^{-0.67} = 0.0071704 \times 2.35857 / 0.26717 \times 1017.717 \times 0.713^{-0.67} = 80.809 \text{ W/m}^2\text{K}$$

The fin efficiency of a continuous plate fin having a staggered tube array using equation (5.3.2) is

$$\eta_f = \tanh(bd_o\phi/2) / (bd_o\phi/2)$$

where from equation (5.3.3)

$$b = (2h_a / k_{tf})^{0.5} = (2 \times 80.809 / 204 \times 0.24 \times 10^{-3})^{0.5} = 57.455$$

and for a staggered tube layout

$$d_{fe}/d_r = 2.54(L_1/d_r)(L_2/L_1 - 0.3)^{0.5} = 2.54(10/10)(10/10 - 0.3)^{0.5} = 2.12512$$

hence

$$\phi = (d_{fe}/d_r - 1)(1 + 0.35\ln(d_{fe}/d_r)) = (2.12512 - 1)(1 + 0.35\ln(2.12512)) = 1.421966$$

The fin efficiency is thus

$$\eta_f = \tanh(57.455 \times 0.01 \times 1.421966 \times 0.5) / (59.972 \times 0.01 \times 1.421966 \times 0.5) = 0.94786$$

Surface effectiveness is given as

$$e_f = 1 - A_f(1 - \eta_f) / A_a = 1 - 49.899(1 - 0.94786) / 56.614 = 0.95404$$

A characteristic flow parameter, R_y , is found using equation (3.4.5)

$$R_y = m_a / (A_{fr} \times \mu_a) = 2.35857 / (0.5808 \times 1.864 \times 10^{-5}) = 217859.3756 \text{ m}^{-1}$$

Similarly, a characteristic heat transfer parameter is given by

$$\begin{aligned} N_y &= h_a e_f A_a / k_a A_{fr} Pr^{0.333} \\ &= 80.809 \times 0.95404 \times 56.614 / (2.66066 \times 10^{-2} \times 0.5808 \times 0.713^{0.333}) = 316122.684 \text{ m}^{-1} \end{aligned}$$

The characteristic heat transfer parameter for this bundle was also determined at other air-flow rates and the data may be correlated by the following empirical relation over the range tested:

$$N_y = 8 \times 10^{-4} R_y^{1.6329}$$

5.4.2 Evaluating the pressure drop parameter.

The correlating parameter necessary for the evaluation of the friction data is

$$\frac{R^*}{R} = \frac{A / A_t}{(P_t - d_o) P_f^{-1} + 1} = \frac{7.7575}{(0.02 - 0.01) / 0.003 + 1} = 1.7902$$

A parameter to be used to obtain the fanning friction factor, f , is evaluated as follows

$$\begin{aligned} FP &= Re_D^{-0.25} \left(\frac{R}{R^*} \right)^{0.25} \left[\frac{(P_t - d_o) P_f^{-1}}{4(1 - P_f^{-1} t_f)} \right]^{-0.4} \left[\frac{P_t}{2R^*} - 1 \right]^{-0.5} \quad (5.4.7) \\ &= 4736.04^{-0.25} (1.7902)^{-0.25} \left[\frac{(20 - 10)/3}{4(1 - 0.24/3)} \right]^{-0.4} \left[\frac{20}{1.7902 \times 10} - 1 \right]^{-0.5} = 0.31669 \end{aligned}$$

The fanning friction factor is hence given by

$$f = 4.904 \times 10^{-3} + 1.382(FP)^2 = 4.904 \times 10^{-3} + 1.382(0.31669)^2 = 0.14352$$

The approach air velocity is given by

$$v_a = m_a / (\rho_a A_{fr}) = 2.35857 / (1.12759 \times 0.5808) = 3.6014 \text{ m/s}$$

The isothermal heat exchanger bundle loss coefficient is found using equation (3.4.16)

$$K_{he} = \frac{2\rho_a \Delta p_{bundle}}{(m_a / A_{fr})^2}$$

where

$$\begin{aligned} \Delta p_{bundle} &= f_D (L/D_h) \rho_a v_a^2 / 2 = 4 \times 0.14352 \times (160/3.02) \times 1.12759 \times 3.6014^2 / 2 \\ &= 222.403 \text{ N/m}^2 \end{aligned}$$

hence

$$K_{he} = \frac{2 \times 1.12759 \times 222.407}{(2.35857 / 0.5808)^2} = 30.415$$

It is noted that the Darcy friction factor, f_D , is $f_D = 4f$.

The loss coefficient for this bundle was also determined at other air flow rates and the data may be correlated by the following empirical equation over the range tested:

$$K_{he} = 12165 R_y^{-0.4875}$$

This bundle was further installed in a forced draught ACHE and the thermal-flow performance thereof evaluated. Results are presented in table 5.1 below.

Table 5.1: Performance evaluation of a forced draught ACHE.

	Force draught ACHE
Heat rejected, Q_{rem} (MW)	5.022
Air mass flow rate, m_a (kg/s)	210.0379
Fan shaft power, P_F (kW)	20.796
Air outlet temperature, °K	324.8489
Pressure drop across tube, Δp_f (Pa)	107912.9
Water velocity in tube, v_w (m/s)	2.86

5.5 Performance comparison of different finned tubes in a forced draught ACHE.

Table 5.2 below presents the finned tube bundle specifications for the different commercial tubes as tested by the author and then installed in a forced draught ACHE.

Table 5.2: Finned tube bundle geometries installed in a forced ACHE.

	R-2.3D	F-3.0	ED-2.5S	ED-2.5L	AE-2.5 DE
Effective length of finned tube, L_t (m ²)	10.203	10.203	10.203	10.203	10.203
Cross-sectional tube inside area, A_{ts} (m ²)	3.418×10^{-4}	2.553×10^{-4}	2.881×10^{-4}	5.994×10^{-4}	1.33×10^{-3}
Inside/hydraulic diameter of tube, d_i (m)	0.02086	0.01502	0.014316	0.020848	0.025922
Number of tube rows per pass, n_r	2	2	2	1	1
Number of tubes per row, n_{tr}	55	117	92	72	72
Number of tube passes, n_p	2	2	2	2	2

From the results obtained in sections 5.2 and 5.3, a performance evaluation of the forced draught ACHE was done and the results are presented in table 5.3 below.

Table 5.3: Performance evaluation of a forced ACHE for different finned tubes.

	Reference	R-2.3D	F-3.0	ED-2.5S	ED-2.5L	AE-2.5DE
Heat rejected, Q_{rem} (MW)	5.022	5.022	5.022	5.022	5.022	5.022
Air mass flow rate, m_a (kg/s)	258.4607	317.7933	274.8075	243.2662	223.312	201.171
Fan shaft power, P_F (kW)	27.5085	32.0583	33.5807	28.2515	19.5147	17.9184
Fan rotational speed, N_F (rpm)	248	265	265	250	221	215
Air outlet temperature, T_{a6} (K)	320.4046	316.7982	319.2743	321.62	323.4227	325.8787
Pressure drop across tube, Δp_f (Pa)	25763.5	30446.96	15465.74	22967.61	21204.21	3617.18
Water velocity in tube, v_w (m/s)	2.52	2.71	1.70	1.92	2.36	1.06

From the results presented in table 5.3 above, the AE-2.5 DE finned tube heat exchanger performs best as it rejects the specified heat of $Q_{rem} = 5.022$ MW with the least amount of fan shaft power of $P_F = 17.9184$ kW. It also has the smallest pressure drop across the tube of $\Delta p_f = 3617.18$ Pa resulting in the least amount of process fluid pumping power required.

The two ED-type elliptical finned tube heat exchanger bundles perform better than the standard reference round tube heat exchanger bundle. Only the R-2.3D (poor quality tube due to high thermal contact resistance) as well as the F-3.0 elliptical finned tube bundles performs poorly when compared to the standard reference round tube heat exchanger bundle.

Chapter 6

CONCLUSIONS

The objective of this thesis was to evaluate the thermal-flow performance characteristics of commercially available elliptical finned tubes, with a view to comparing their performance in forced and induced draught air-cooled heat exchangers.

The first step, in chapter 2, was to consider two types of mechanical draught ACHE's commonly in use in the petro-chemical industry. These are of the forced draught type as well as the induced draught type. The governing equations to evaluate the performance of these two types of ACHE's are employed in a computer performance evaluation program. With this program, it is possible to determine the process fluid outlet temperature and fan shaft power consumption for a given set of ambient conditions and design parameters. The induced draught system generally requires more fan shaft power than the forced draught system for a given heat rejection rate as is seen from table F.1 in appendix F. This is so because the fan draws hot air, which has a low density, through the tube bundle.

After outlining the method for data presentation in chapter 3, a presentation of experimental and calculated results performed for the different finned tubes is given in chapter 4. It is concluded from figures A.5 through to A.7 in appendix A that there is an increase in the heat transfer parameter with a decrease in the fin pitch. The decrease in fin pitch however also results in an increase in the pressure drop across the bundle. Varying the water mass flowrate has a negligible effect on the heat transfer parameter, everything else being held constant. A less than 1 % variation (figure A.8) of the Ny-value, the heat transfer parameter, was obtained by performing such a test. Furthermore, thermal-flow characteristics of the different finned tubes (see figures 3.1 and 3.2) are presented in appendices C, D and E.

Finally, in chapter 5, different heat exchanger bundles are installed in a forced draught ACHE with the view to comparing their respective thermal-flow performance. Performance characteristics of a reference extruded finned round tube as tested by Kröger [98KR1] is also presented. Comparison is also made between the experimentally

determined heat transfer characteristics for the R-2.3D finned tube tested and the theoretical prediction by Ganguli [85GA1]. It is shown in figure 5.1 that the R-2.3D finned tube, due to its poor quality (as seen from the high contact resistance calculated), has a lower heat transfer parameter when compared to that of the reference extruded finned round tube, which compares very well with Ganguli correlation. It is also shown that the thermal contact resistance of the R-2.3D finned tube, at $R_c = 1.7219 \times 10^{-4} \text{ m}^2\text{K/W}$, is almost five times higher than the specified value for the reference round tube which has a value of $R_c = 4 \times 10^{-5} \text{ m}^2\text{K/W}$. The McQuiston correlation was also used to determine the heat transfer and airside pressure drop characteristics for a staggered plate-finned round tubes heat exchanger. The heat exchanger bundle was then incorporated in a forced draught ACHE and a thermal-flow performance thereof evaluated.

Lastly, using the computer performance evaluation program for a forced draught ACHE, it is shown in table 5.2 that the AE-2.5 DE finned tube heat exchanger requires the least amount of fan shaft power of $P_F = 17.9184 \text{ kW}$ for a specified heat rejection rate of $Q_{rem} = 5.022 \text{ MW}$ at a water mass flowrate of 100 kg/s . Less process fluid pumping power is required as it has the smallest pressure drop across the tube of $\Delta p_f = 3617.18 \text{ Pa}$. The two ED-type finned tube heat exchanger also have better performance characteristics when compared to the standard reference extruded finned round tube heat exchanger bundle. The R-2.3D and the F-3.0 finned tube bundles perform poorly when compared to the standard reference extruded finned round tube bundles.

Based on the above conclusions, it is recommended that the use of elliptical finned tubes in a petrochemical industry as a better alternative, performance-wise, to the conventional finned round tube heat exchanger be considered for application where the process fluid pressure is not excessive.

REFERENCES

- [46SC1] Schmidt, T.E., La Production Calorifique des Surfaces Munies Dailettes, Annexe Du Bulletin De L'Institut International Du Froid, Annex G-5 1945 –1946.
- [50KA1] Kays, W.M., Loss Coefficients for Abrupt Changes in Flow Cross Section with Low Reynolds Number Flow in Single and Multiple-Tube Systems, Transactions of ASME, Vol. 72, No. 8, pp 1067-1074, 1950.
- [54FI1] Filonenko, G.K., Teploenergetika No.4, 1954.
- [73RI1] Rich, D.G., The Effect of Fin Spacing on the Heat Transfer and Friction Performance of Multi-Row, Smooth Plate-Fin-and-Tube Exchangers, ASHRAE Trans., Vol. 79, Part 2, 1973.
- [75GN1] Gnielinski, V., Forsch. Ing. Wesen, Vol. 41, No. 1, 1975.
- [75RI1] Rich, D.G., The Effect of the Number of Tube Rows on Heat Transfer Performance of Smooth Plate-Fin-Tube Heat Exchangers, ASHRAE Trans., Vol. 81, Part 1, 1975.
- [78MC1] McQuiston, F.C., Correlation of Heat, Mass and Momentum Transport Coefficients for Plate-Fin-Tube Heat Transfer Surfaces with Staggered Tubes, ASHRAE Trans., Vol. 84, Part 1, pp. 294 – 309, 1978.
- [80KE1] Kern, J., Zur Bewertung von Kompakt-Wärmeaustauschern, Wärme-und Stoffübertragung, Vol. 13, pp. 205 – 215, 1980.
- [81SH1] Shah, R.K., Compact Heat Exchangers, in Heat Exchangers, Thermal-Hydraulic Fundamentals and Design, eds Kakac, S., Bergles, A.E. and Mayinger, F., pp. 111-151, MacGraw-Hill Book Co., New York, 1981.

- [84KA1] Kays, W.M. and London, A.L., Compact Heat Exchangers, MacGraw-Hill Book Co., New York, 1984.
- [85GA1] Ganguli, A., Tung, S.S. and Taborek, J., Parametric Study of Air-cooled Heat Exchanger Finned Tube Geometry, AIChE Symposium Series, Vol. 81, No. 245, pp. 122-128, 1985.
- [86KR1] Kröger, D.G., Performance Characteristics of Industrial Finned Tubes Presented in Dimensional Form, Int. J. Heat Mass Transfer, Vol. 29, No. 8, 1986.
- [91AS1] ASME PTC 30-1991, Air-cooled Heat Exchangers Performance Test Codes, ASME, New York, 1991.
- [91BE1] Beiler, M.G., Effect of Flow Maldistribution on Performance of Induced and Forced Draft Air-cooled Heat Exchangers, M. Eng thesis, Department of Mechanical Engineering, University of Stellenbosch, Republic of South Africa, January 1991.
- [98AB1] Abu-Madi, M., Johns, R.A., and Heikal, M.R., Performance Characteristics Correlation for Round Tube and Plate Finned Heat Exchangers, Int. J. of Refrigeration, Vol. 21, No. 7, pp. 507-517, 1998.
- [98KR1] Kröger, D.G., Air-cooled Heat Exchangers and Cooling Towers, Thermal-flow performance evaluation and design, 1998.
- [98ME1] Meyer, C.J., and Kröger, D.G., Plenum Chamber Flow Losses in Forced Draught Air-cooled Heat Exchangers, Applied Thermal Engineering, Vol. 18, pp. 875 – 893, 1998.

APPENDIX A

Effect of fin pitch and water mass flowrate on the thermal-flow performance of a heat exchanger bundle

Table A.1.1: Tube specifications.

Name: AE-2.2 (2.2 mm fin pitch, 0.48875 mm fin thickness)

No	Tube mass,kg	No. of fins	L_t ,mm	P_f ,mm
1	4.075	214	468.5	2.18925
2	4.055	213	468	2.19718
3	4.01	209	469	2.24402
4	4.06	214	466	2.17757
5	4.05	214	467	2.18224
6	4.05	211	468	2.21801
7	4.005	209	461	2.20574
8	4.055	214	467	2.18224
9	4.045	209	468	2.23923
10	4.075	214	469	2.19159
Average	4.048	212.1	467.15	2.2027085

Table A.1.2a: Test data.

Run no.	T_{ai} °C	T_{ao} °C	T_{wi} °C	T_{wo} °C	P_{atm} N/m ²	m_a kg/s	m_w kg/s
1	24.95925	37.33766	65.5401	64.03753	100103.6	2.4724873	4.28044
2	25.28283	39.08679	65.33853	63.99107	100098.33	1.9706344	4.2590853
3	25.21611	41.1575	65.36698	64.17437	100099.42	1.5280545	4.260266
4	25.25604	43.83281	65.37377	64.35564	100098.77	1.1382156	4.2780567
5	25.52157	46.3568	65.50876	64.6232	100094.44	0.8901218	4.2864099
6	25.47576	49.96894	65.70552	64.97584	100095.19	0.638672	4.279248

Table A.1.2b: Test data.

Run no.	Δp_{bundle} N/m ²	Δp_n N/m ²	Δp_{up} N/m ²
1	462	431	1298
2	323	740	865
3	213	445	540
4	134	248	316
5	92	153	205
6	57	80	115

Table A.1.3: Pressure drops for isothermal tests. $(P_{atm} = 100820 \text{ N/m}^2, T_{aiwb} = 17.5^\circ\text{C}, T_{aidb} = 23.5^\circ\text{C})$

Run no.	Δp_{bundle} N/m ²	Δp_n N/m ²	Δp_{up} N/m ²
1	426	400	1200
2	320	756	890
3	210	454	543
4	131	250	312
5	89	154	215
6	56	82	110

Table A.1.4a: Test results.

Run no	LMTD °C	F_T ---	Q_a W	Q_w W	Q_w/Q_a ---	%error %
1	33.35312136	0.9810046	31364.529	29521.918	0.9412517	5.8748272
2	32.08727217	0.9806031	27875.744	26607.73	0.9545119	4.5488069
3	31.0128674	0.9807224	24964.196	23853.161	0.9554949	4.4505141
4	29.46764403	0.9816576	21670.896	20827.487	0.961081	3.8918952
5	27.96770359	0.9828238	19007.581	18489.283	0.972732	2.7267952
6	25.84409028	0.9845631	16034.619	15665.804	0.9769989	2.3001126

Table A.1.4b: Test results.

Run no.	Re_w ---	h_w W/m ² K	R_y m ⁻¹	N_y m ⁻¹	K_{he}
1	193444.9179	17554.869	570208.1	183295.5	9.4499855
2	192132.3063	17469.291	453279.85	168192.98	10.365316
3	192482.3403	17483.451	350622.99	154756.02	11.331016
4	193550.921	17553.879	260305.97	140070.54	12.790973
5	194497.1067	17601.939	202867.18	128323.16	14.294931
6	194947.217	17603.279	144935.72	115935.98	17.104573

Correlating equations: $N_y = 2164.3479R_y^{0.334505}$
 $K_{he} = 2621.945R_y^{-0.425420}$

Table A.1.5: Isothermal test results.

Run no.	R_y m ⁻¹	K_{heiso}
1	572576.0191	9.2199913
2	479721.4624	9.8664041
3	373010.7934	10.709365
4	277427.0139	12.077054
5	217746.82	13.31906
6	158626.428	15.791528

Correlating equation: $K_{heiso} = 2099.6263R_y^{-0.410382}$

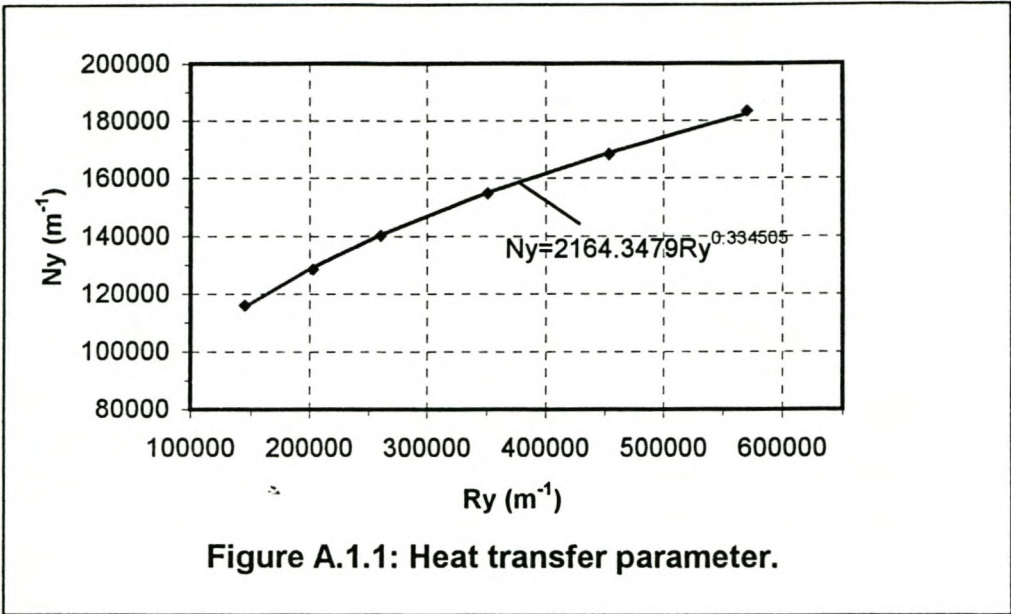


Figure A.1.1: Heat transfer parameter.

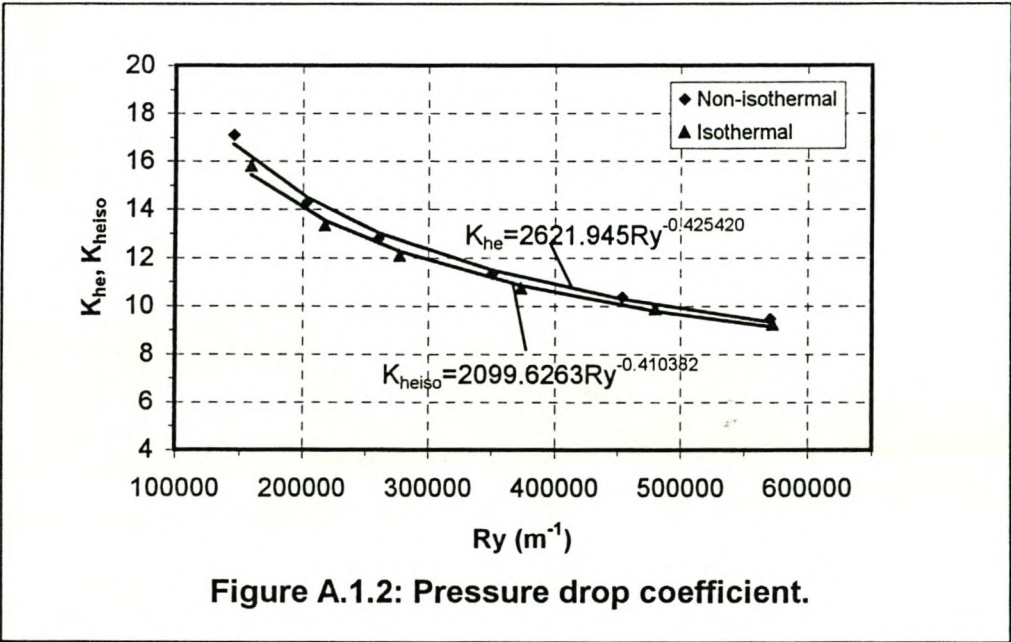


Figure A.1.2: Pressure drop coefficient.

Table A.2.1: Tube specifications.

Name: AE-2.3 (2.3 mm fin pitch, 0.463920 mm fin thickness)

No	Tube mass,kg	No. of fins	L_t ,mm	P_f ,mm
1	3.885	201	468	2.32836
2	3.91	201	468	2.32836
3	3.92	202	466	2.30693
4	3.665	201	468	2.32836
5	3.875	200	465	2.32500
6	3.9	203	468	2.30542
7	3.885	200	468	2.34000
8	3.89	199	468	2.35176
9	3.885	201	467	2.32338
10	3.88	200	470	2.35000
Average	3.8695	200.8	467.6	2.3287566

Table A.2.2a: Test data.

Run no.	T_{ai} °C	T_{ao} °C	T_{wi} °C	T_{wo} °C	P_{atm} N/m ²	m_a kg/s	m_w kg/s
1	26.94005	37.55132	63.06423	61.73734	100101.21	2.4738871	4.3597672
2	27.4969	39.13672	62.97453	61.76826	100092.14	1.9831436	4.3347139
3	27.84769	41.08774	62.95214	61.90222	100086.43	1.5330234	4.3192619
4	27.84497	43.23277	62.86764	61.96936	100086.48	1.1482015	4.3274
5	27.94133	45.49372	62.85996	62.08626	100084.91	0.8674404	4.2976692
6	27.97915	48.54143	63.11699	62.48605	100084.29	0.6318639	4.3457313

Table A.2.2b: Test data.

Run no.	Δp_{bundle} N/m ²	Δp_n N/m ²	Δp_{up} N/m ²
1	432	432	1294
2	302	750	864
3	197.5	448	534
4	124.5	252	313
5	82	145	190
6	50.5	78	110

Table A.2.3: Pressure drops for isothermal tests.

($P_{atm} = 100360$ N/m², $T_{aiwb} = 26^\circ\text{C}$, $T_{aidb} = 27^\circ\text{C}$)

Run no.	Δp_{bundle} N/m ²	Δp_n N/m ²	Δp_{up} N/m ²
1	439	438	1335
2	295	742	853
3	198.5	462	546
4	123.5	258	316
5	83.5	158	202
6	53.5	88	118

Table A.2.4a: Test results.

Run no	LMTD °C	F_T ---	Q_a W	Q_w W	Q_w/Q_a ---	%error %
1	29.92034008	0.9824207	26923.339	25970.645	0.9646146	3.5385442
2	28.74546391	0.9817977	23671.474	23632.78	0.9983654	0.1634642
3	27.51795631	0.9818705	20813.273	20722.065	0.9956178	0.4382224
4	26.22460502	0.9825785	18118.657	18014.38	0.9942448	0.575521
5	24.82845077	0.9836653	15614.395	15649.709	1.0022616	-0.226158
6	23.14152432	0.9855811	13325.452	13228.622	0.9927334	0.7266604

Table A.2.4b: Test results.

Run no.	Re_w ---	h_w W/m ² K	R_y m ⁻¹	N_y m ⁻¹	K_{he}
1	190214.7618	17593.975	569270.13	174143.61	8.7900039
2	189038.7672	17505.791	455089.91	158271.9	9.5293375
3	188521.755	17458.681	350781.92	144297.7	10.390061
4	188852.5011	17485.548	262045.44	130773.86	11.63515
5	187707.8354	17389.598	197401.12	118080.69	13.375857
6	190737.1445	17585.896	143256.93	107045.17	15.448128

Correlating equations: $N_y = 1646.0652R_y^{0.350891}$
 $K_{he} = 1948.849R_y^{-0.408734}$

Table A.2.5: Isothermal test results.

Run no.	R_y m ⁻¹	K_{heiso}
1	590141.2328	8.6929661
2	468649.6864	9.262767
3	370937.0728	9.948908
4	277829.1369	11.033842
5	217447.0658	12.178527
6	162025.0696	14.054155

Correlating equation: $K_{heiso} = 1143.0382R_y^{-0.368724}$

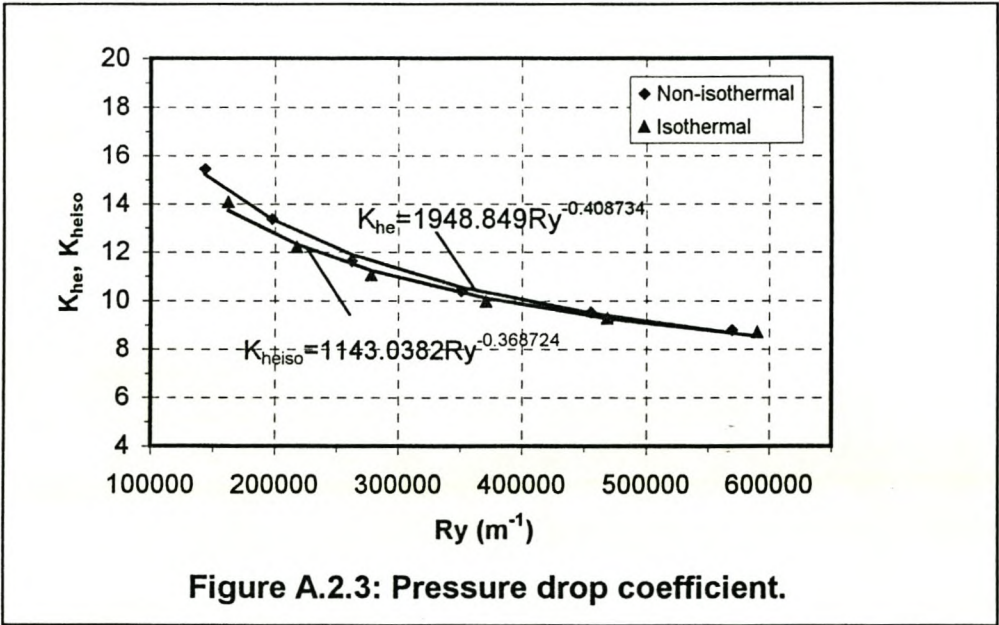
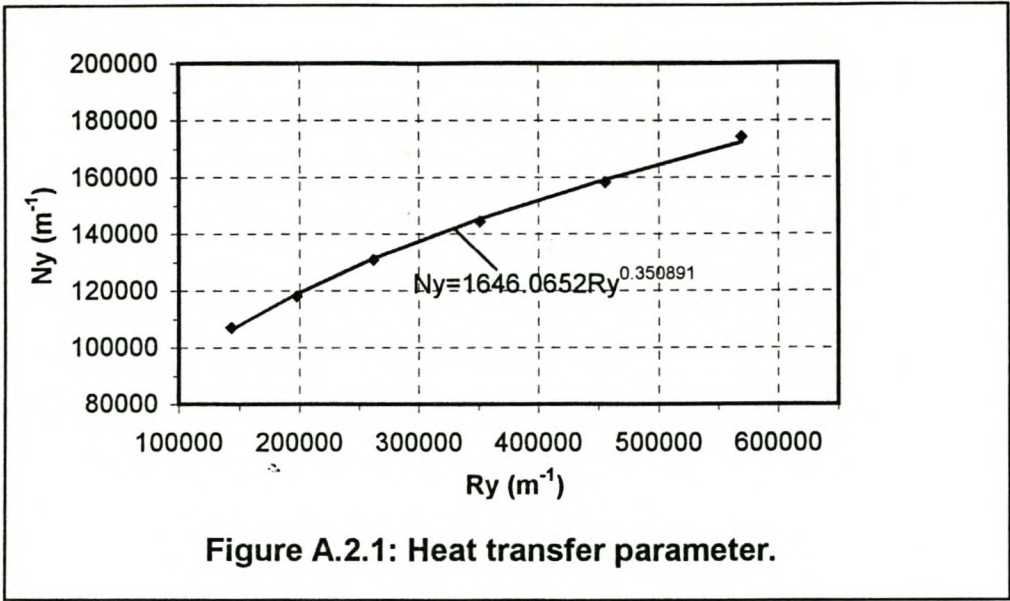


Table A.3.1: Tube specifications.

Name: AE-2.4 (2.4 mm fin pitch, 0.50417 mm fin thickness)

No	Tube mass,kg	No. of fins	L_t ,mm	P_f ,mm
1	3.845	193	468	2.425
2	3.845	192	468	2.438
3	3.785	193	470	2.435
4	3.865	193	468	2.425
5	3.835	192	470	2.448
6	3.87	193	470	2.435
7	3.835	192	468	2.438
8	3.86	192	468	2.438
9	3.835	193	470	2.435
10	3.895	193	469	2.430
Average	3.847	192.6	468.9	2.4345909

Table A.3.2a: Test data.

Run no.	T_{ai} °C	T_{ao} °C	T_{wi} °C	T_{wo} °C	P_{atm} N/m ²	m_a kg/s	m_w kg/s
1	28.35868	37.0178	60.94835	58.32739	100088.06	2.4879917	2.009746111
2	29.02352	38.57636	61.03271	58.67113	100077.23	1.9857809	2.003994642
3	29.47976	40.48772	61.16273	59.0604	100069.8	1.5432355	2.011583053
4	29.51082	42.52892	61.2469	59.39182	100069.3	1.1484482	1.998794526
5	29.76281	44.84549	61.493	59.90401	100065.19	0.858496	2.003603695
6	29.84254	46.68411	61.4953	60.10833	100063.89	0.676669	1.988474838

Table A.3.2b: Test data.

Run no.	Δp_{bundle} N/m ²	Δp_n N/m ²	Δp_{up} N/m ²
1	411	437	1286
2	286.5	752	854
3	190	454	534
4	118	252	308
5	75	142	182
6	53	89	120

Table A.3.3: Pressure drops for isothermal tests.

($P_{atm} = 100450$ N/m², $T_{aiwb} = 25^\circ\text{C}$, $T_{aidb} = 25^\circ\text{C}$)

Run no.	Δp_{bundle} N/m ²	Δp_n N/m ²	Δp_{up} N/m ²
1	416.5	446	1320
2	278	738	832
3	189	458	533
4	119	256	310
5	78.5	148	187

Table A.3.4a: Test results.

Run no	LMTD °C	F _T ---	Q _a W	Q _w W	Q _w /Q _a ---	%error %
1	26.83680248	0.9584434	22151.902	22103.588	0.9978189	0.218106
2	25.88607172	0.9601778	19502.112	19866.228	1.0186706	-1.867059
3	24.86302887	0.9613991	17463.068	17760.2	1.0170148	-1.701483
4	23.86656541	0.9631467	15369.696	15579.971	1.0136812	-1.368117
5	22.73149989	0.9665464	13311.345	13387.441	1.0057166	-0.571656
6	21.62681115	0.9696059	11716.025	11605.561	0.9905716	0.942841

Table A.3.4b: Test results.

Run no.	Re _w ---	h _w W/m ² K	Ry m ⁻¹	Ny m ⁻¹	K _{he}
1	84093.32779	9025.1597	572861.24	171780.43	8.2406326
2	84128.36029	9015.5347	455914.62	154523.78	8.9851654
3	84782.99946	9058.7982	353252.93	142369.65	9.8287332
4	84511.55686	9022.0805	262222.48	128973.72	10.98527
5	85204.96741	9061.4643	195399.4	115514.51	12.443564
6	84694.28324	9009.7728	153656.25	105677.36	14.110631

Correlating equations: $Ny = 1426.4684Ry^{0.360576}$
 $K_{he} = 1664.625Ry^{-0.4011}$

Table A.3.5: Isothermal test results.

Run no.	Ry m ⁻¹	K _{heiso}
1	600748.8212	8.0990687
2	471547.1426	8.7740578
3	372600.158	9.5539214
4	279189.3667	10.714086
5	212291.8196	12.22388

Correlating equation: $K_{heiso} = 1510.285Ry^{-0.393805}$

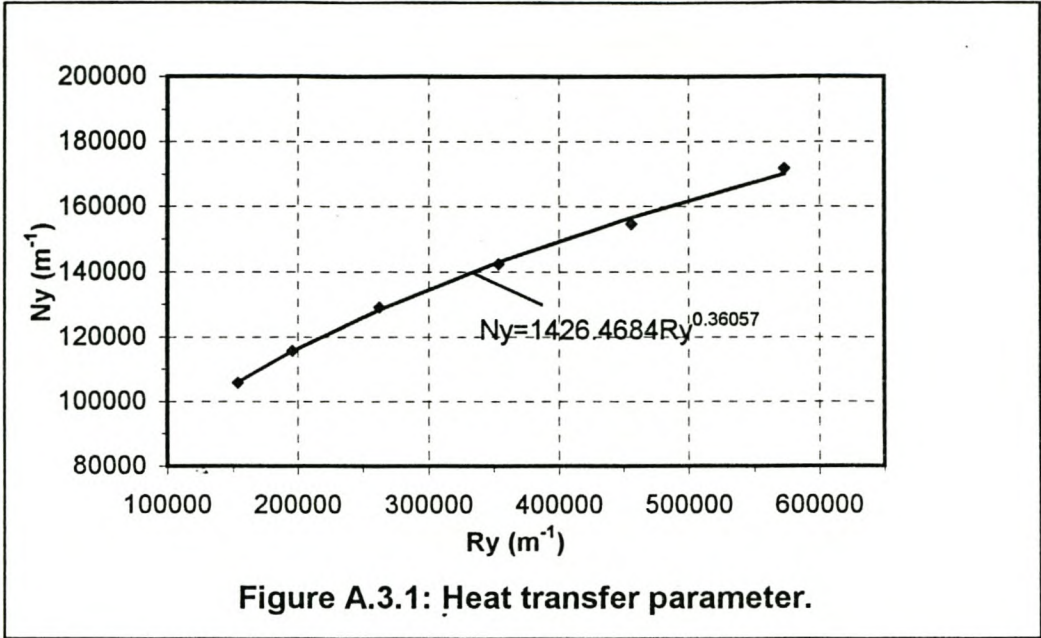


Figure A.3.1: Heat transfer parameter.

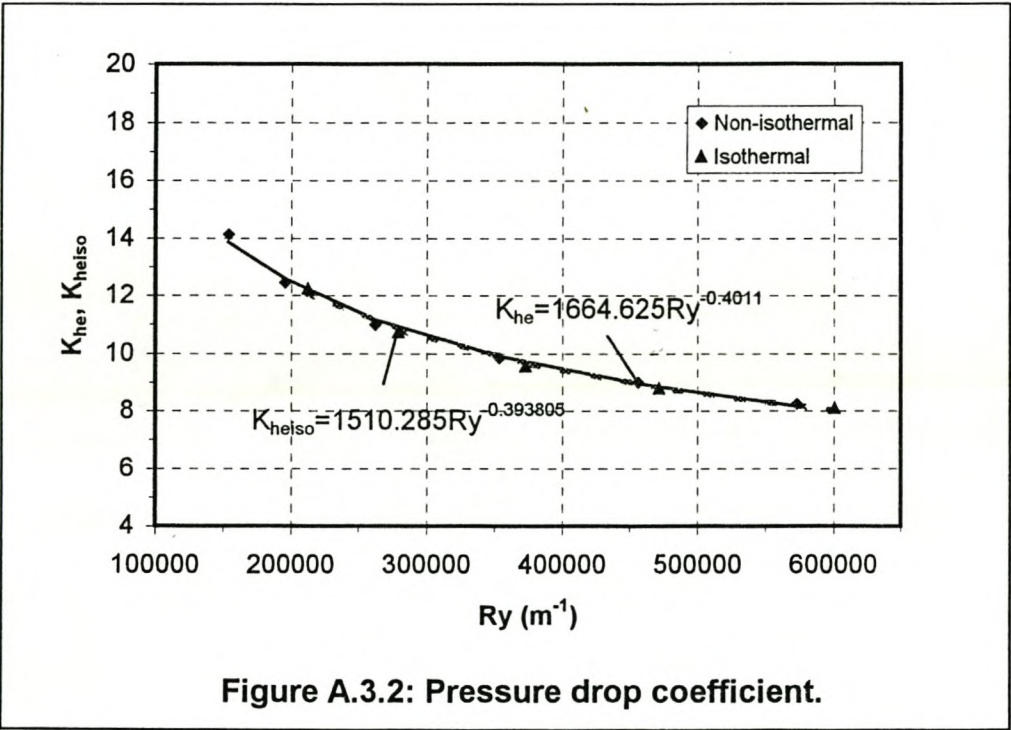


Figure A.3.2: Pressure drop coefficient.

Table A.4.1: Tube specifications.

Name: AE-2.5 (2.5 mm fin pitch, 0.5252 mm fin thickness)

No	Tube mass,kg	No. of fins	L_t ,mm	P_f ,mm
1	3.785	187	469	2.5080
2	3.79	187	467	2.4973
3	3.815	187	467	2.4973
4	3.805	187	466	2.4920
5	3.72	187	470	2.5134
6	3.73	188	469	2.4947
7	3.715	187	467	2.4973
8	3.71	187	467	2.4973
9	3.705	187	467	2.4973
10	3.72	187	469	2.5080
Average	3.7495	187.1	467.8	2.5002702

Table A.4.2a: Test data.

Run no.	T_{ai} °C	T_{ao} °C	T_{wi} °C	T_{wo} °C	p_{atm} N/m ²	m_a kg/s	m_w kg/s
1	28.61717	37.51778	62.65179	59.89692	99844.965	2.4999128	1.971599974
2	28.60199	38.77568	62.45247	60.02759	99845.211	1.9946626	1.991749573
3	28.61008	40.38286	62.63118	60.45633	99845.08	1.5332256	1.982006204
4	28.43224	42.3869	62.74792	60.81269	99847.97	1.1534004	1.982771951
5	28.30862	44.36552	62.67126	60.9669	99849.979	0.8879161	1.956566806
6	27.90576	46.8413	62.82766	61.33433	99856.525	0.6504746	1.965057332

Table A.4.2b: Test data.

Run no.	Δp_{bundle} N/m ²	Δp_n N/m ²	Δp_{up} N/m ²
1	398.5	440	1275
2	277	756	844
3	181	446	518
4	114	253	304
5	76	151	190
6	48	82	110

Table A.4.3: Pressure drops for isothermal tests.

($P_{atm} = 100010 \text{ N/m}^2$, $T_{aiwb} = 22.5^\circ\text{C}$, $T_{aidb} = 28^\circ\text{C}$)

Run no.	Δp_{bundle} N/m ²	Δp_n N/m ²	Δp_{up} N/m ²
1	401	449	1302
2	275	764	848
3	179	453	520
4	112	254	302
5	75	155	191
6	45	80	104

Table A.4.4a: Test results.

Run no	LMTD °C	F _T ---	Q _a W	Q _w W	Q _w /Q _a ---	%error %
1	28.09433824	0.9589205	22659.027	22595.246	0.9971852	0.2814792
2	27.36783627	0.9619296	20666.23	20075.477	0.9714146	2.858539
3	26.76005056	0.9636161	18382.988	17904.27	0.9739587	2.6041331
4	25.90642774	0.9652182	16393.787	15923.402	0.9713071	2.8692855
5	24.79186633	0.9676208	14522.956	13822.497	0.9517688	4.8231162
6	23.64276977	0.9706595	12549.22	12147.414	0.9679816	3.2018416

Table A.4.4b: Test results.

Run no.	Re _w ---	h _w W/m ² K	Ry m ⁻¹	Ny m ⁻¹	K _{he}
1	84578.12287	8971.5453	571375.79	166964.42	7.9382045
2	85398.23932	9046.4515	455207.66	154331.36	8.6497517
3	85370.50143	9026.0089	349214.03	138611.3	9.5408682
4	85707.75249	9041.8831	262132.79	126233.53	10.586997
5	84624.25133	8943.7275	201349.83	115646.5	11.873808
6	85325.82056	8990.4399	147151.61	103375.31	13.926268

Correlating equations:

$$Ny = 1556.625Ry^{0.352482}$$

$$K_{he} = 1168.125Ry^{-0.37809}$$

Table A.4.5: Isothermal test results.

Run no.	Ry m ⁻¹	K _{heiso}
1	593021.2925	7.7447379
2	471883.865	8.388134
3	364581.4855	9.1467484
4	273596.2732	10.162501
5	213729.9005	11.151509
6	153253.4224	13.013529

Correlating equation:

$$K_{heiso} = 1168.125Ry^{-0.37809}$$

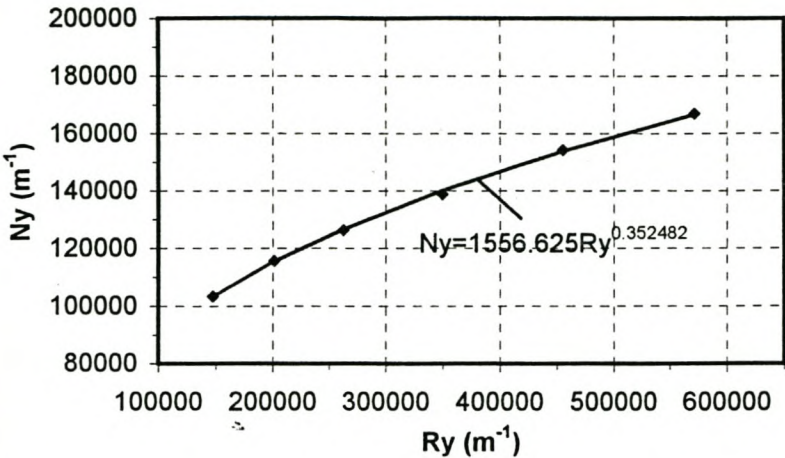


Figure A.4.1: Heat transfer parameter.

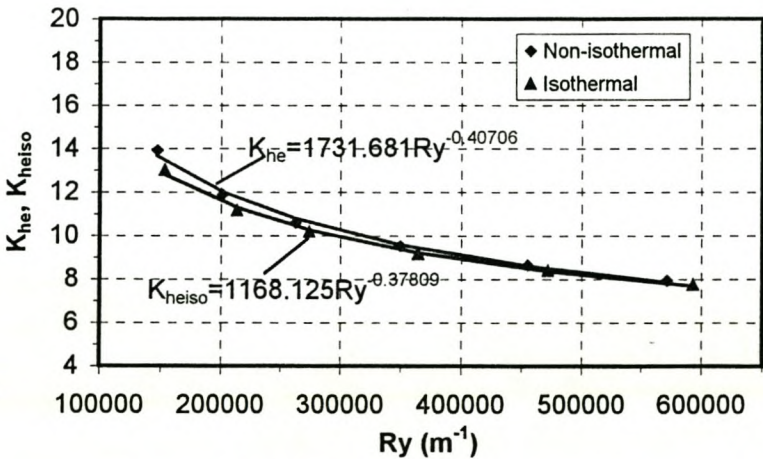


Figure A.4.2: Pressure drop coefficient.

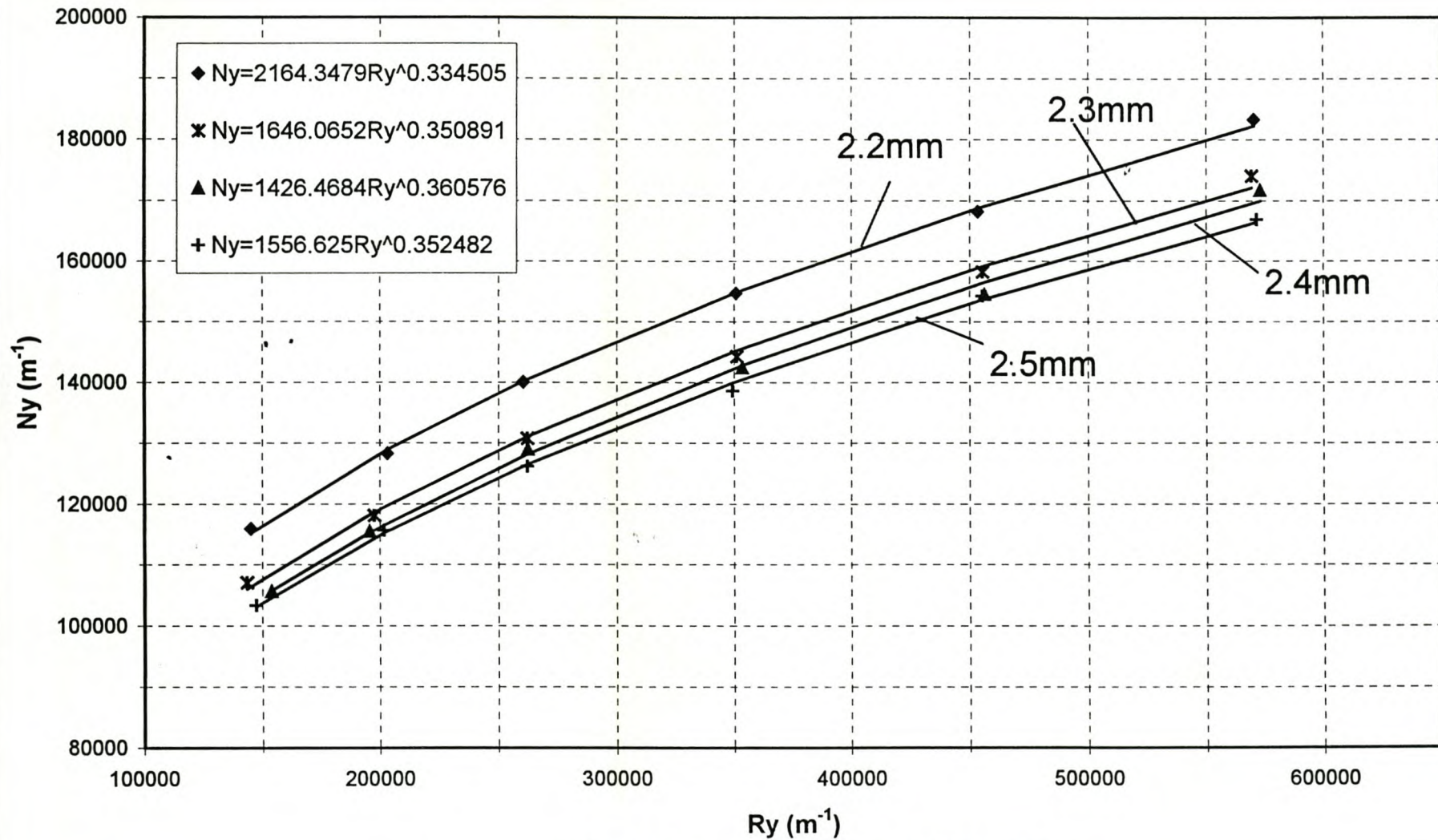


Figure A.5: Heat transfer parameter.

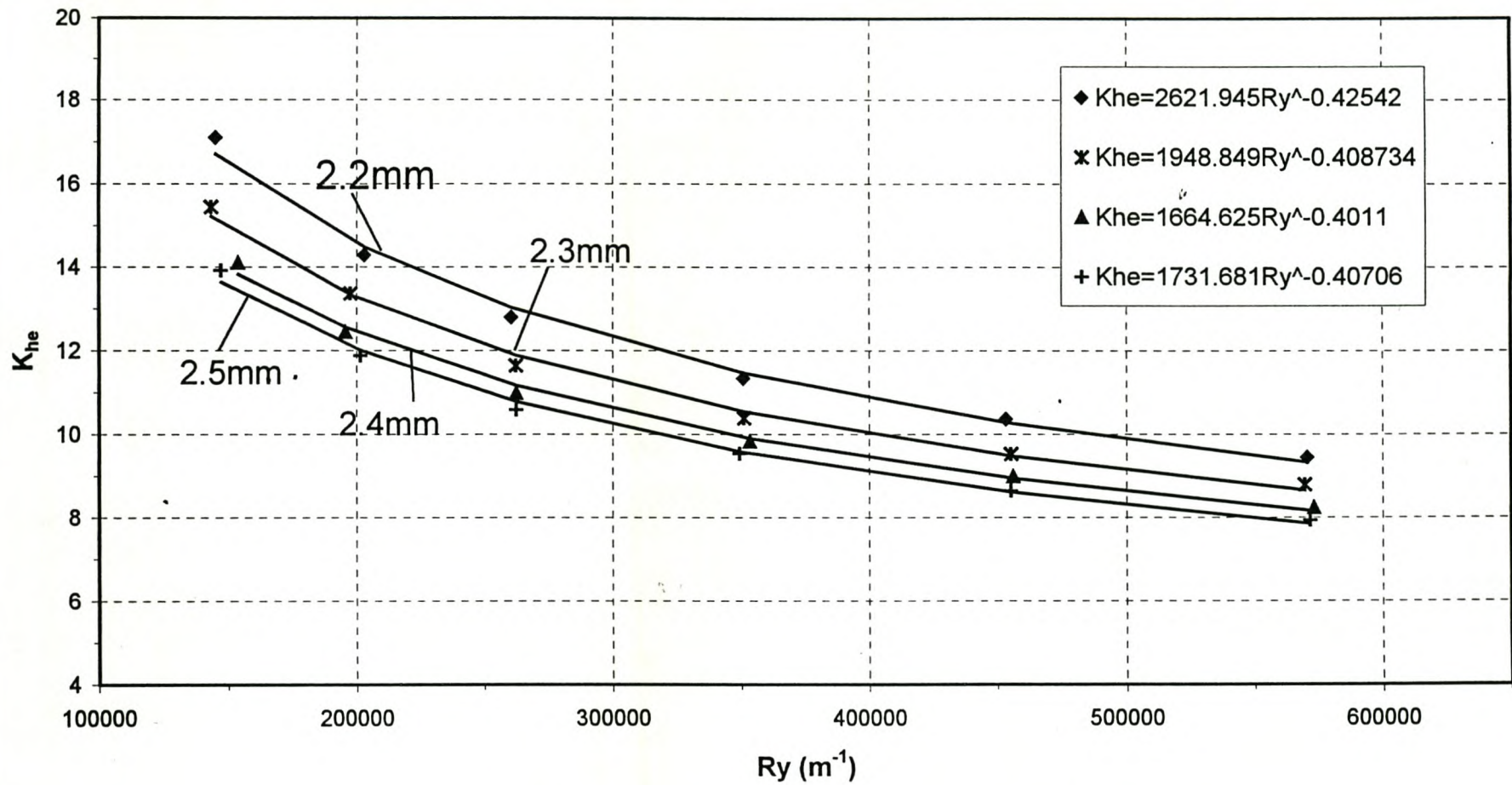


Figure A.6: Non-isothermal pressure drop.

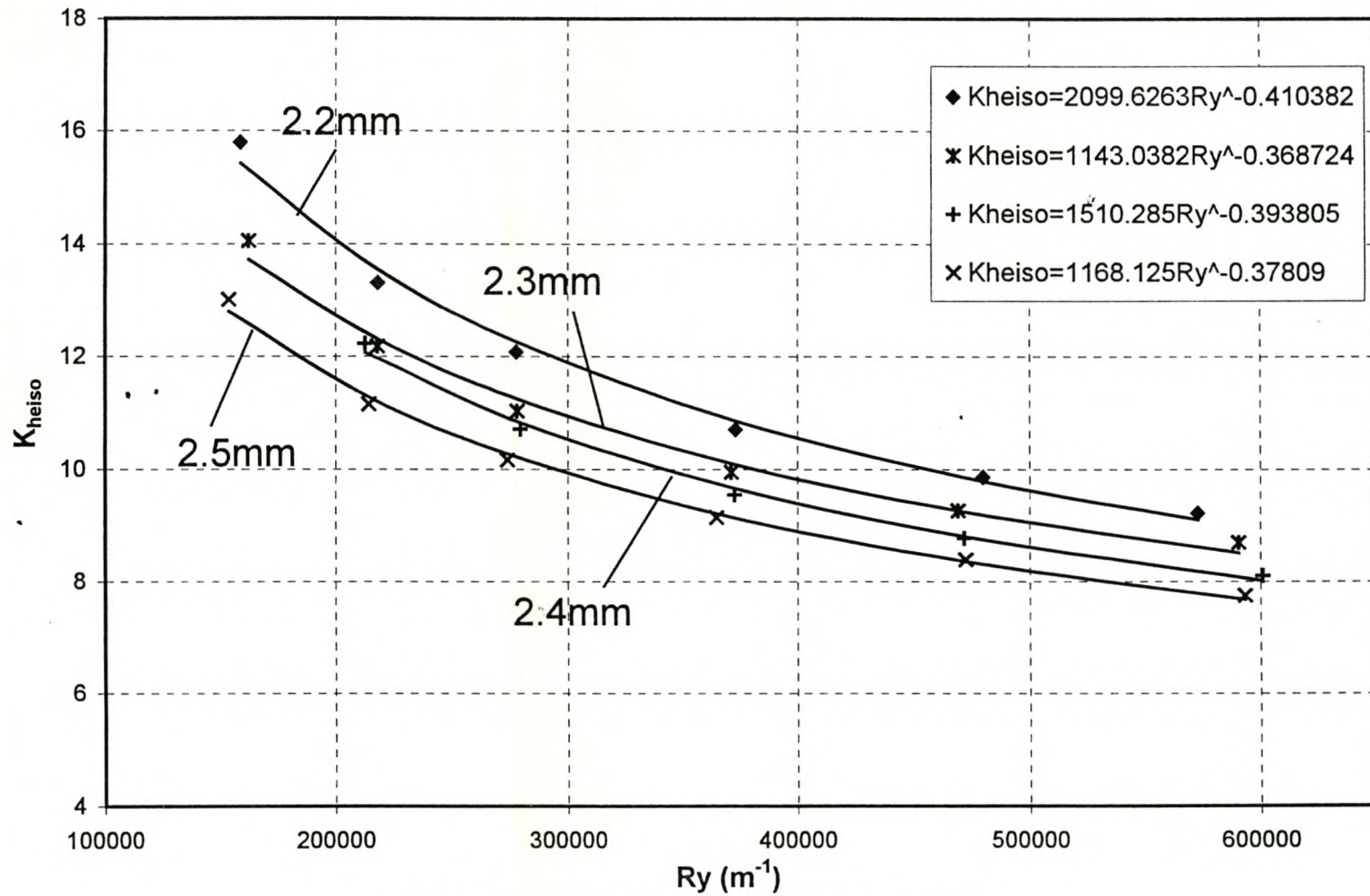


Figure A.7: Isothermal pressure drop.

Testing heat exchanger bundle at different water flow rates.

Table A.5.1a: Test data.

Name: AE-2.4 (2.4 mm fin pitch, 0.50417 mm fin thickness)

Run no.	T_{ai} °C	T_{ao} °C	T_{wi} °C	T_{wo} °C	P_{atm} N/m ²	m_a kg/s	m_w kg/s
1	27.11008	41.24413	60.69384	59.38481	100048.66	1.1558117	3.1432124
2	27.39349	41.30084	60.76997	59.19934	100044.05	1.1557197	2.5665074
3	27.94464	41.42713	60.62866	58.80418	100035.08	1.155517	2.1108332
4	28.67481	41.75583	60.76402	58.63624	100023.19	1.1572083	1.7496198
5	29.24338	41.97449	61.02282	58.51398	100013.94	1.1522899	1.4503038

Table A.5.1b: Test data.

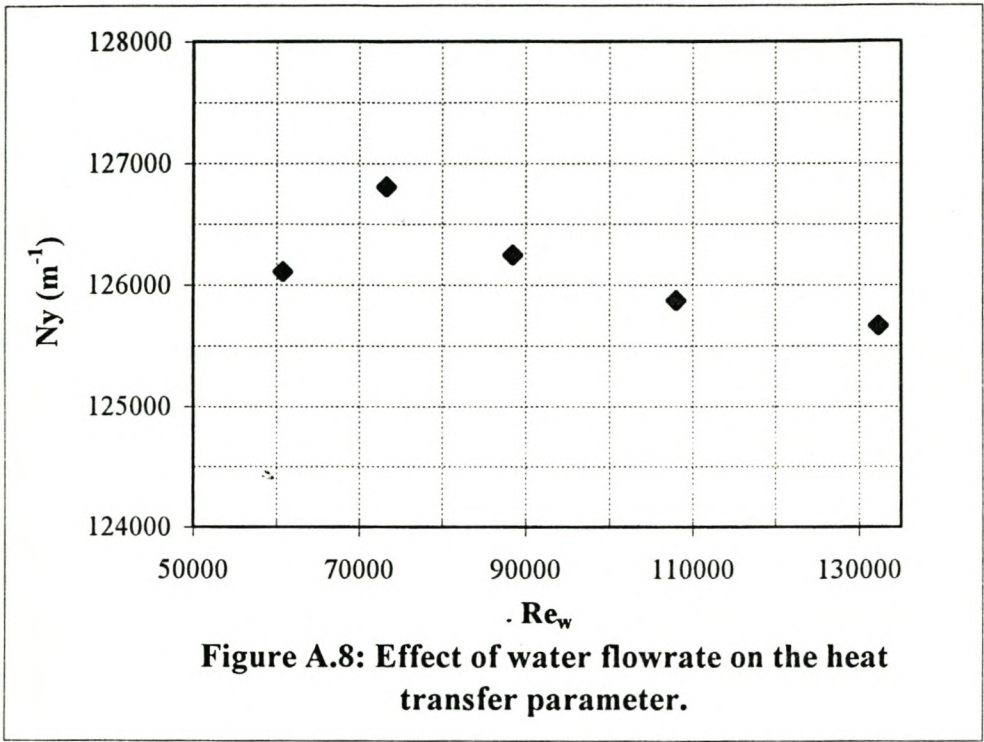
Run no.	Δp_{bundle} N/m ²	Δp_n N/m ²	Δp_{up} N/m ²
1	118	254	310
2	118	254	310
3	118	254	309
4	118	255	310
5	117	253	309

Table A.5.2a: Test results.

Run no.	LMTD °C	F_T ---	Q_a W	Q_w W	Q_w/Q_a ---	%error %
1	25.321537	0.9949909	16768.073	16952.775	1.0110151	-1.101507
2	25.133255	0.9938396	16496.348	16651.412	1.0093999	-0.939991
3	24.56972	0.9925507	15986.84	15936.335	0.9968408	0.3159188
4	24.069355	0.9909735	15530.04	15429.447	0.9935226	0.6477355
5	23.793178	0.9891201	15047.752	15102.257	1.0036222	-0.362219

Table A.5.2b: Test results.

Run no.	Re_w ---	h_w W/m ² K	R_y m ⁻¹	N_y m ⁻¹
1	132332.06	13173.928	264833.6	125666.84
2	107961.97	11105.96	264685.28	125872.01
3	88429.62	9409.2413	264386.72	126246.72
4	73278.91	8037.542	264388.16	126805.98
5	60806.358	6870.4	262978.24	126108.99



From the above figure, it is noticed that there is less than 1% variation on the Ny -value when testing at different water flow rates.

APPENDIX B

Sample calculation for determining the heat transfer characteristics for a single pass air-cooled heat exchanger bundle

Sample calculation for determining the heat transfer characteristics of a heat exchanger bundle.

Finned tube bundle specification (2.4mm fin pitch).

The following sample calculation shows how the heat transfer characteristics for the elliptical tube air-cooled heat exchanger bundle, consisting of one tube-pass, single tube row, is determined.

Test Data: Run no.3 in Appendix A (Table A.5)

The finned tube bundle specifications used for this test are:

Bundle width: W_b	0.47 m
Bundle height: H_b	0.50 m
Number of tubes per row: n_{tr}	10.0
Number of rows: n_r	1.00
Frontal area: A_{fr}	0.235 m ²
Tube length per pass: L_t	0.47 m
Tube length along all passes: L	4.70 m

(for waterside heat transfer coefficient)

Hydraulic diameter: d_e	0.0259221 m
Waterside surface area per tube: A_w	0.096464 m ²

(for determination of air mass flowrate)

Nozzle diameter: d_n	0.2509 m
Windtunnel upstream cross-section: A_{tus}	1.44 m ²

Table B.1 below shows temperature as well as pressure readings used for this sample calculation.

Table B.1: Test data.

T_{ai} °C	T_{ao} °C	T_{wi} °C	T_{wo} °C
27.94464	41.42713	60.62866	58.80418
p_{meas} Pa	Δp_{bundle} Pa	Δp_n Pa	Δp_{up} Pa
100490	118	254	309

The wetbulb temperature of the inlet air is, $T_{aiwb} = 26.5^\circ\text{C}$

A corrected ambient pressure value is given by the following equation from the barometer used.

$$p_{amb} = p_{meas} - 0.000162 \times p_{meas} \times T_{ai} = 100035.154 \text{ N/m}^2$$

Hence pressure upstream of the nozzle is

$$p_u = p_{amb} - \Delta p_{up} = 100035.154 - 309 = 99726.154 \text{ N/m}^2$$

The following thermophysical properties of the airstream are required to determine air mass flowrate through the flow nozzles in the windtunnel.

Water vapour pressure at 26.5°C (299.65°K) from Kröger [98KR1],

$$\begin{aligned} z &= 10.79586\left(1 - \frac{273.16}{T}\right) + 5.02808 \log_{10}\left(\frac{273.16}{T}\right) + 1.50474 \times 10^{-4} \left[1 - 10^{-8.29692\left(\frac{T}{273.16} - 1\right)}\right] \\ &\quad + 4.2873 \times 10^{-4} \left[10^{4.76955\left(1 - \frac{273.16}{T}\right)} - 1\right] + 2.786118312 \\ &= 10.79586\left(1 - \frac{273.16}{299.65}\right) + 5.02808 \log_{10}\left(\frac{273.16}{299.65}\right) + 1.50474 \times 10^{-4} \left[1 - 10^{-8.29692\left(\frac{299.65}{273.16} - 1\right)}\right] \\ &\quad + 4.2873 \times 10^{-4} \left[10^{4.76955\left(1 - \frac{273.16}{299.65}\right)} - 1\right] + 2.786118312 \\ &= 3.53922 \end{aligned}$$

Therefore,

$$p_v = 10^z = 10^{3.53922} = 3461.16 \text{ N/m}^2$$

Humidity ratio is calculated using the following equation

$$w = \frac{\left[\{2501.6 - 2.3263(T_{wb} - 273.15)\} x \left\{ \frac{0.62509 p_{vwb}}{p_{abs} - 1.005 p_{vwb}} \right\} - 1.00416(T - T_{wb}) \right]}{[2501.6 + 1.8577(T - 273.15) - 4.184(T_{wb} - 273.15)]}$$

$$= \frac{\left[\{2501.6 - 2.3263(299.65 - 273.15)\} \times \left\{ \frac{0.62509 \times 3461.16}{100035.154 - 1.005 \times 3461.16} \right\} - 1.00416(301.09 - 299.65) \right]}{[2501.6 + 1.8577(301.09 - 273.15) - 4.184(299.65 - 273.15)]}$$

$$= 0.0223824 \text{ kg/kg dry air}$$

Air density after bundle and before nozzle at 314.577 °K is

$$\begin{aligned} \rho_{ao} &= (1 + w) \left\{ 1 - \frac{w}{w + 0.62198} \right\} \times \frac{P_u}{287.08T} \\ &= (1 + 0.0223824) \left\{ 1 - \frac{0.0223824}{0.0223824 + 0.62198} \right\} \times \frac{99726.154}{287.08 \times 314.577} \\ &= 1.089779 \text{ kg/m}^3 \end{aligned}$$

Dynamic viscosity of dry air is

$$\begin{aligned} \mu_{ao} &= 2.287973 \times 10^{-6} + 6.259793 \times 10^{-8} T - 3.131956 \times 10^{-11} T^2 \\ &\quad + 8.15038 \times 10^{-15} T^3 \\ &= 2.287973 \times 10^{-6} + 6.259793 \times 10^{-8} (314.577) - 3.131956 \times 10^{-11} (314.577)^2 \\ &\quad + 8.15038 \times 10^{-15} (314.577)^3 = 1.9134 \times 10^{-5} \text{ kg/ms} \end{aligned}$$

Dynamic viscosity of water vapour in air,

$$\begin{aligned} \mu_{vo} &= 2.562435 \times 10^{-6} + 1.816683 \times 10^{-8} T + 2.579066 \times 10^{-11} T^2 - 1.067299 \times 10^{-14} T^3 \\ &= 2.562435 \times 10^{-6} + 1.816683 \times 10^{-8} (314.577) + 2.579066 \times 10^{-11} (314.577)^2 \\ &\quad - 1.067299 \times 10^{-14} (314.577)^3 = 1.04973 \times 10^{-5} \text{ kg/ms} \end{aligned}$$

Calculating the dynamic viscosity of the air-vapour mixtures,

$$X_a = \frac{1}{1 + 1.608w} = \frac{1}{1 + 1.608 \times 0.0223824} = 0.965259$$

$$X_v = \frac{w}{w + 0.622} = \frac{0.0223824}{0.0223824 + 0.622} = 0.0347347$$

with these values, the dynamic viscosity of the air-vapour mixtures is

$$\begin{aligned}\mu_{avo} &= \frac{X_a \mu_{ao} M_a^{0.5} + X_v \mu_{vo} M_v^{0.5}}{X_a M_a^{0.5} + X_v M_v^{0.5}} \\ &= \frac{0.965259 \times 1.9134 \times 10^{-5} \times 28.97^{0.5} + 0.0347347 \times 1.04973 \times 10^{-5} \times 18.016^{0.5}}{0.965259 \times 28.97^{0.5} + 0.0347347 \times 18.016^{0.5}} \\ &= 1.8895 \times 10^{-5} \text{ kg/ms}\end{aligned}$$

where $M_a = 28.97 \text{ kg/mole}$, $M_v = 18.016 \text{ kg/mole}$, $X_a = 1 / (1 + 1.608w)$ and $X_v = w / (w + 0.622)$

For this particular test, only one nozzle was open in the windtunnel. The air mass flow is given by equation (3.3.1)

$$m_a = C_n \phi_g Y \pi d_n^2 (2 \rho_{avo} \Delta p_n)^{0.5} / 4$$

The gas expansion factor is given by equation (3.3.3)

$$\begin{aligned}\phi_g &= 1 - \frac{3 \Delta p_n}{(4 p_{up} \frac{c_p}{c_v})} \\ &= 1 - \frac{3 \times 254}{(4 \times 99726.154 \times 1.4)} = 0.99864\end{aligned}$$

For a compressible fluid, it can be shown that the approach velocity factor is approximately,

$$\begin{aligned}Y &= 1 + 0.5(A_n / A_{tus})^2 + 2(A_n / A_{tus})^2 \Delta p_n / (p_{up} \frac{c_p}{c_v}) \\ &= 1 + 0.5\left(\frac{\pi \times 0.2509^2}{4 \times 1.44}\right)^2 + 2\left(\frac{\pi \times 0.2509^2}{4 \times 1.44}\right)^2 \times \frac{254}{99726.154 \times 1.4} = 1.000594\end{aligned}$$

The nozzle coefficient of discharge is a function of the nozzle Reynolds number. Initially, assume $C_n = 1$.

Therefore, air mass flowrate

$$m_a = 1 \times 0.99864 \times 1.000594 \times \pi \times 0.2509^2 (2 \times 1.089779 \times 254)^{0.5} / 4 = 1.1624 \text{ kg/s}$$

and the nozzle Re number

$$Re_n = \frac{4m_a}{\pi d_n \mu_{avo}} = \frac{4 \times 1.1624}{\pi \times 0.2509 \times 1.8895 \times 10^{-5}} = 312192.06$$

Since $100000 < Re_n < 350000$, use equation. (3.3.2b) to find a new C_n .

$$\begin{aligned} C_n &= 0.9758 + 1.08 \times 10^{-7} (312675.3) - 1.6 \times 10^{-13} (312675.3)^2 \\ &= 0.993926 \end{aligned}$$

A calculated new air mass flowrate is:

$$m_a = 0.993926 \times 1.1624 = 1.15534 \text{ kg/s}$$

As before, a new Re_n is calculated. Using equation. (3.3.2), a new coefficient of discharge, C_n is again calculated. This is an iterative procedure to find C_n . The ultimate converged value of $C_n = 0.993901$ and the corresponding air mass flow $m_a = 1.155326 \text{ kg/s}$.

Evaluate the arithmetic mean temperature of the air,

$$T_{am} = (T_{ai} + T_{ao}) / 2 = (301.09 + 314.577) / 2 = 307.8335 \text{ K}$$

The specific heat of dry air is found using

$$\begin{aligned} c_{pa} &= 1045.356 - 3.161783 \times 10^{-1} T + 7.083814 \times 10^{-4} T^2 - 2.705209 \times 10^{-7} T^3 \\ &= 1045.356 - 3.161783 \times 10^{-1} (307.8335) + 7.083814 \times 10^{-4} (307.8335)^2 \\ &\quad - 2.705209 \times 10^{-7} (307.8335)^3 = 1007.262 \text{ J/kgK} \end{aligned}$$

Dynamic viscosity of dry air is

$$\begin{aligned}\mu_a &= 2.287973 \times 10^{-6} + 6.259793 \times 10^{-8} T - 3.131956 \times 10^{-11} T^2 + 8.15038 \times 10^{-15} T^3 \\ &= 2.287973 \times 10^{-6} + 6.259793 \times 10^{-8} (307.8335) - 3.131956 \times 10^{-11} (307.8335)^2 \\ &\quad + 8.15038 \times 10^{-15} (307.8335)^3 = 1.88276 \times 10^{-5} \text{ kg/ms}\end{aligned}$$

Thermal conductivity of dry air is similarly calculated using the following equation

$$\begin{aligned}k_a &= -4.937787 \times 10^{-4} + 1.018087 \times 10^{-4} T - 4.627937 \times 10^{-8} T^2 + 1.250603 \times 10^{-11} T^3 \\ &= -4.937787 \times 10^{-4} + 1.018087 \times 10^{-4} (307.8335) - 4.627937 \times 10^{-8} (307.8335)^2 \\ &\quad + 1.250603 \times 10^{-11} (307.8335)^3 = 2.68257 \times 10^{-2} \text{ W/mK}\end{aligned}$$

Now, evaluating properties of water vapour in air at 307.8335 °K.

Specific heat of water vapour is

$$\begin{aligned}c_{pv} &= 1.3605 \times 10^3 + 2.31334 T - 2.46784 \times 10^{-10} T^5 + 5.91332 \times 10^{-13} T^6 \\ &= 1.3605 \times 10^3 + 2.31334 (307.8335) - 2.46784 \times 10^{-10} (307.8335)^5 + 5.91332 \times 10^{-13} \\ &\quad \times (307.8335)^6 = 1893.63 \text{ J / kgK}\end{aligned}$$

Dynamic viscosity of water vapour is

$$\begin{aligned}\mu_v &= 2.562435 \times 10^{-6} + 1.816683 \times 10^{-8} T + 2.579066 \times 10^{-11} T^2 - 1.067299 \times 10^{-14} T^3 \\ &= 2.562435 \times 10^{-6} + 1.816683 \times 10^{-8} (307.8335) + 2.579066 \times 10^{-11} (307.8335)^2 \\ &\quad - 1.067299 \times 10^{-14} (307.8335)^3 = 1.02874 \times 10^{-5} \text{ kg/ms}\end{aligned}$$

Thermal conductivity of water vapour is calculated using

$$\begin{aligned}k_v &= 1.3046 \times 10^{-2} - 3.756191 \times 10^{-5} T + 2.217964 \times 10^{-7} T^2 - 1.111562 \times 10^{-10} T^3 \\ &= 1.3046 \times 10^{-2} - 3.756191 \times 10^{-5} (307.8335) + 2.217964 \times 10^{-7} (307.8335)^2 \\ &\quad - 1.111562 \times 10^{-10} (307.8335)^3 = 1.9258 \times 10^{-2} \text{ W/mK}\end{aligned}$$

Finally, properties of air containing water vapour at 307.8335 °K are:

Specific heat of air is

$$c_{pav} = \frac{(c_{pa} + w c_{pv})}{(1 + w)} = \frac{(1007.262 + 0.0223824 \times 1893.63)}{(1 + 0.0223824)} = 1026.667 \text{ J/kgK}$$

Thermal conductivity of air is

$$k_{av} = \frac{(X_a k_a M_a^{0.33} + X_v k_v M_v^{0.33})}{(X_a M_a^{0.33} + X_v M_v^{0.33})}$$

$$= \frac{(0.965259 \times 2.68257 \times 10^{-2} \times 28.97^{0.33} + 0.0347347 \times 1.9258 \times 10^{-2} \times 18.016^{0.33})}{(0.965259 \times 28.97^{0.33} + 0.0347347 \times 18.016^{0.33})}$$

$$= 2.6599 \times 10^{-2} \text{ W/mK}$$

Dynamic viscosity of air is found using

$$\mu_{av} = \frac{(X_a \mu_a M_a^{0.5} + X_v \mu_v M_v^{0.5})}{(X_a M_a^{0.5} + X_v M_v^{0.5})}$$

$$= \frac{(0.965259 \times 1.88276 \times 10^{-5} \times 28.97^{0.5} + 0.0347347 \times 1.02874 \times 10^{-5} \times 18.016^{0.5})}{(0.965259 \times 28.97^{0.5} + 0.0347347 \times 18.016^{0.5})}$$

$$= 1.859 \times 10^{-5} \text{ J/kgK}$$

Prandtl number of the air is given by,

$$Pr_{av} = \frac{\mu_{av} c_{pav}}{k_{av}} = \frac{1.859 \times 10^{-5} \times 1026.667}{2.6599 \times 10^{-2}} = 0.71761$$

Properties of water stream evaluated at the arithmetic mean temperature,

$$T_{wm} = (T_{wi} + T_{wo}) / 2 = (333.77866 + 331.95418) / 2 = 332.866 \text{ K}$$

Density of water is found using the following equation

$$\begin{aligned} \rho_w &= (1.49343 \times 10^{-3} - 3.7164 \times 10^{-6} T + 7.09782 \times 10^{-9} T^2 - 1.90321 \times 10^{-20} T^6)^{-1} \\ &= (1.49343 \times 10^{-3} - 3.7164 \times 10^{-6} (332.866) + 7.09782 \times 10^{-9} (332.866)^2 - 1.90321 \times 10^{-20} \\ &\quad \times (332.866)^6)^{-1} = 983.366 \text{ kg/m}^3 \end{aligned}$$

Specific heat of water is

$$\begin{aligned} c_{pw} &= 8.15599 \times 10^3 - 2.80627 \times 10 T + 5.11283 \times 10^{-2} T^2 - 2.17582 \times 10^{-13} T^6 \\ &= 8.15599 \times 10^3 - 2.80627 \times 10 (332.866) + 5.11283 \times 10^{-2} (332.866)^2 - 2.17582 \times 10^{-13} \\ &\quad \times (332.866)^6 = 4183.91 \text{ J / kgK} \end{aligned}$$

Dynamic viscosity of water is

$$\begin{aligned} \mu_w &= 2.414 \times 10^{-5} \times 10^{\frac{247.8}{T-140}} = 2.414 \times 10^{-5} \times 10^{\frac{247.8}{332.866-140}} \\ &= 4.612 \times 10^{-4} \text{ kg/ms} \end{aligned}$$

Thermal conductivity of water is found from

$$\begin{aligned} k_w &= -6.14255 \times 10^{-1} + 6.9962 \times 10^{-3} T - 1.01075 \times 10^{-5} T^2 + 4.74737 \times 10^{-12} T^4 \\ &= -6.14255 \times 10^{-1} + 6.9962 \times 10^{-3} (332.866) - 1.01075 \times 10^{-5} (332.866)^2 \\ &\quad + 4.74737 \times 10^{-12} (332.866)^4 = 0.65292 \text{ W/mK} \end{aligned}$$

The Prandtl number of water is then found to be

$$Pr_w = \frac{\mu_w c_{pw}}{k_w} = \frac{4.612 \times 10^{-4} \times 4183.91}{0.65292} = 2.9805$$

The heat transferred to the air stream is given by equation (3.4.9)

$$Q_a = m_a c_{p_{av}} (T_{ao} - T_{ai}) = 1.155326 \times 1026.667 \times (314.577 - 301.09) = 15997.404 \text{ W}$$

Similarly, the heat removed from the water stream is given by

$$Q_w = m_w c_{p_w} (T_{wi} - T_{wo}) = 2.1108 \times 4183.91 \times (333.77866 - 331.95418) = 16112.71 \text{ W}$$

The two heat transfer values compare very well, i.e.

$$\frac{Q_a}{Q_w} = \frac{15997.404}{16112.71} = 0.99284$$

We now determine the waterside heat transfer coefficient. Firstly, calculating the waterside Reynolds number.

$$\text{Re}_w = \frac{m_w d_e}{A_{ts} \mu_w} = \frac{2.1108 \times 0.0259221}{1330.082 \times 10^{-6} \times 4.6512 \times 10^{-4}} = 88445.112$$

From equation (3.4.15), it follows for smooth tubes that the friction factor is

$$f_w = (1.82 \log_{10} \text{Re}_w - 1.64)^{-2} = (1.82 \log_{10} (88445.112) - 1.64)^{-2} = 0.018446$$

From the Gnielinski equation (3.4.14), with $L_t = 0.47\text{m}$, the water-side heat transfer coefficient is,

$$\begin{aligned} h_w &= \frac{k_w f_w (\text{Re}_w - 1000) \text{Pr}_w \left[1 + \left(\frac{d_e}{L_t} \right)^{0.67} \right]}{d_e \times 8 \left[1 + 12.7 \left(\frac{f_w}{8} \right)^{0.5} (\text{Pr}_w^{0.67} - 1) \right]} \\ &= \frac{0.65292 \times 0.018446 (88445.112 - 1000) \times 2.9805 \left[1 + \left(\frac{0.0259221}{0.47} \right)^{0.67} \right]}{0.0259221 \times 8 \left[1 + 12.7 \left(\frac{0.018446}{8} \right)^{0.5} (2.9805^{0.67} - 1) \right]} \\ &= 10404.68 \text{ W/m}^2 \text{ K} \end{aligned}$$

Furthermore, the logarithmic mean temperature difference (LMTD) is given by equation (3.4.8)

$$\Delta T_{lm} = \frac{(T_{wo} - T_{ai}) - (T_{wi} - T_{ao})}{\ln \left[\frac{(T_{wo} - T_{ai})}{(T_{wi} - T_{ao})} \right]}$$

$$= \frac{(331.95418 - 301.09) - (333.77866 - 314.577)}{\ln \left[\frac{(331.95418 - 301.09)}{(333.77866 - 314.577)} \right]} = 24.573K$$

The temperature correction factor as given by equation (3.4.10) is

$$F_T = 1 - \sum_{i=1}^4 \sum_{k=1}^4 a_{i,k} (1 - \phi_3)^k \sin \left[2i \arctan \left(\frac{\phi_1}{\phi_2} \right) \right] \quad (a)$$

$$\text{where } \phi_1 = \frac{T_{wi} - T_{wo}}{T_{wi} - T_{ai}} = \frac{60.62866 - 58.80418}{60.62866 - 27.94} = 0.05581$$

$$\phi_2 = \frac{T_{ao} - T_{ai}}{T_{wi} - T_{ai}} = \frac{41.427 - 27.94}{60.62866 - 27.94} = 0.4126$$

$$\phi_3 = \frac{\phi_1 - \phi_2}{\ln \left[\frac{(1 - \phi_2)}{(1 - \phi_1)} \right]} = \frac{0.05581 - 0.4126}{\ln \left[\frac{(1 - 0.4126)}{(1 - 0.05581)} \right]} = 0.75176$$

Substituting into equation (a) above, one obtains,

$$F_T = 1 - \sum_{i=1}^4 \sum_{k=1}^4 a_{i,k} (0.2482)^k \sin(2i(7.7033))$$

For crossflow with one tube row [98KR1] (using Table B.2)

Table B.2: Sixteen values of the empirical constant $a_{i,k}$.

$F_T = 1 - \sum$	$i = 1$	$i = 2$	$i = 3$	$i = 4$	
	-0.03046	-0.00398	-0.03118	-0.00917	$k = 1$
	0.08314	0.01669	0.05871	0.01881	$k = 2$
	-0.06377	-0.01856	-0.03235	-0.01147	$k = 3$
	<u>0.01734</u>	<u>0.006182</u>	<u>0.00453</u>	<u>0.002167</u>	<u>$k = 4$</u>
	0.00625	<u>0.006182</u>	<u>0.000633</u>	<u>0.000337</u>	<u>0.007552</u>

therefore $F_T = 1 - 0.007552 = 0.992448$

Upon substitution of equation (3.4.7) into equation (3.4.6) find

$$\begin{aligned}
 N_y &= \left\{ \left[\frac{F_T \Delta T_{lm}}{Q_a} - \frac{1}{h_w A_w} \right] A_{fr} k_{av} Pr_{av}^{0.333} \right\}^{-1} \\
 &= \left\{ \left[\frac{0.992448 \times 24.573}{15997.404} - (10404.68 \times 0.96464)^{-1} \right] \times 2.6599 \times 10^{-2} \times 0.71761^{0.333} \times 0.235 \right\}^{-1} \\
 &= 125398.862 \text{ m}^{-1}
 \end{aligned}$$

The corresponding characteristic flow parameter is according to equation (3.4.5)

$$Ry = \frac{m_a}{\mu_{av} A_{fr}} = \frac{1.155326}{1.859 \times 10^{-5} \times 0.235} = 2.6446 \times 10^5 \text{ m}^{-1}$$

APPENDIX C

Thermal-flow performance of C-2.5 and C-4.3 elliptical finned tubes

Table C.1.1: Tube specifications.

Name: C-2.5 (2.5 mm fin pitch, 0.6676 mm fin thickness)

No	Tube mass,kg	No. of fins	L_o ,mm	P_f ,mm
1	4.63	188	468	2.48936
2	4.7	191	470	2.46073
3	4.69	188	468	2.48936
4	4.72	188	468	2.48936
5	4.67	191	467	2.44503
6	4.79	189	468	2.47619
7	4.835	193	480	2.48705
8	4.69	189	469	2.48148
9	4.76	189	468	2.47619
10	4.735	189	470	2.48677
Average	4.722	189.5	469.6	2.4781526

Table C.1.2a: Test data.

Run no.	T_{ai} °C	T_{ao} °C	T_{wi} °C	T_{wo} °C	p_{atm} N/m ²	m_a kg/s	m_w kg/s
1	22.63694	35.46069	60.88855	58.01786	100450.27	2.4114289	2.5673188
2	22.74278	37.00472	60.97183	58.49038	100448.55	1.9983866	2.7362994
3	22.70082	39.07977	60.9907	58.78043	100449.23	1.5429923	2.7319314
4	22.34937	41.40487	61.09417	59.00447	100454.97	1.1567169	2.5795728
5	22.0392	44.14231	61.17526	59.39847	100460.04	0.854929	2.5767677
6	22.15795	46.48541	61.24638	59.69843	100458.1	0.6689474	2.5791408

Table C.1.2b: Test data.

Run no.	Δp_{bundle} N/m ²	Δp_n N/m ²	Δp_{up} N/m ²
1	547	404	1354
2	401	750	958
3	260	447	592
4	162	252	350
5	100	139	202
6	68	86	132

Table C.1.3: Pressure drops for isothermal tests.

($p_{atm} = 101430 \text{ N/m}^2$, $T_{aiwb} = 15^\circ\text{C}$, $T_{aidb} = 19^\circ\text{C}$)

Run no.	Δp_{bundle} N/m ²	Δp_n N/m ²	$\Delta \tilde{p}_{up}$ N/m ²
1	564	433	1425
2	392	755	954
3	250	443	580
4	156	245	347
5	101	150	213
6	61	79	119

Table C.1.4a: Test results.

Run no	LMTD °C	F _T ---	Q _a W	Q _w W	Q _w /Q _a ---	%error %
1	30.13090638	0.9564751	31442.12	30834.09	0.9806619	1.9338069
2	29.46590932	0.9608632	28978.869	28408.779	0.9803274	1.9672594
3	28.4088203	0.9630261	25698.099	25264.392	0.983123	1.6877041
4	27.29914972	0.9634797	22416.793	22554.668	1.0061505	-0.615053
5	25.87918025	0.9679135	19221.341	19157.203	0.9966632	0.3336818
6	24.40400448	0.9708886	16553.842	16705.725	1.0091751	-0.917508

Table C.1.4b: Test results.

Run no.	Re _w ---	h _w W/m ² K	Ry m ⁻¹	Ny m ⁻¹	K _{he}
1	107119.3103	11072.746	556126.26	220160.37	11.949575
2	114658.2384	11702.131	459919.53	203468.03	12.720941
3	114746.4968	11697.439	354227.47	184690.82	13.788712
4	108618.9239	11157.846	264928.35	166386.9	15.237687
5	108895.0306	11163.784	195241.93	148034.52	17.14994
6	109303.8378	11185.002	152307.21	133392.27	18.971854

Correlating equations:

$$Ny = 1413.3189Ry^{0.381476}$$

$$K_{he} = 1295.972Ry^{-0.354874}$$

Table C.1.5: Isothermal test results.

Run no.	Ry m ⁻¹	K _{heiso}
1	608310.4794	11.305539
2	490022.2449	12.10925
3	376688.2366	13.068888
4	280759.9983	14.67969
5	219739.4802	15.515577
6	159188.9651	17.85528

Correlating equation:

$$K_{heiso} = 979.4976Ry^{-0.335451}$$

Table C.2.1: Tube specifications.

Name: C-4.3 (4.3 mm fin pitch, 0.62383 mm fin thickness)

No	Tube mass,kg	No. of fins	L_t ,mm	P_f ,mm
1	3.24	109	463	4.24771
2	3.235	110	466	4.23636
3	3.26	110	466	4.23636
4	3.29	111	470	4.23423
5	3.23	110	470	4.27273
6	3.25	111	470	4.23423
7	3.225	109	470	4.31193
8	3.23	109	471	4.32110
9	3.285	111	471	4.24324
10	3.245	109	470	4.31193
Average	3.249	109.9	468.7	4.2649827

Table C.2.2a: Test data.

Run no.	T_{ai} °C	T_{ao} °C	T_{wi} °C	T_{wo} °C	p_{atm} N/m ²	m_a kg/s	m_w kg/s
1	23.90791	32.15374	62.732685	60.740225	100608.82	2.6455679	2.6408696
2	24.43415	33.67472	62.557835	60.789945	100600.21	2.0239515	2.5962942
3	23.41977	34.48564	62.702545	61.098195	100616.81	1.5587699	2.5659763
4	23.54864	36.54361	62.888465	61.579035	100614.7	1.153519	2.7679944
5	23.29122	38.31861	63.186735	62.030035	100618.91	0.8917813	2.7248441
6	23.63806	41.08453	63.224555	62.278015	100613.23	0.6263262	2.7080537

Table C.2.2b: Test data.

Run no.	Δp_{bundle} N/m ²	Δp_n N/m ²	Δp_{up} N/m ²
1	288	480	1250
2	179	758	746
3	114	448	450
4	69	246	253
5	45	148	156
6	25	74	81

Table C.2.3: Pressure drops for isothermal tests.

($p_{atm} = 100750 \text{ N/m}^2$, $T_{aiwb} = 21^\circ\text{C}$, $T_{aidb} = 26^\circ\text{C}$)

Run no.	Δp_{bundle} N/m ²	Δp_n N/m ²	Δp_{up} N/m ²
1	278	485	1278
2	170	743	740
3	109	456	462
4	68	252	262
5	44	152	160
6	26	79	86

Table C.2.4a: Test results.

Run no	LMTD °C	F _T ---	Q _a W	Q _w W	Q _w /Q _a ---	%error %
1	33.60872537	0.9823922	22169.363	22022.052	0.9933552	0.6644799
2	32.47629485	0.9825484	19003.755	19209.937	1.0108495	-1.084951
3	32.71998598	0.9824204	17533.16	17229.974	0.9827078	1.729215
4	31.83093291	0.9835946	15236.864	15170.651	0.9956544	0.4345555
5	31.29278531	0.9840678	13623.623	13193.08	0.9683973	3.1602694
6	29.62818508	0.9854135	11108.093	10729.771	0.9659417	3.4058294

Table C.2.4b: Test results.

Run no.	Re _w ---	h _w W/m ² K	Ry m ⁻¹	Ny m ⁻¹	K _{he}
1	114079.6738	11496.069	611476.7	129856.32	5.254843
2	112048.7172	11328.741	466557.47	114108.19	5.5616406
3	111117.5092	11232.655	359500.24	104086.49	5.9731223
4	120465.5305	11993.992	265310.77	91786.089	6.5780278
5	119252.206	11862.733	204739.91	82969.924	7.1597403
6	118769.6297	11811.16	143235.51	70657.235	8.022957

Correlating equations:

$$Ny = 536.9496Ry^{0.411508}$$

$$K_{he} = 269.315Ry^{-0.296708}$$

Table C.2.5: Isothermal test results.

Run no.	Ry m ⁻¹	K _{heiso}
1	623628.3068	4.9708387
2	471204.8223	5.3243425
3	370234.2651	5.5298047
4	275810.3367	6.216191
5	214200.2188	6.6688257
6	154119.4907	7.611929

Correlating equation:

$$K_{heiso} = 282.3795Ry^{-0.304296}$$

Table C.3.1a: Test data.

Name: B-4.3 & B-2.5 (4.3 mm and 2.5 mm fin pitch)

Run no.	T_{ai} °C	T_{ao} °C	T_{wi} °C	T_{wo} °C	P_{atm} N/m ²	m_a kg/s	m_w kg/s
1	24.01777	42.8982	60.79502	57.95466	100198.62	2.2342124	3.6239146
2	24.5186	44.52581	60.79723	58.2151	100190.46	1.9290934	3.603546
3	25.01257	46.95918	61.33446	59.05827	100182.41	1.5348638	3.5825708
4	25.08054	49.90852	61.77853	59.86683	100181.3	1.1351751	3.5750793
5	24.94244	52.51865	62.50963	60.92291	100183.55	0.8812734	3.5495136
6	25.20503	55.31199	62.89511	61.64023	100179.27	0.6432988	3.5717599

Table C.3.1b: Test data.

Run no.	Δp_{bundle} N/m ²	Δp_n N/m ²	Δp_{up} N/m ²
1	688	356	1394
2	540	718	1072
3	366	455	706
4	226	250	411
5	150	152	262
6	91.5	82	152

Table C.3.2: Pressure drops for isothermal tests.

($P_{atm} = 101070 \text{ N/m}^2$, $T_{aiwb} = 17^\circ\text{C}$, $T_{aidb} = 21^\circ\text{C}$)

Run no.	Δp_{bundle} N/m ²	Δp_n N/m ²	Δp_{up} N/m ²
1	685	397	1472
2	503	742	1050
3	332	456	670
4	200	250	385
5	129	147	238
6	77	78	136

Table C.3.3a: Test results.

Run no	LMTD °C	F_T ---	Q_a W	Q_w W	Q_w/Q_a ---	%error %
1	25.067326	0.9949094	42879.931	43063.689	1.0042854	-0.428541
2	23.936083	0.9949537	39228.798	38929.31	0.9923656	0.7634386
3	22.814387	0.995272	34234.239	34120.698	0.9966834	0.3316595
4	21.31334	0.9957998	28645.268	28599.785	0.9984122	0.1587783
5	20.28379	0.9962498	24702.737	23571.593	0.9542098	4.5790245
6	18.38168	0.9962257	19686.894	18760.465	0.9529418	4.7058161

Table C.3.3b: Test results.

Run no.	Re_w ---	h_w $W/m^2 K$	Ry m^{-1}	Ny m^{-1}	K_{he}
1	151022.7	14628.276	509549	327665.32	17.219154
2	150477.55	14570.47	438772.45	312218.9	18.066432
3	151191.7	14558.944	347829.07	283141.22	19.252307
4	152320.06	14587.24	256314.13	250911.54	21.627792
5	153284.57	14575.26	198402.1	225438.13	23.723018
6	155524.92	14698.801	144290.34	196299.7	27.026035

Correlating equations:

$$Ny = 1552.2323Ry^{0.407909}$$

$$K_{he} = 1838.65Ry^{-0.356195}$$

Table C.3.4: Isothermal test results.

Run no.	Ry m^{-1}	K_{heiso}
1	576611.2	14.977924
2	480713.44	15.824232
3	378150.49	16.878582
4	280711.59	18.451705
5	215303.11	20.230951
6	156560.52	22.837755

Correlating equation:

$$K_{heiso} = 1027.948Ry^{-0.319399}$$

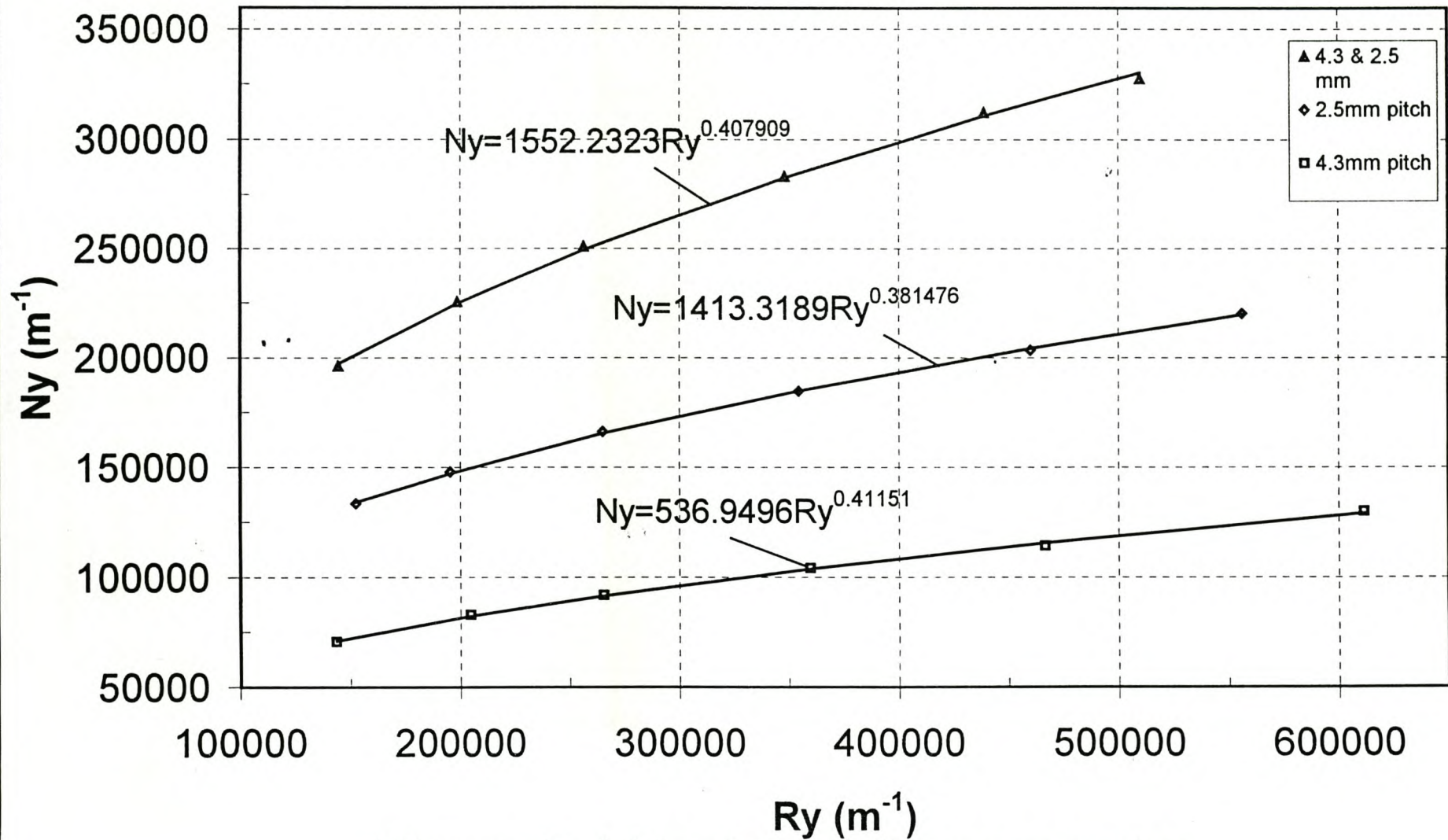


Figure C.1 Heat transfer parameter.

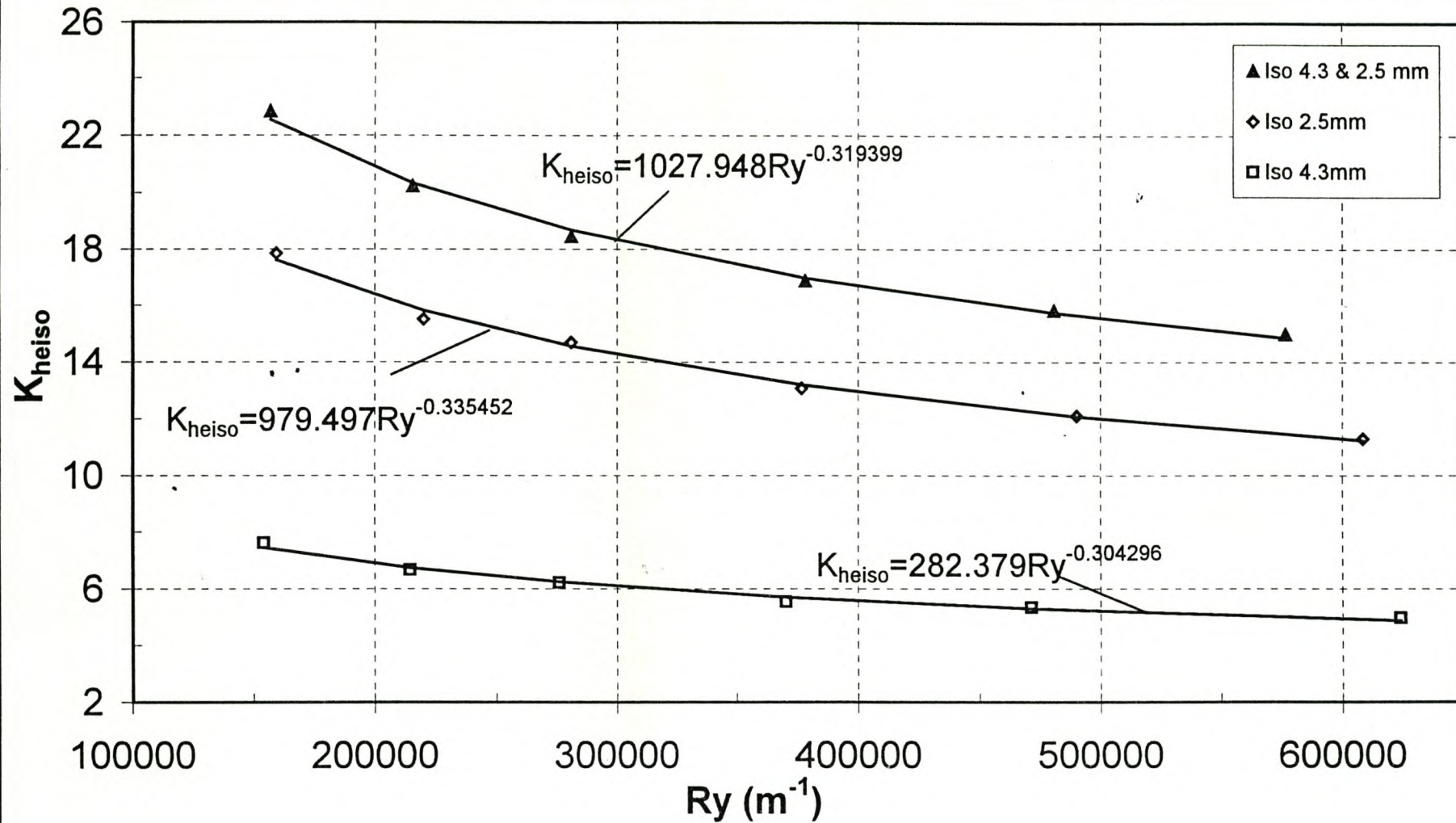


Figure C.2 Isothermal pressure drop coefficient.

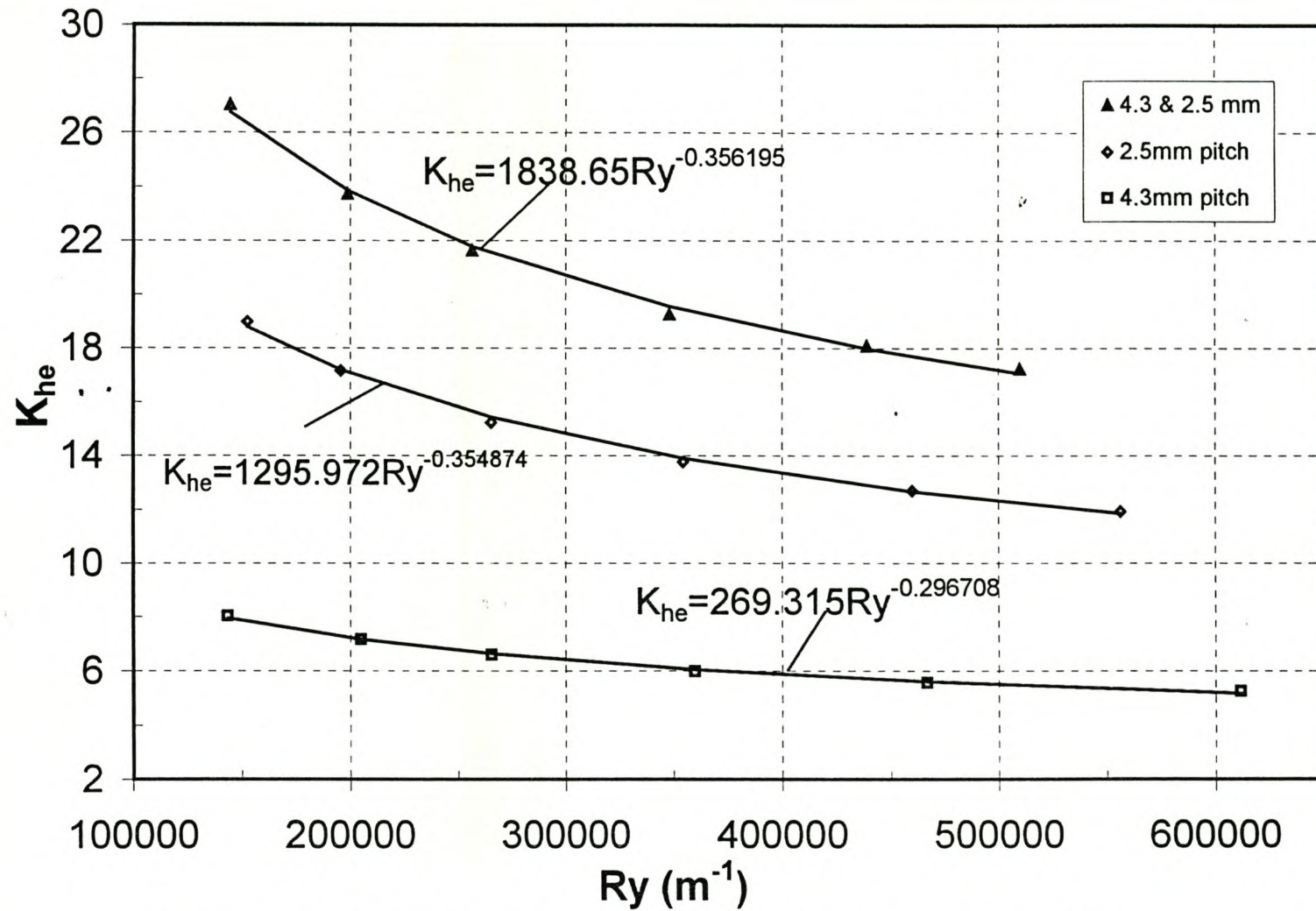


Figure C.3 Non-isothermal pressure drop coefficient.

APPENDIX D

Thermal-flow performance of AE elliptical finned tubes

Table D.1.1: Tube specifications.

Name: AE-2.5 DE (2.5 mm fin pitch, 0.54373 mm fin thickness)

No	Tube mass,kg	No. of fins	L_t ,mm	P_f ,mm
1	4.515	188	472	2.5106
2	4.51	194	470	2.4227
3	4.515	193	470	2.4352
4	4.525	195	470	2.4103
5	4.515	193	467	2.4197
6	4.585	195	468	2.4000
7	4.645	195	470	2.4103
8	4.58	194	470	2.4227
9	4.665	196	470	2.3980
10	4.47	192	469	2.4427
11	4.56	191	470	2.4607
12	4.585	196	470	2.3980
13	4.53	193	469	2.4301
14	4.585	195	467	2.3949
15	4.58	193	470	2.4352
16	4.545	194	470	2.4227
17	4.515	192	469	2.4427
18	4.52	192	470	2.4479
19	4.535	194	469	2.4175
20	4.635	196	469	2.3929
21	4.445	192	466	2.4271
22	4.51	193	471	2.4404
Average	4.548636364	193.45455	469.36364	2.42646077

Table D.1.2a: Test data.

Run no.	T_{ai} °C	T_{ao} °C	T_{wi} °C	T_{wo} °C	P_{atm} N/m ²	m_a kg/s	m_w kg/s
1	18.000756	41.94349	60.049115	55.542005	101084.36	2.1918986	2.771560778
2	17.78178	43.43756	60.222875	56.009055	101087.96	1.8905878	2.728565636
3	18.253286	46.04914	60.281075	56.583625	101080.22	1.5120793	2.676699839
4	18.057246	49.05049	60.586235	57.399735	101083.44	1.145452	2.670944692
5	18.014246	51.4846	60.657525	58.011875	101084.14	0.8889927	2.755934015
6	17.76322	53.97822	60.694525	58.554575	101088.26	0.6589948	2.724975279

Table D.1.2b: Test data.

Run no.	Δp_{bundle} N/m ²	Δp_n N/m ²	Δp_{up} N/m ²
1	834	339	1467
2	675.5	682	1164
3	468	437	781
4	303.5	252	488
5	206	153	318
6	130	85	182

Table D.1.3: Pressure drops for isothermal tests.

($p_{atm} = 101030 \text{ N/m}^2$, $T_{aiwh} = 14^\circ\text{C}$, $T_{aidh} = 14.8^\circ\text{C}$)

Run no.	Δp_{bundle} N/m^2	Δp_n N/m^2	Δp_{up} N/m^2
1	895	369	1598
2	721	746	1257
3	466	443	788
4	288	244	467
5	184	141	287
6	126	87	190

Table D.1.4a: Test results.

Run no	LMTD $^\circ\text{C}$	F_T ---	Q_a W	Q_w W	Q_w/Q_a ---	%error %
1	26.65270693	0.9921082	53390.416	52249.4479	0.9786297	2.1370271
2	26.05199401	0.9924196	49351.249	48093.8428	0.9745213	2.5478716
3	24.3233134	0.9928793	42759.475	41400.0653	0.968208	3.1792012
4	22.66506879	0.9931419	36122.946	35605.2306	0.985668	1.4332032
5	20.93267572	0.9930501	30278.329	30504.1172	1.0074571	-0.745709
6	18.88932046	0.9919963	24288.959	24397.3442	1.0044623	-0.446234

Table D.1.4b: Test results.

Run no.	Re_w ---	h_w $\text{W/m}^2 \text{K}$	R_y m^{-1}	N_y m^{-1}	K_{he}
1	112705.0131	11558.43	504521.43	401259.989	22.115088
2	111513.4369	11430.366	434505.7	377015.779	24.025639
3	109933.999	11269.615	346163.17	346266.837	25.891566
4	110655.0516	11288.538	261345.05	310018.961	29.125196
5	114779.5945	11614.276	202244.48	277864.616	32.692161
6	113997.1768	11524.943	149522.25	244765.023	37.407998

Correlating equations: $N_y = 1983.295R_y^{0.404505}$
 $K_{he} = 5811.972R_y^{-0.42394}$

Table D.1.5: Isothermal test results.

Run no.	R_y m^{-1}	K_{heiso}
1	570669.2945	21.076518
2	494521.257	22.610501
3	382605.6777	24.413381
4	284718.1952	27.246259
5	216530.3702	30.097126
6	169890.4147	33.479398

Correlating equation: $K_{heiso} = 2891.203R_y^{-0.37098}$

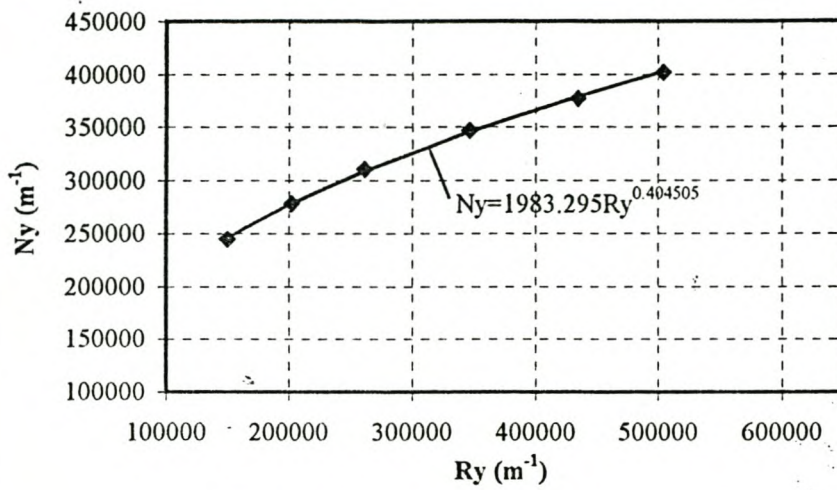
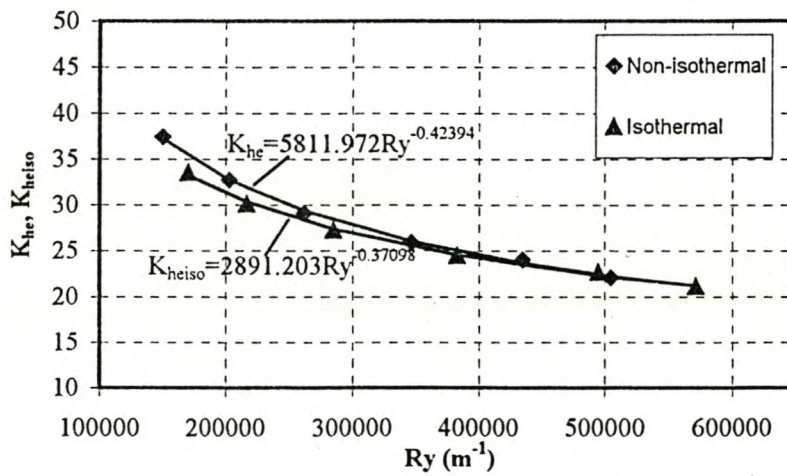


**Figure D.1.1: Heat transfer parameter
(2.5mm pitch Double-Row).**



**D.1.2: Pressure drop coefficient
(2.5mm pitch Double row).**

Table D.2.1: Tube specifications.

Name: AE-4.0 DE (4.0 mm fin pitch, 0.60250 mm fin thickness)

No	Tube mass,kg	No. of fins	L_t ,mm	P_f ,mm
1	3.36	116	469	4.04310
2	3.355	116	468	4.03448
3	3.335	115	465	4.04348
4	3.365	115	469	4.07826
5	3.39	116	469	4.04310
6	3.375	116	468	4.03448
7	3.36	116	469	4.04310
8	3.385	116	468	4.03448
9	3.34	116	469	4.04310
10	3.39	116	469	4.04310
11	3.355	116	470	4.05172
12	3.37	114	469	4.11404
13	3.37	116	470	4.05172
14	3.375	116	470	4.05172
15	3.35	115	466	4.05217
16	3.375	116	466	4.01724
17	3.36	116	468	4.03448
18	3.415	118	471	3.99153
19	3.37	116	467	4.02586
20	3.345	117	469	4.00855
21	3.355	116	468	4.03448
22	3.36	116	468	4.03448
Average	3.366136364	115.90909	468.40909	4.04130501

Table D.2.2a: Test data.

Run no.	T_{ai} °C	T_{ao} °C	T_{wi} °C	T_{wo} °C	P_{atm} N/m ²	m_a kg/s	m_w kg/s
1	22.19607	37.61024	60.70259	57.4983	100447.51	2.5153157	2.757777389
2	22.10328	39.47038	60.82777	57.97027	100449.03	1.9813804	2.724005892
3	22.34393	41.56862	60.88971	58.35859	100445.1	1.5585997	2.725377256
4	22.59647	44.07004	60.90774	58.7297	100440.97	1.1469529	2.71334254
5	22.35981	46.19174	60.96447	59.03818	100444.84	0.8968511	2.710278721
6	22.31902	49.02559	61.06252	59.4862	100445.5	0.6502227	2.70559338

Table D.2.2b: Test data.

Run no.	Δp_{bundle} N/m ²	Δp_n N/m ²	Δp_{up} N/m ²
1	476.5	443	1313
2	324	743	856
3	217	460	550
4	132	250	315
5	88.5	154	202
6	53	82	114

Table D.2.3: Pressure drops for isothermal tests.

($p_{atm} = 100840 \text{ N/m}^2$, $T_{aiwb} = 18 \text{ }^\circ\text{C}$, $T_{aidb} = 20 \text{ }^\circ\text{C}$)

Run no.	Δp_{bundle} N/m^2	Δp_n N/m^2	Δp_{up} N/m^2
1	493	472	1384
2	324	760	871
3	206	442	527
4	127	246	307
5	84	149	194
6	51.5	81	109

Table D.2.4a: Test results.

Run no.	LMTD $^\circ\text{C}$	F_T ---	Q_a W	Q_w W	Q_w/Q_a ---	%error %
1	28.76671289	0.9970376	39472.107	36968.5979	0.9365752	6.3424764
2	27.98814159	0.9962921	35035.322	32565.3508	0.9295005	7.0499451
3	26.80712556	0.9959376	30506.62	28861.2872	0.9460664	5.3933629
4	25.26940676	0.9959642	25075.1	24726.3346	0.9860912	1.3908843
5	24.08790033	0.9962174	21763.585	21844.2484	1.0037064	-0.370636
6	22.28952395	0.9966965	17683.596	17845.4211	1.0091512	-0.915116

Table D.2.4b: Test results.

Run no.	Re_w ---	h_w $\text{W/m}^2 \text{ K}$	R_y m^{-1}	N_y m^{-1}	K_{he}
1	114442.2599	11604.064	579338.22	265110.644	9.5319021
2	113562.2411	11505.578	455376.58	240198.43	10.414614
3	114013.293	11526.344	357162	216532.894	11.229621
4	113849.0981	11497.202	261931.63	186812.723	12.557716
5	114038.8833	11499.073	204356.96	168899.551	13.727409
6	114317.4415	11501.406	147660.3	146904.476	15.569253

Correlating equations: $N_y = 823.0402R_y^{0.435418}$

$$K_{he} = 1068.022R_y^{-0.35579}$$

Table D.2.5: Isothermal test results.

Run no.	R_y m^{-1}	K_{heiso}
1	631030.3873	9.0667601
2	488675.764	9.9359446
3	373955.2601	10.78782
4	279588.8366	11.897886
5	217616.1529	12.989809
6	160178.6806	14.699534

Correlating equation: $K_{heiso} = 928.4973R_y^{-0.34682}$

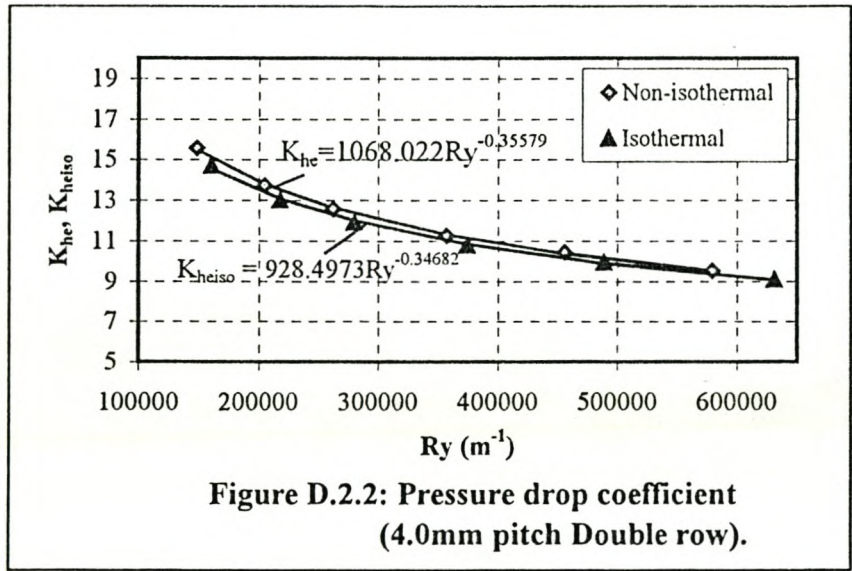
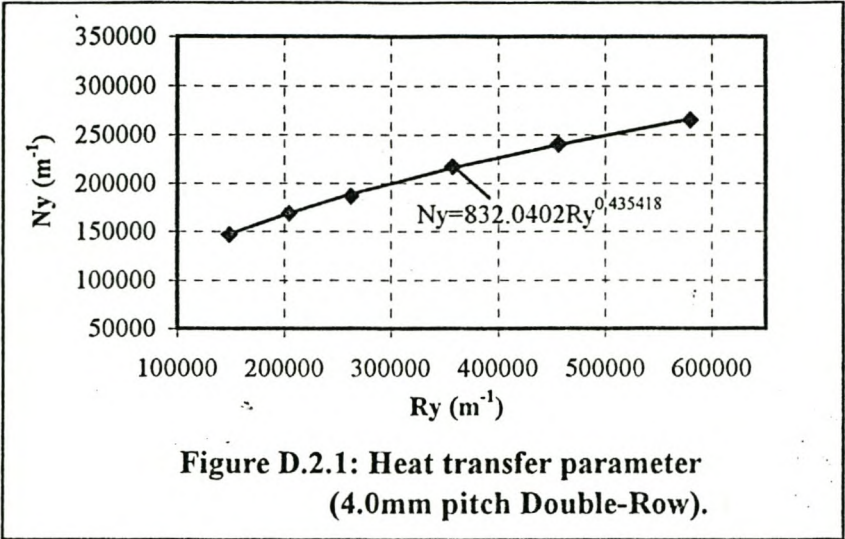


Table D.3.1: Tube specifications.

Name: AE-4.3 DA (4.3 mm fin pitch, 0.59120 mm fin thickness)

No	Tube mass,kg	No. of fins	L_t ,mm	P_f ,mm
1	3.155	110	468	4.25455
2	3.13	109	468	4.29358
3	3.125	109	469	4.30275
4	3.15	109	469	4.30275
5	3.13	109	469	4.30275
6	3.18	111	469	4.22523
7	3.155	109	470	4.31193
8	3.14	110	465	4.22727
9	3.135	108	467	4.32407
10	3.15	109	469	4.30275
11	3.115	108	469	4.34259
12	3.17	110	468	4.25455
13	3.185	111	469	4.22523
14	3.15	109	468	4.29358
15	3.115	112	470	4.19643
16	3.16	111	467	4.20721
17	3.15	108	469	4.34259
18	3.16	110	468	4.25455
19	3.17	110	469	4.26364
20	3.18	110	468	4.25455
21	3.17	111	467	4.20721
22	3.135	108	470	4.35185
Average	3.150454545	109.59091	468.40909	4.2746176

Table D.3.2a: Test data.

Run no.	T_{ai} °C	T_{ao} °C	T_{wi} °C	T_{wo} °C	p_{atm} N/m ²	m_a kg/s	m_w kg/s
1	22.15542	37.99629	60.8552	57.58429	100428.25	2.4815448	2.77640066
2	22.47405	39.77207	60.94714	57.99116	100423.04	1.9887458	2.768342594
3	22.33467	41.95096	61.01423	58.38749	100425.32	1.5402497	2.745846812
4	22.60989	44.40295	61.04463	58.7831	100420.83	1.1641088	2.711969902
5	22.42287	46.795	61.12537	59.20583	100423.88	0.8660041	2.686798435
6	22.42957	49.06822	61.1892	59.5537	100423.77	0.6618538	2.674419377

Table D.3.2b: Test data.

Run no.	Δp_{bundle} N/m ²	Δp_n N/m ²	Δp_{up} N/m ²
1	509	432	1329
2	351	750	891
3	225	450	551
4	142	258	332
5	88	144	195
6	57	85	120

Table D.3.3: Pressure drops for isothermal tests.

($p_{atm} = 100810 \text{ N/m}^2$, $T_{aiwb} = 17.5^\circ\text{C}$, $T_{aidb} = 21^\circ\text{C}$)

Run no.	Δp_{bundle} N/m^2	Δp_n N/m^2	Δp_{up} N/m^2
1	528	462	1393
2	343	740	875
3	222	450	546
4	138.5	258	328
5	90	154	203
6	49	74	103

Table D.3.4a: Test results.

Run no	LMTD $^\circ\text{C}$	F_T ---	Q_a W	Q_w W	Q_w/Q_a ---	%error %
1	28.68635374	0.9966653	40043.456	37992.727	0.9487874	5.1212582
2	27.73069827	0.9960661	35041.333	34236.347	0.9770275	2.2972461
3	26.66191632	0.9956645	30779.185	30176.9133	0.9804325	1.9567494
4	25.15625804	0.9957708	25843.436	25661.5474	0.9929619	0.7038104
5	23.8184941	0.9961961	21503.367	21579.6695	1.0035484	-0.354838
6	22.33761717	0.9965787	17963.618	18302.3363	1.0188558	-1.885578

Table D.3.4b: Test results.

Run no.	Re_w ---	h_w $\text{W/m}^2 \text{K}$	Ry m^{-1}	Ny m^{-1}	K_{he}
1	115427.3457	11678.509	571534.74	269899.528	10.448912
2	115535.1961	11667.853	456821.99	242254.559	11.180471
3	115004.9345	11604.521	352927.74	219720.849	11.90841
4	113957.4399	11498.98	265835.25	193689.742	13.098725
5	113335.0635	11426.69	197238.76	168673.613	14.615221
6	113167.6295	11396.643	150325.69	149038.025	16.147594

Correlating equations: $Ny = 778.019Ry^{0.441216}$
 $K_{he} = 770.0977Ry^{-0.32518}$

Table D.3.5: Isothermal test results.

Run no.	Ry m^{-1}	K_{heiso}
1	621343.6689	9.9204324
2	479950.011	10.800965
3	375477.1724	11.42211
4	284917.2478	12.375784
5	220185.9277	13.465542
6	152313.3386	15.320772

Correlating equation: $K_{heiso} = 565.441Ry^{-0.30335}$

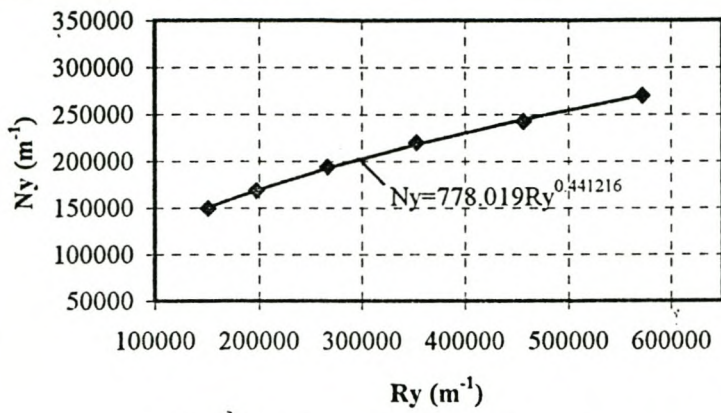


**Figure D.3.1: Heat transfer parameter
(4.3mm pitch Double-Row).**

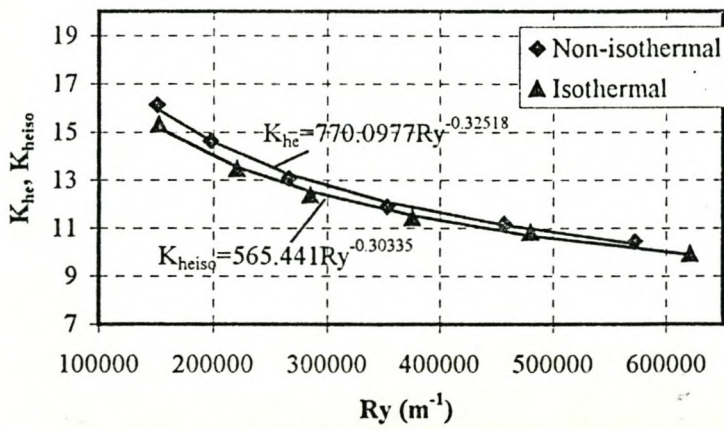


**Figure D.3.2 Pressure drop coefficient
(4.3mm pitch Double row).**

Table D.4.1: Tube specifications.

Name: AE-4.5 DA (4.5 mm fin pitch, 0.59020 mm fin thickness)

No	Tube mass,kg	No. of fins	L_t ,mm	P_f ,mm
1	3.155	107	471	4.40187
2	3.15	108	470	4.35185
3	3.145	107	469	4.38318
4	3.135	106	467	4.40566
5	3.14	106	470	4.43396
6	3.155	106	466	4.39623
7	3.135	106	465	4.38679
8	3.125	106	465	4.38679
9	3.135	107	468	4.37383
10	3.145	106	467	4.40566
11	3.13	106	466	4.39623
12	3.15	106	470	4.43396
13	3.15	106	467	4.40566
14	3.115	105	468	4.45714
15	3.16	107	469	4.38318
16	3.18	108	473	4.37963
17	3.13	106	470	4.43396
18	3.14	109	466	4.27523
19	3.13	106	467	4.40566
20	3.14	108	471	4.36111
21	3.1	105	470	4.47619
22	3.145	106	469	4.42453
Average	3.140454545	106.5	468.36364	4.3981048

Table D.4.2a: Test data.

Run no.	T_{ai} °C	T_{ao} °C	T_{wi} °C	T_{wo} °C	P_{atm} N/m ²	m_a kg/s	m_w kg/s
1	24.55259	38.70659	60.890515	57.854315	100269.58	2.5187336	2.793056647
2	24.51718	40.46827	60.974365	58.250885	100270.16	1.9699321	2.770165948
3	24.10778	42.28182	60.992925	58.584095	100276.84	1.5328636	2.740891816
4	23.4151	44.42199	61.079555	58.968735	100288.13	1.1368095	2.738389246
5	23.11823	46.36214	61.093505	59.244675	100292.98	0.8904905	2.729749142
6	23.02898	49.17038	61.224655	59.742825	100294.43	0.6337169	2.717479639

Table D.4.2b: Test data.

Run no.	Δp_{bundle} N/m ²	Δp_n N/m ²	Δp_{up} N/m ²
1	457	446	1312
2	308.5	737	844
3	201	446	526
4	124	246	306
5	83	152	195
6	49	78	106

Table D.4.3: Pressure drops for isothermal tests.

($p_{atm} = 100680 \text{ N/m}^2$, $T_{aiwb} = 17^\circ\text{C}$, $T_{aidb} = 20.5^\circ\text{C}$)

Run no.	Δp_{bundle} N/m^2	Δp_n N/m^2	Δp_{up} N/m^2
1	479	475	1374
2	308	752	857
3	196	446	522
4	123	255	312
5	81.5	155	197
6	44	73	98

Table D.4.4a: Test results.

Run no	LMTD $^\circ\text{C}$	F_T ---	Q_a W	Q_w W	Q_w/Q_a ---	%error %
1	27.36748042	0.9973872	36228.781	35478.8759	0.9793008	2.069915
2	26.5734545	0.996492	31934.341	31564.9821	0.9884338	1.1566185
3	25.7957482	0.996049	28317.128	27623.9194	0.9755198	2.4480189
4	24.92300179	0.996044	24280.946	24185.1839	0.9960561	0.394393
5	23.85058738	0.9963319	21048.385	21117.0131	1.0032605	-0.32605
6	22.14133494	0.9968762	16848.058	16849.9569	1.0001127	-0.011269

Table D.4.4b: Test results.

Run no.	Re_w ---	h_w $\text{W/m}^2\text{K}$	R_y m^{-1}	N_y m^{-1}	K_{he}
1	116393.2542	11748.412	576938.37	253576.138	9.0612569
2	115866.4748	11684.569	450280.97	228625.732	9.9714874
3	114951.8051	11593.114	349809.94	207609.198	10.70497
4	115261.8899	11600.844	259012.11	182822.2	11.978254
5	115152.9544	11580.254	202499.59	164493.401	13.031539
6	115186.4964	11558.469	143637.93	140437.453	15.123945

Correlating equations: $N_y = 941.0388R_y^{0.422242}$
 $K_{he} = 1087.139R_y^{-0.36117}$

Table D.4.5: Isothermal test results.

Run no.	R_y m^{-1}	K_{heiso}
1	630926.5652	8.7532727
2	484519.1784	9.5438004
3	374385.1311	10.17212
4	283683.6542	11.118061
5	221224.1211	12.113935
6	151491.9293	13.946533

Correlating equation: $K_{heiso} = 641.4488R_y^{-0.32206}$

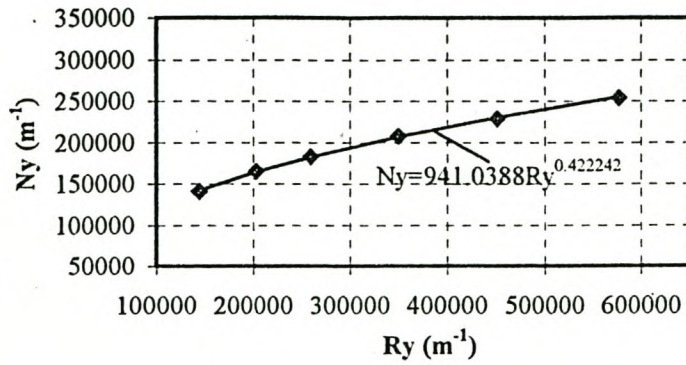


**Figure D.4.1: Heat transfer parameter
(4.5mm pitch Double-Row).**

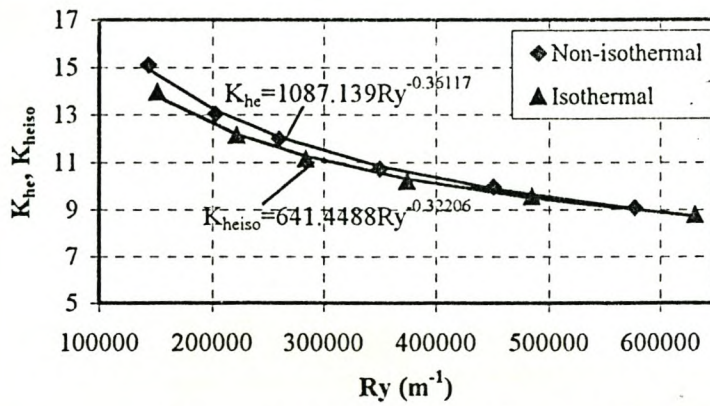


**Figure D.4.2: Pressure drop coefficient
(4.5mm pitch Double row).**

Table D.5.1a: Test data.

Name: AE-4.0 DE & AE-2.5 DE (4mm and 2.5mm fin pitch)

Run no.	T_{ai} °C	T_{ao} °C	T_{wi} °C	T_{wo} °C	P_{atm} N/m ²	m_a kg/s	m_w kg/s
1	18.74359	38.57344	60.26727	56.29777	100304.5	2.3191244	2.766332329
2	19.5019	40.77964	60.57182	56.89674	100292.14	1.972282	2.746788075
3	19.40351	43.18701	60.50535	57.26594	100293.75	1.5331779	2.684653362
4	19.46064	46.38157	60.75912	57.99044	100292.81	1.1512463	2.696304122
5	19.31336	49.05874	60.79094	58.43243	100295.22	0.8866112	2.684422916
6	19.22826	52.31005	60.9337	59.07283	100296.6	0.6224236	2.675602114

Table D.5.1b: Test data.

Run no.	Δp_{bundle} N/m ²	Δp_n N/m ²	Δp_{up} N/m ²
1	700	378	1420
2	546	741	1082
3	359	448	687
4	226	254	414
5	148	152	262
6	85	76	142

Table D.5.2: Pressure drops for isothermal tests. $(P_{atm} = 100700 \text{ N/m}^2, T_{aiwb} = 13.5 \text{ }^\circ\text{C}, T_{aidb} = 16.5 \text{ }^\circ\text{C})$

Run no.	Δp_{bundle} N/m ²	Δp_n N/m ²	Δp_{up} N/m ²
1	733	416	1511
2	540	746	1084
3	346	443	668
4	216	250	402
5	140.5	149	252
6	82	77	140

Table D.5.3a: Test results.

Run no	LMTD °C	F_T ---	Q_a W	Q_w W	Q_w/Q_a ---	%error %
1	28.90232967	0.9941802	46727.283	45933.52	0.9830129	1.6987149
2	27.66644516	0.9939555	42632.059	42228.947	0.9905444	0.9455588
3	26.26472348	0.9941692	37046.673	36381.632	0.9820486	1.7951425
4	24.50104676	0.9946919	31489.478	31232.124	0.9918273	0.8172672
5	22.74141567	0.9950639	26798.497	26488.915	0.9884478	1.1552236
6	20.39946082	0.9949696	20925.794	20832.394	0.9955366	0.4463386

Table D.5.3b: Test results.

Run no.	Re_w ---	h_w $W/m^2 K$	Ry m^{-1}	Ny m^{-1}	K_{he}
1	113350.7401	11575.402	535120.3	318088.99	16.538449
2	113342.4858	11538.99	453343.8	300944.11	17.750011
3	111038.5288	11329.7	351420.45	273144.48	19.239769
4	112365.4392	11405.425	262825.39	246007.9	21.367383
5	112278.5191	11379.695	201793.98	223558.64	23.495152
6	112583.1554	11375.429	141124.41	192370.18	27.239267

Correlating equations:

$$Ny = 2268.266Ry^{0.37518}$$

$$K_{he} = 2103.001Ry^{-0.3673}$$

Table D.5.4: Isothermal test results.

Run no.	Ry m^{-1}	K_{heiso}
1	600304.7199	15.306581
2	490276.7922	16.905531
3	379223.3951	18.105211
4	285563.5814	19.932687
5	220545.8536	21.736833
6	158270.2086	24.633903

Correlating equation:

$$K_{heiso} = 1529.082Ry^{-0.3452}$$

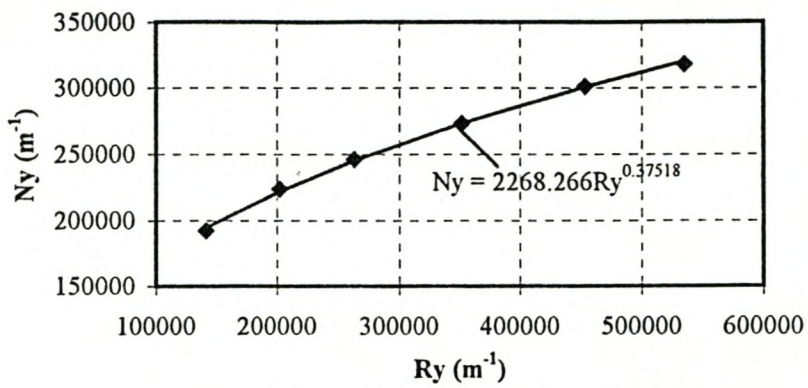


Figure D.5.1: Heat transfer coefficient (4.0mm & 2.5mm pitch).

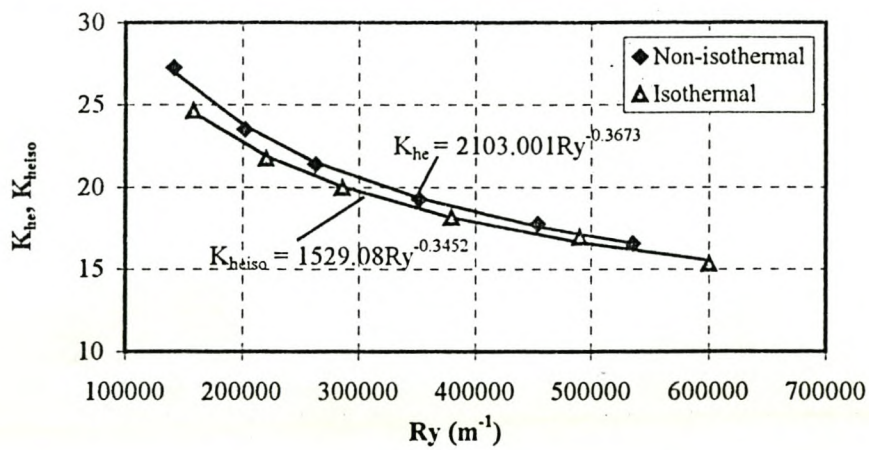


Figure D.5.2: Pressure drop coefficient (4.0mm & 2.5mm pitch).

Table D.6.1a: Test data.

Name: AE-4.3 DA & AE-2.5 DE (4.3mm and 2.5mm fin pitch)

Run no.	T_{ai} °C	T_{ao} °C	T_{wi} °C	T_{wo} °C	P_{atm} N/m ²	m_a kg/s	m_w kg/s
1	20.23787	39.481	60.43598	56.42867	101446.31	2.3292644	2.696660247
2	20.58714	40.9979	60.45496	56.77465	101440.55	1.983066	2.676553685
3	20.54239	43.70613	60.64041	57.43307	101441.29	1.540773	2.65767884
4	20.35085	46.60748	60.81694	58.08058	101444.45	1.1574643	2.663203682
5	20.10528	49.11873	60.85023	58.50358	101448.5	0.89164	2.656653018
6	19.81653	52.24388	60.95499	59.08623	101453.26	0.6260712	2.641734513

Table D.6.1b: Test data.

Run no.	Δp_{bundle} N/m ²	Δp_n N/m ²	Δp_{up} N/m ²
1	706	380	1429
2	553	751	1098
3	357	445	680
4	223	250	406
5	146	148	255
6	84	74	140

Table D.6.2: Pressure drops for isothermal tests.

($p_{atm} = 101880 \text{ N/m}^2$, $T_{aiwb} = 15 \text{ }^\circ\text{C}$, $T_{aidb} = 17 \text{ }^\circ\text{C}$)

Run no.	Δp_{bundle} N/m ²	Δp_n N/m ²	Δp_{up} N/m ²
1	745	415	1524
2	551	757	1120
3	357	456	690
4	213	246	393
5	146	154	260
6	88	82	148

Table D.6.3a: Test results.

Run no	LMTD °C	F_T ---	Q_a W	Q_w W	Q_w/Q_a ---	%error %
1	27.88254413	0.9938709	45656.924	45204.14	0.9900829	0.9917082
2	26.96267675	0.9938342	41390.851	41207.002	0.9955582	0.4441779
3	25.63050818	0.9940862	36141.048	35660.327	0.9866988	1.3301239
4	24.08530061	0.9946609	30638.252	30488.943	0.9951267	0.4873279
5	22.48966695	0.9950515	25941.101	26083.327	1.0054827	-0.548265
6	20.29319566	0.995003	20360.501	20655.964	1.0145116	-1.45116

Table D.6.3b: Test results.

Run no.	Re_w ---	h_w $W/m^2 K$	Ry m^{-1}	Ny m^{-1}	K_{he}
1	110753.7444	11340.259	537201.62	322045.85	16.572975
2	110239.9372	11281.936	458090.44	299729.49	17.713392
3	110179.9233	11244.423	351275.3	272595.67	19.236271
4	111112.433	11292.736	261820.2	243120.93	21.393373
5	111228.3201	11285.169	200046.94	218418.47	23.77469
6	111187.5731	11255.491	139984.52	187912.38	27.619274

Correlating equations:

$$Ny = 1740.4518Ry^{0.395564}$$

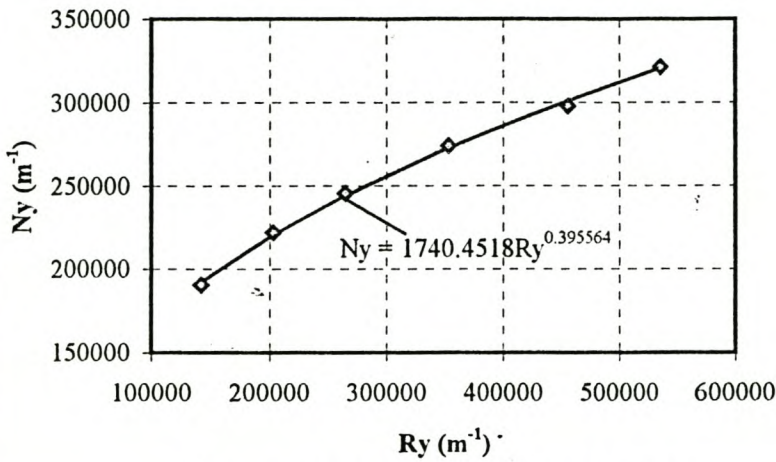
$$K_{he} = 2288.692Ry^{-0.3737}$$

Table D.6.4: Isothermal test results.

Run no.	Ry m^{-1}	K_{heiso}
1	602009.409	15.592907
2	495786.4628	17.003552
3	386240.6393	18.152216
4	284431.1905	19.971126
5	225130.2108	21.850565
6	164024.5017	24.810905

Correlating equation:

$$K_{heiso} = 1553.914Ry^{-0.34554}$$



**Figure D.6.1: Heat transfer parameter
(4.3mm & 2.5mm pitch).**

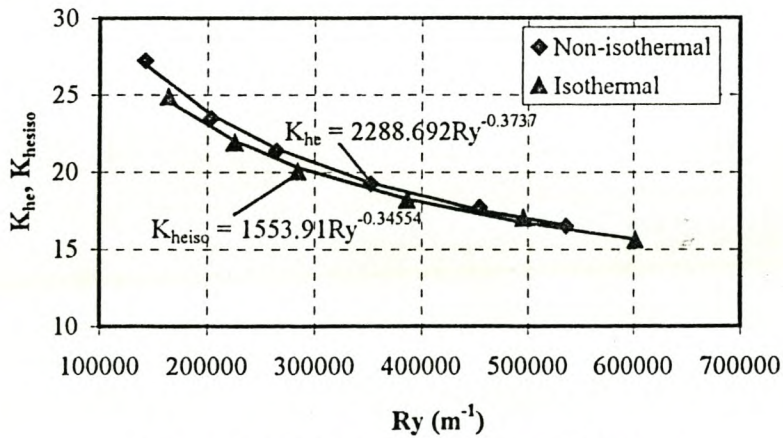


**Figure D.6.2: Pressure drop coefficient
(4.3mm & 2.5mm pitch).**

Table D.7.1a: Test data.
Name: AE-4.5 DA & AE-2.5 DE (4.5mm and 2.5mm fin pitch)

Run no.	T_{ai} °C	T_{ao} °C	T_{wi} °C	T_{wo} °C	p_{atm} N/m ²	m_a kg/s	m_w kg/s
1	20.4924	39.62135	60.41722	56.58973	101073.34	2.3317917	2.736249786
2	20.82835	41.3171	60.49746	56.98384	101067.82	1.9899757	2.716681336
3	21.21732	44.11418	60.72111	57.65881	101061.43	1.5479413	2.717167134
4	21.17278	46.97646	60.74664	58.16289	101062.16	1.1507769	2.694865551
5	20.8809	49.23565	60.88678	58.61902	101066.96	0.9048953	2.667432046
6	20.72247	52.28189	60.92827	59.11453	101069.56	0.6456072	2.692434005

Table D.7.1b: Test data.

Run no.	Δp_{bundle} N/m ²	Δp_n N/m ²	Δp_{up} N/m ²
1	692	380	1414
2	539	749	1080
3	357	454	690
4	219	252	403
5	150	157	266
6	87.5	81	147

Table D.7.2: Pressure drops for isothermal tests.

($p_{atm} = 101390 \text{ N/m}^2$, $T_{aiwb} = 17 \text{ }^\circ\text{C}$, $T_{aidb} = 20 \text{ }^\circ\text{C}$)

Run no.	Δp_{bundle} N/m ²	Δp_n N/m ²	Δp_{up} N/m ²
1	728	409	1507
2	525	745	1058
3	346	457	674
4	208	246	387
5	141	152	254
6	90	87	154

Table D.7.3a: Test results.

Run no	LMTD °C	F_T ---	Q_a W	Q_w W	Q_w/Q_a ---	%error %
1	27.74695419	0.9941304	45249.803	43810.011	0.9681813	3.1818728
2	26.7771041	0.9940429	41358.841	39931.186	0.9654812	3.4518751
3	25.23840924	0.9942618	35950.851	34810.629	0.9682839	3.171613
4	23.49850014	0.9948346	30122.316	29130.822	0.9670844	3.2915611
5	22.19663934	0.9951676	26031.901	25309.02	0.972231	2.7769013
6	19.95403625	0.9951235	20674.535	20432.567	0.9882963	1.1703661

Table D.7.3b: Test results.

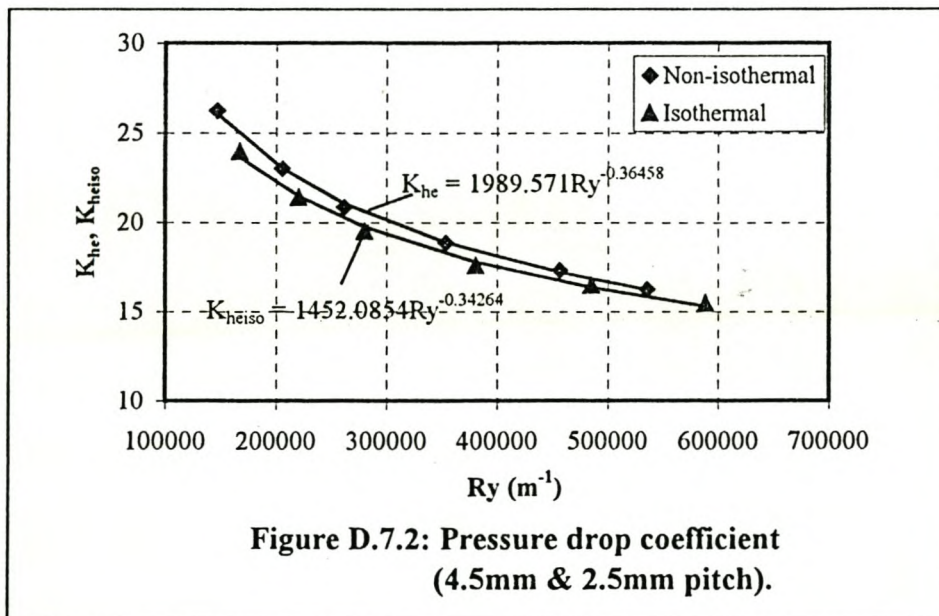
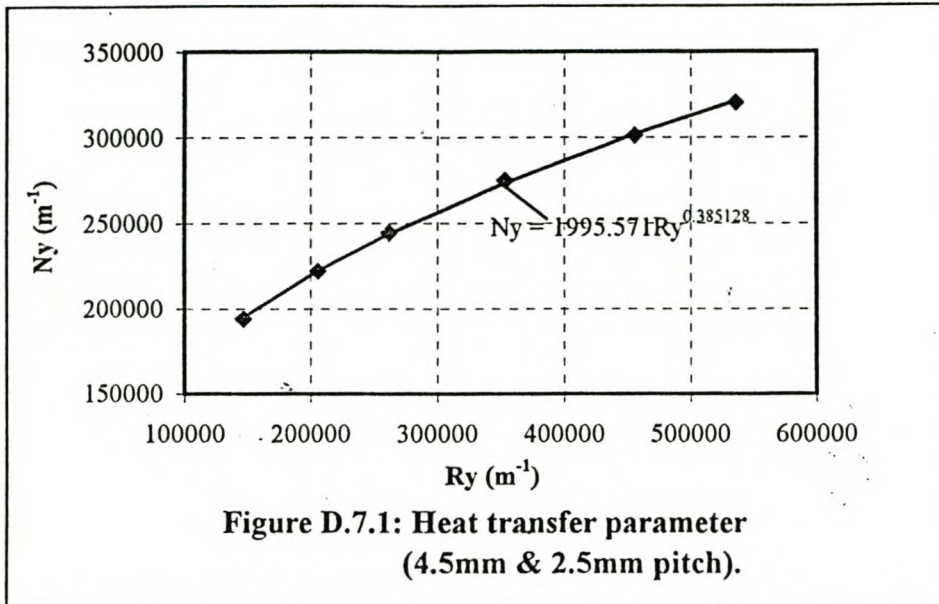
Run no.	Re_w ---	h_w $W/m^2 K$	Ry m^{-1}	Ny m^{-1}	K_{he}
1	112504.0367	11485.24	535595.38	319942.71	16.239807
2	112111.238	11432.971	455905.35	301021.98	17.310386
3	112912.8699	11466.526	353221.03	274645.86	18.8503
4	112443.794	11405.914	261695.29	244438.12	20.826828
5	111809.8782	11328.91	205302.98	221869.33	22.996265
6	113322.8254	11436.803	145970.46	193872.78	26.23002

Correlating equations: $Ny = 1995.571Ry^{0.385128}$
 $K_{he} = 1989.517Ry^{-0.36458}$

Table D.7.4: Isothermal test results.

Run no.	Ry m^{-1}	K_{heiso}
1	588670.0634	15.457794
2	484579.7327	16.450869
3	380847.916	17.552256
4	280143.8445	19.501193
5	220266.5509	21.38366
6	166413.8492	23.912424

Correlating equation: $K_{heiso} = 1452.0854Ry^{-0.34264}$



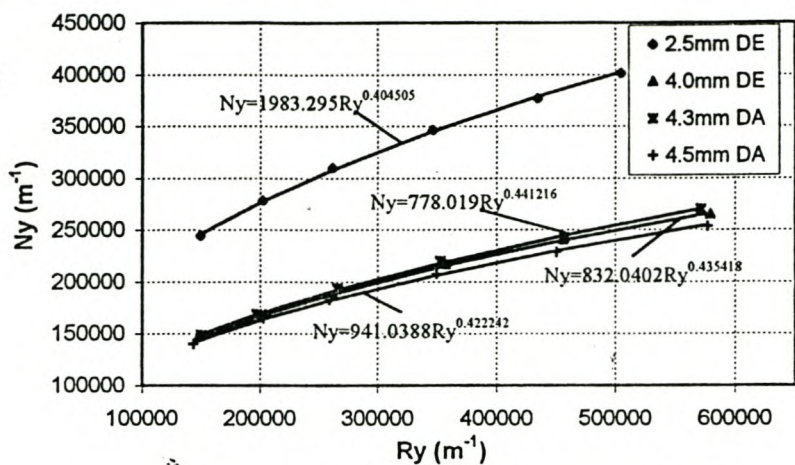


Figure D.8: Heat transfer parameter (Double-Row).

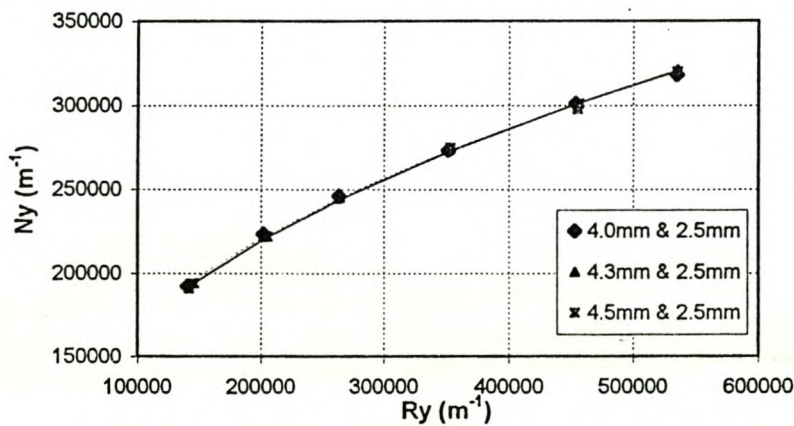


Figure D.9: Heat transfer parameter (Combination).

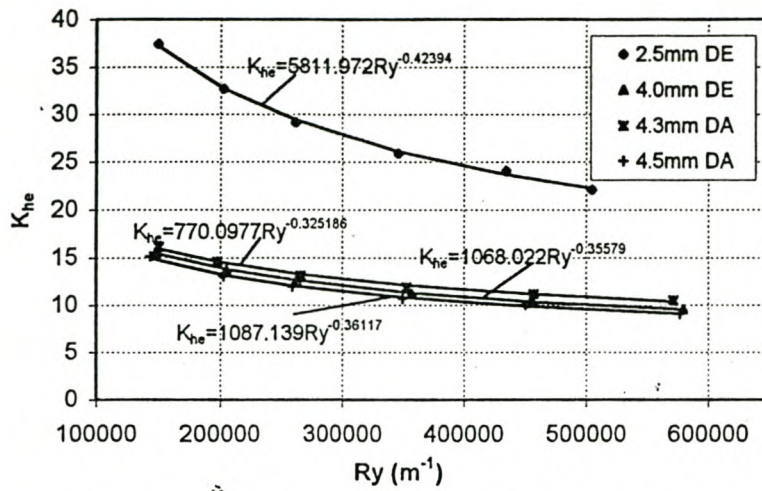


Figure D.10: Pressure drop coefficient (Double row).

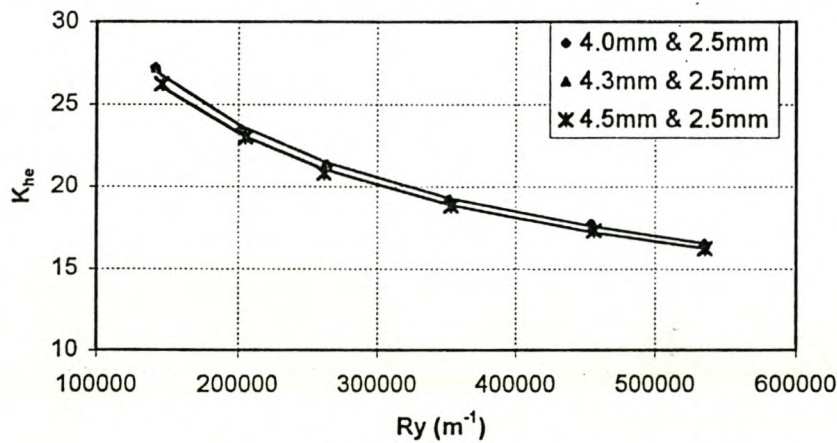


Figure D.11: Pressure drop coefficient (Combination).

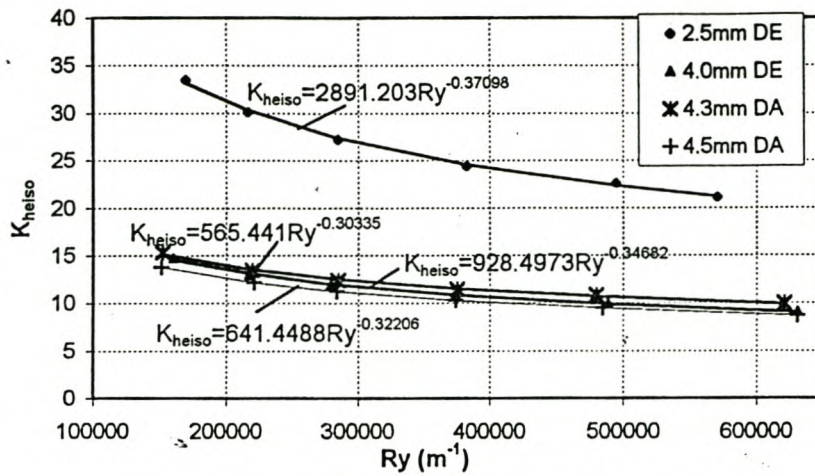


Figure D.12: Isothermal pressure drop coefficient (Double row).

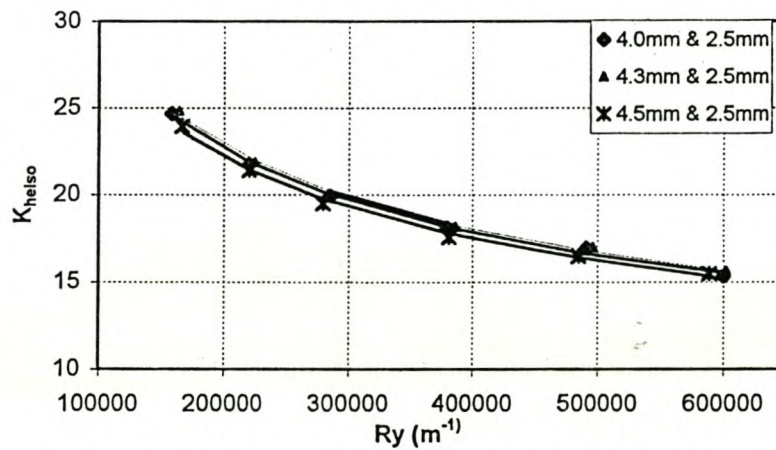


Figure D.13: Isothermal Pressure drop coefficient (Combination).

APPENDIX E

Thermal-flow performance of ED-, F- and R-finned tubes

Table E.1.1: Tube specifications.

Name: ED-2.5L (2.5 mm fin pitch, 0.61846 mm fin thickness)

No	Tube mass,kg	No. of fins	L_t ,mm	P_f ,mm
1	2.19	200	495	2.47500
2	2.19	199	500	2.51256
3	2.19	199	496	2.49246
4	2.19	198	496	2.50505
5	2.195	200	496	2.48000
6	2.195	200	497	2.48500
7	2.18	199	497	2.49749
8	2.18	200	499	2.49500
9	2.185	199	494	2.48241
10	2.205	200	498	2.49000
Average	2.19	199.4	496.8	2.4914975

Table E.1.2a: Test data.

Run no.	T_{ai} °C	T_{ao} °C	T_{wi} °C	T_{wo} °C	P_{atm} N/m ²	m_a kg/s	m_w kg/s
1	26.98155	44.68019	59.830495	56.232685	99921.325	2.2715039	2.6829761
2	27.33121	46.49938	60.158635	56.853585	99915.64	1.9358056	2.6558297
3	27.378	48.59884	60.205515	57.257475	99914.88	1.5060331	2.627708
4	27.47149	50.69472	60.172075	57.673035	99913.36	1.1609276	2.6754144
5	27.46811	52.92584	60.385805	58.272835	99913.415	0.892454	2.660742
6	27.63577	55.31053	60.404725	58.746605	99910.689	0.6256489	2.6477528

Table E.1.2b: Test data.

Run no.	Δp_{bundle} N/m ²	Δp_n N/m ²	Δp_{up} N/m ²
1	570	373	1718
2	528	736	1750
3	368	444	1096
4	223	264	680
5	152	157	420
6	92	78	224

Table E.1.3: Pressure drops for isothermal tests.

($p_{atm} = 100300$ N/m², $T_{aiwb} = 20^\circ\text{C}$, $T_{aidb} = 24^\circ\text{C}$)

Run no.	Δp_{bundle} N/m ²	Δp_n N/m ²	Δp_{up} N/m ²
1	426	400	1200
2	320	756	890
3	210	454	543
4	131	250	312
5	89	154	215
6	56	82	110

Table E.1.4a: Test results.

Run no	LMTD °C	F _T ---	Q _a W	Q _w W	Q _w /Q _a ---	%error %
1	21.43316466	0.9985728	40969.643	40376.516	0.9855228	1.4477221
2	20.58191144	0.998611	37811.557	36718.251	0.9710854	2.8914611
3	19.32420229	0.9983243	32568.606	32406.237	0.9950146	0.4985422
4	17.88128379	0.9978654	27475.381	27970.143	1.0180075	-1.800748
5	16.46179687	0.9973123	23155.345	23520.849	1.0157849	-1.578488
6	14.37816761	0.9968155	17646.912	18368.196	1.0408731	-4.087309

Table E.1.4b: Test results.

Run no.	Re _w ---	h _w W/m ² K	Ry m ⁻¹	Ny m ⁻¹	K _{he}
1	195468.7295	23449.242	515888.77	352421.03	13.634871
2	194926.0282	23315.139	438461.71	337292.15	17.330229
3	193537.6314	23137.588	340234.51	307835.49	19.887208
4	197635.0543	23518.915	261577.24	279054.45	20.210057
5	197788.9969	23466.541	200551.41	254250.96	23.227271
6	197570.6283	23403.782	140163.67	220494.11	28.490071

Correlating equations: $Ny = 3039.7200Ry^{0.36213}$

Table E.1.5: Isothermal test results.

Run no.	Ry m ⁻¹	K _{heiso}
1	571362.0432	13.759583
2	477196.1601	14.995303
3	380012.4885	16.576413
4	285565.1238	19.253155
5	209515.3955	23.256454
6	154972.8439	28.43596

Correlating equation: $K_{heiso} = 13216.347Ry^{-0.518865}$

Table E.2.1: Tube specifications.

Name: ED-2.5S (2.5 mm fin pitch, 0.53111 mm fin thickness)

No	Tube mass,kg	No. of fins	L_t ,mm	P_t ,mm
1	1.105	188	468	2.48936
2	1.145	188	469	2.49468
3	1.19	189	467	2.47090
4	1.105	189	467	2.47090
5	1.195	188	468	2.48936
6	1.19	188	468	2.48936
7	1.105	192	468	2.43750
8	1.2	189	469	2.48148
9	1.2	191	469	2.45550
10	1.2	189	469	2.48148
Average	1.1635	189.1	468.2	2.4760525

Table E.2.2a: Test data.

Run no.	T_{ai} °C	T_{ao} °C	T_{wi} °C	T_{wo} °C	p_{atm} N/m ²	m_a kg/s	m_w kg/s
1	27.72707	44.24221	59.99608	56.50789	100028.67	2.3375712	2.6844607
2	28.12587	45.87716	60.14224	57.00182	100022.17	1.9357609	2.6478809
3	28.40576	47.52677	60.05287	57.28438	100017.62	1.5398504	2.6361929
4	28.25957	49.451	60.27647	57.89052	100020	1.1837585	2.6594341
5	28.12684	51.4501	60.41146	58.43543	100022.16	0.8866234	2.6332658
6	28.25523	54.35312	60.51618	59.09616	100020.07	0.5676216	2.6368504

Table E.2.2b: Test data.

Run no.	Δp_{bundle} N/m ²	Δp_n N/m ²	Δp_{up} N/m ²
1	500	394	1714
2	460	733	1676
3	330	462	1074
4	253	273	654
5	163	154	380
6	102	64	167

Table E.2.3: Pressure drops for isothermal tests.

($p_{atm} = 100500 \text{ N/m}^2$, $T_{aiwb} = 20^\circ\text{C}$, $T_{aidb} = 25^\circ\text{C}$)

Run no.	Δp_{bundle} N/m ²	Δp_n N/m ²	Δp_{up} N/m ²
1	512	410	1796
2	483	764	1734
3	325	476	1106
4	240	264	635
5	174	152	375
6	122	92	240

Table E.2.4a: Test results.

Run no	LMTD °C	F_T ---	Q_a W	Q_w W	Q_w/Q_a ---	%error %
1	21.61707551	0.9986563	39331.324	39169.21	0.9958783	0.4121732
2	20.71892293	0.9988395	35005.574	34785.168	0.9937037	0.6296325
3	19.57712594	0.9988104	29993.441	30530.523	1.0179066	-1.790664
4	18.67628248	0.998583	25556.736	26545.532	1.0386902	-3.869023
5	17.51913776	0.9982348	21069.54	21769.643	1.0332282	-3.322824
6	15.32530618	0.9977846	15094.247	15666.37	1.0379034	-3.790337

Table E.2.4b: Test results.

Run no.	Re_w ---	h_w W/m ² K	R_y m ⁻¹	N_y m ⁻¹	K_{he}
1	280375.9704	45883.178	530598.45	330351.5	11.302577
2	277935.0898	45437.739	438274.92	305472.78	15.113997
3	277123.2708	45293.231	347806.19	275815.87	17.082161
4	281366.9275	45742.466	266815.29	245341	22.097131
5	280061.9319	45450.114	199402.81	214790.28	25.30167
6	282096.1656	45603.21	127195.27	174844.22	38.443986

Correlating equations: $N_y = 919.5229R_y^{0.446805}$

Table E.2.5: Isothermal test results.

Run no.	R_y m ⁻¹	K_{heiso}
1	573686.3178	10.878471
2	476657.2052	14.865574
3	378036.3222	15.902419
4	282536.361	21.023714
5	214564.3464	26.429018
6	166756.8703	30.678862

Correlating equation: $K_{heiso} = 867074.55R_y^{-0.846683}$

Table E.3.1: Tube specifications.

Name: F-3.0 (3.0 mm fin pitch, 0.30609 mm fin thickness)

No	Tube mass,kg	No. of fins	L_t ,mm	P_f ,mm
1	0.955	157	467	2.975
2	0.965	158	466	2.949
3	0.98	158	468	2.962
4	0.96	158	468	2.962
5	0.97	158	468	2.962
6	0.96	158	467	2.956
7	0.965	158	468	2.962
8	0.965	158	468	2.962
9	0.95	158	467	2.956
10	0.965	158	468	2.962
Average	0.9635	157.9	467.5	2.9607434

Table E.3.2a: Test data.

Run no.	T_{ai} °C	T_{ao} °C	T_{wi} °C	T_{wo} °C	p_{atm} N/m ²	m_a kg/s	m_w kg/s
1	25.55694	40.85775	60.1856	57.00498	100004.24	2.2711979	2.7168352
2	25.76049	42.13849	60.26346	57.29422	100000.93	1.9487529	2.7169084
3	25.76083	44.01583	60.2806	57.62017	100000.92	1.5478272	2.7059731
4	24.8886	45.96716	60.28356	57.98824	100015.11	1.1769354	2.6782224
5	25.3336	48.62603	60.43309	58.50058	100007.87	0.8788067	2.7128158
6	25.25841	51.74997	60.57148	59.08844	100009.1	0.5962203	2.7048417

Table E.3.2b: Test data.

Run no.	Δp_{bundle} N/m ²	Δp_n N/m ²	Δp_{up} N/m ²
1	628	368	1745
2	496	735	1786
3	366	462	1140
4	250	267	675
5	162	150	392
6	103	70	186

Table E.3.3: Pressure drops for isothermal tests. $(p_{atm} = 100200 \text{ N/m}^2, T_{aiwb} = 24^\circ\text{C}, T_{aidb} = 27^\circ\text{C})$

Run no.	Δp_{bundle} N/m ²	Δp_n N/m ²	Δp_{up} N/m ²
1	645	378	1805
2	538	737	1776
3	358	437	1075
4	242	260	669
5	194	179	462
6	120	78	208

Table E.3.4a: Test results.

Run no	LMTD °C	F _T ---	Q _a W	Q _w W	Q _w /Q _a ---	%error %
1	24.89821069	0.9994333	35384.988	36148.019	1.0215637	-2.15637
2	24.21371199	1.0004546	32497.758	33747.49	1.0384559	-3.845592
3	23.19484369	1.0014246	28771.474	30116.71	1.0467559	-4.675592
4	22.41124727	1.0013194	25269.552	25717.819	1.0177394	-1.773942
5	20.68042043	1.00011	20848.846	21933.503	1.0520248	-5.20248
6	18.60537281	0.9980167	16089.331	16783.585	1.0431499	-4.314995

Table E.3.4b: Test results.

Run no.	Re _w ---	h _w W/m ² K	Ry m ⁻¹	Ny m ⁻¹	K _{he}
1	337758.0576	51568.709	540504.27	270185.41	13.985068
2	338729.7489	51624.803	462907.84	254103.73	14.967159
3	338263.2036	51499.189	366833.51	233720.05	17.453467
4	335754.9702	51104.648	278624.28	211889.02	20.582098
5	341830.0607	51763.263	207246.07	188556.85	23.802363
6	342730.3425	51741.018	140092.88	161122.98	32.71775

Correlating equations: $Ny = 1794.6929Ry^{0.379978}$

Table E.3.5: Isothermal test results.

Run no.	Ry m ⁻¹	K _{heiso}
1	568907.1506	13.696957
2	483424.3457	15.822402
3	374199.4956	17.572106
4	289513.1571	19.84385
5	240427.1901	23.066502
6	158474.9029	32.840324

Correlating equation: $K_{heiso} = 24057.539Ry^{-0.562371}$

Table E.4.1: Tube specifications.

Name: R-2.4G (2.4 mm fin pitch, 0.1415 mm fin thickness)

No	Tube mass,kg	No. of fins	L_t ,mm	P_f ,mm
1	1.62	287	700	2.439
2	1.61	290	702	2.421
3	1.62	274	697	2.544
4	1.605	287	700	2.439
5	1.61	287	702	2.446
6	1.61	287	700	2.439
7	1.615	290	702	2.421
8	1.61	287	700	2.439
9	1.605	287	700	2.439
10	1.615	284	699	2.461
Average	1.612	286	700.2	2.4487558

Table E.4.2a: Test data.

Run no.	T_{ai} °C	T_{ao} °C	T_{wi} °C	T_{wo} °C	P_{atm} N/m ²	m_a kg/s	m_w kg/s
1	28.7483	35.78348	59.28378	57.25881	99902.554	2.4907263	2.160680298
2	28.88517	36.79305	59.40965	57.60362	99900.329	2.004592	2.137262393
3	27.98609	37.303	59.44003	57.79891	99914.948	1.5531638	2.124104739
4	27.61519	39.06605	59.42158	57.99561	99920.979	1.1471432	2.240442187
5	27.51316	41.75605	59.49513	58.11019	99922.638	0.9056368	2.231560957
6	27.76831	44.07007	59.51234	58.38744	99918.489	0.6241827	2.18077852

Table E.4.2b: Test data.

Run no.	Δp_{bundle} N/m ²	Δp_n N/m ²	Δp_{up} N/m ²
1	424	435	1278
2	298	760	857
3	195	454	528
4	120	248	298
5	82	156	194
6	46	75	97

Table E.4.3: Pressure drops for isothermal tests. $(p_{atm} = 1005700 \text{ N/m}^2, T_{aiwb} = 21.5^\circ\text{C}, T_{aidb} = 25^\circ\text{C})$

Run no.	Δp_{bundle} N/m ²	Δp_n N/m ²	Δp_{up} N/m ²
1	430	452	1324
2	288	757	848
3	192	460	532
4	116	247	296
5	75	144	178
6	47	81	104

Table E.4.4a: Test results.

Run no	LMTD °C	F _T ---	Q _a W	Q _w W	Q _w /Q _a ---	%error %
1	25.92476592	0.9989907	17898.622	18301.975	1.0225354	-2.253543
2	25.54618523	0.998534	16191.886	16146.804	0.9972158	0.2784242
3	25.78479057	0.9986576	14785.385	14582.34	0.9862672	1.3732792
4	25.03433034	0.9991921	13423.715	13364.748	0.9956073	0.4392707
5	23.58682011	0.9996535	13183.085	12928.925	0.9807207	1.9279287
6	22.17165213	0.9998447	10399.324	10262.606	0.9868533	1.3146747

Table E.4.4b: Test results.

Run no.	Re _w ---	h _w W/m ² K	R _y m ⁻¹	N _y m ⁻¹	K _{he}
1	295862.5454	35462.368	595380.18	132358.04	7.8497763
2	293729.0519	35184.415	478487.94	121166.03	8.5015515
3	292432.5673	35023.622	370988.18	109456.44	9.2721124
4	308875.7493	36664.59	273564.02	101895.36	10.43576
5	308100.0382	36561.156	215296.29	105865.63	11.393327
6	301775.4934	35884.286	147916.02	88280.158	13.399214

Correlating equations: $N_y = 4082.773R_y^{0.259598}$

Table E.4.5: Isothermal test results.

Run no.	R _y m ⁻¹	K _{heiso}
1	629393.6605	7.6043941
2	496953.2905	8.1696271
3	388629.4006	8.9057564
4	285443.4092	9.9737583
5	217929.1651	11.062963
6	163167.9822	12.367128

Correlating equation: $K_{heiso} = 957.70213R_y^{-0.362919}$

Table E.5.1: Tube specifications.

Name: R-2.3D (2.3 mm fin pitch, 0.2734 mm fin thickness)

No	Tube mass,kg	No. of fins	L_t ,mm	P_f ,mm
1	1.695	295	691	2.342
2	1.715	309	692	2.239
3	1.68	294	693	2.357
4	1.695	294	694	2.361
5	1.695	296	692	2.338
6	1.665	288	680	2.361
7	1.715	302	695	2.301
8	1.695	302	693	2.295
9	1.68	301	694	2.306
10	1.695	294	693	2.357
Average	1.693	297.5	691.7	2.3257308

Table E.5.2a: Test data.

Run no.	T_{ai} °C	T_{ao} °C	T_{wi} °C	T_{wo} °C	P_{atm} N/m ²	m_a kg/s	m_w kg/s
1	27.05794	39.80523	59.21234	55.83373	99959.908	2.3585657	2.187686292
2	27.53387	41.32444	59.24683	56.27968	99952.167	1.9751743	2.176405094
3	27.76648	43.0028	59.29804	56.66443	99948.384	1.5510505	2.175058571
4	27.55348	45.29413	59.47701	57.27427	99951.848	1.1235785	2.175296548
5	27.59625	46.99948	59.50955	57.67888	99951.153	0.8993996	2.169949316
6	27.43821	49.92303	59.63024	58.15447	99953.723	0.6067256	2.157281007

Table E.5.2b: Test data.

Run no.	Δp_{bundle} N/m ²	Δp_n N/m ²	Δp_{up} N/m ²
1	560	394	1340
2	416	747	969
3	274	460	615
4	159	242	335
5	110	156	222
6	61	72	108

Table E.5.3: Pressure drops for isothermal tests. $(P_{atm} = 100350 \text{ N/m}^2, T_{aiwb} = 18.5^\circ\text{C}, T_{aidb} = 23^\circ\text{C})$

Run no.	Δp_{bundle} N/m ²	Δp_n N/m ²	Δp_{up} N/m ²
1	582	435	1400
2	417	766	983
3	266	455	603
4	160	254	348
5	100	148	209
6	57	76	112

Table E.5.4a: Test results.

Run no	LMTD °C	F_T ---	Q_a W	Q_w W	Q_w/Q_a ---	%error %
1	23.78471934	0.9984551	30597.988	30914.732	1.0103518	-1.035179
2	22.90955762	0.9988713	27718.202	27010.734	0.9744764	2.5523604
3	21.99818887	0.9992333	24047.52	23960.346	0.9963749	0.3625068
4	21.00253423	0.9994488	20285.916	20043.666	0.9880582	1.1941765
5	20.02767203	0.999414	17760.824	16617.627	0.9356338	6.4366225
6	18.2382377	0.9989881	13885.987	13318.456	0.9591292	4.0870788

Table E.5.4b: Test results.

Run no.	Re_w ---	h_w W/m ² K	R_y m ⁻¹	N_y m ⁻¹	K_{he}
1	277483.8572	31710.739	560794.31	251315.43	11.554594
2	277094.3462	31617.171	468444.51	234988.95	12.19975
3	277868.4181	31641.529	366984.95	210791.76	12.990573
4	279612.4741	31718.329	265189.19	184830.04	14.317003
5	279873.9826	31692.881	211829.18	168835.51	15.414385
6	279528.4313	31590.973	142429.33	143851.11	18.700295

Correlating equations: $N_y = 1116.6703R_y^{0.409269}$

Table E.5.5: Isothermal test results.

Run no.	R_y m ⁻¹	K_{heiso}
1	621343.2002	10.701522
2	502832.2553	11.707804
3	388939.0396	12.482576
4	291293.3256	13.385807
5	222390.0098	14.35341
6	159059.3029	15.993457

Correlating equation: $K_{heiso} = 430.2697R_y^{-0.275697}$

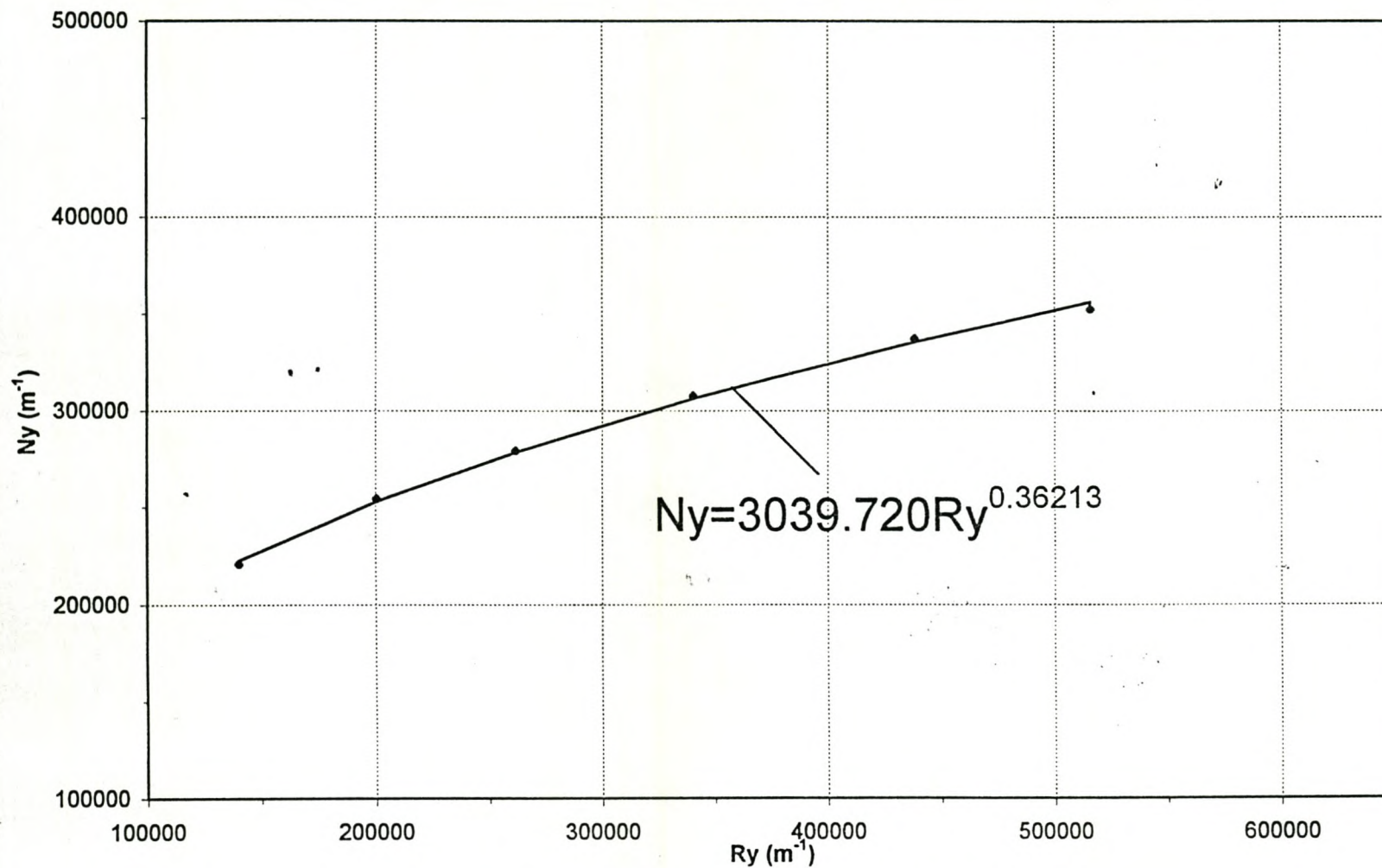


Figure E.1: Heat transfer parameter (ED-2.5L).

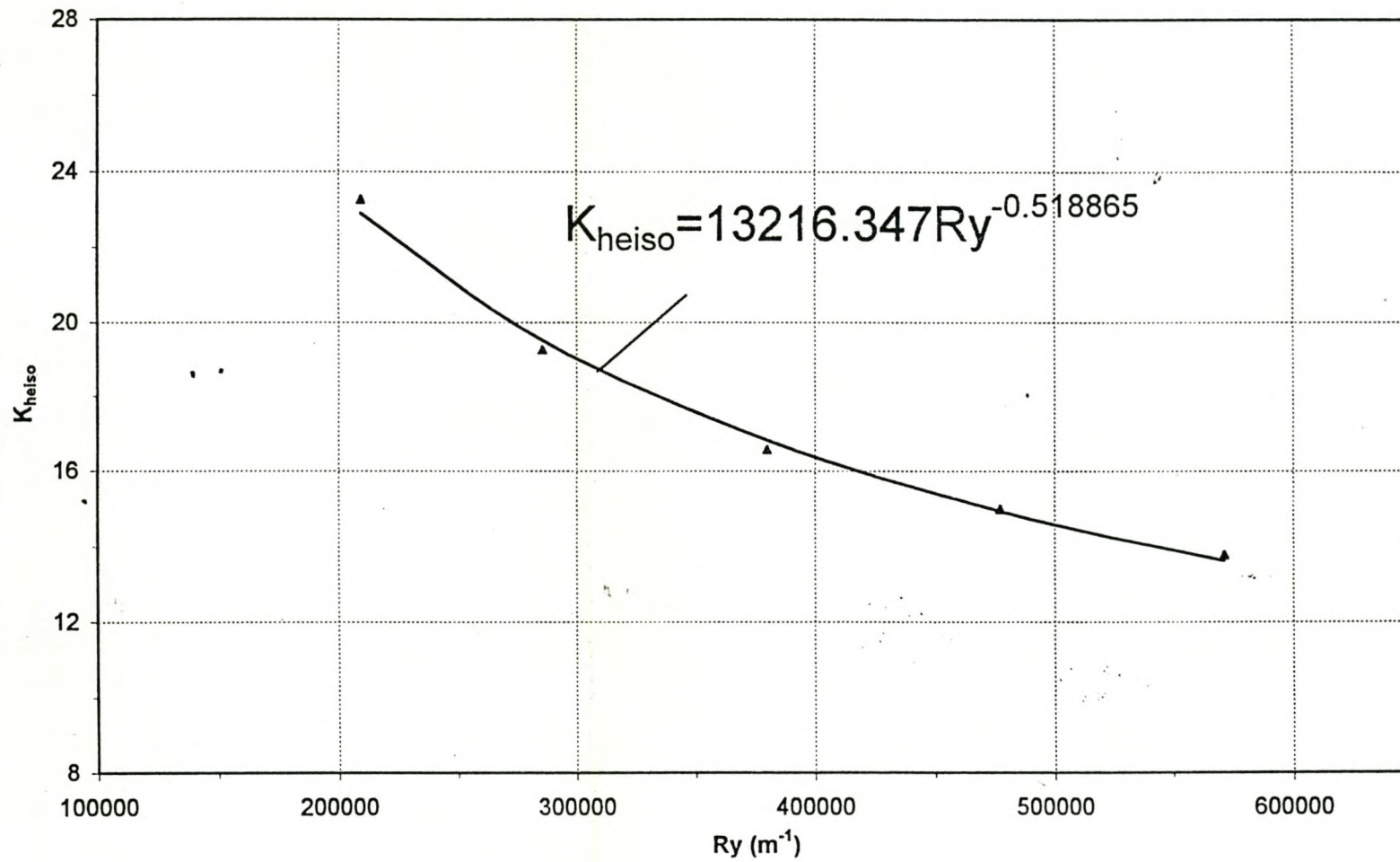


Figure E.2: Pressure drop coefficient (ED-2.5L).

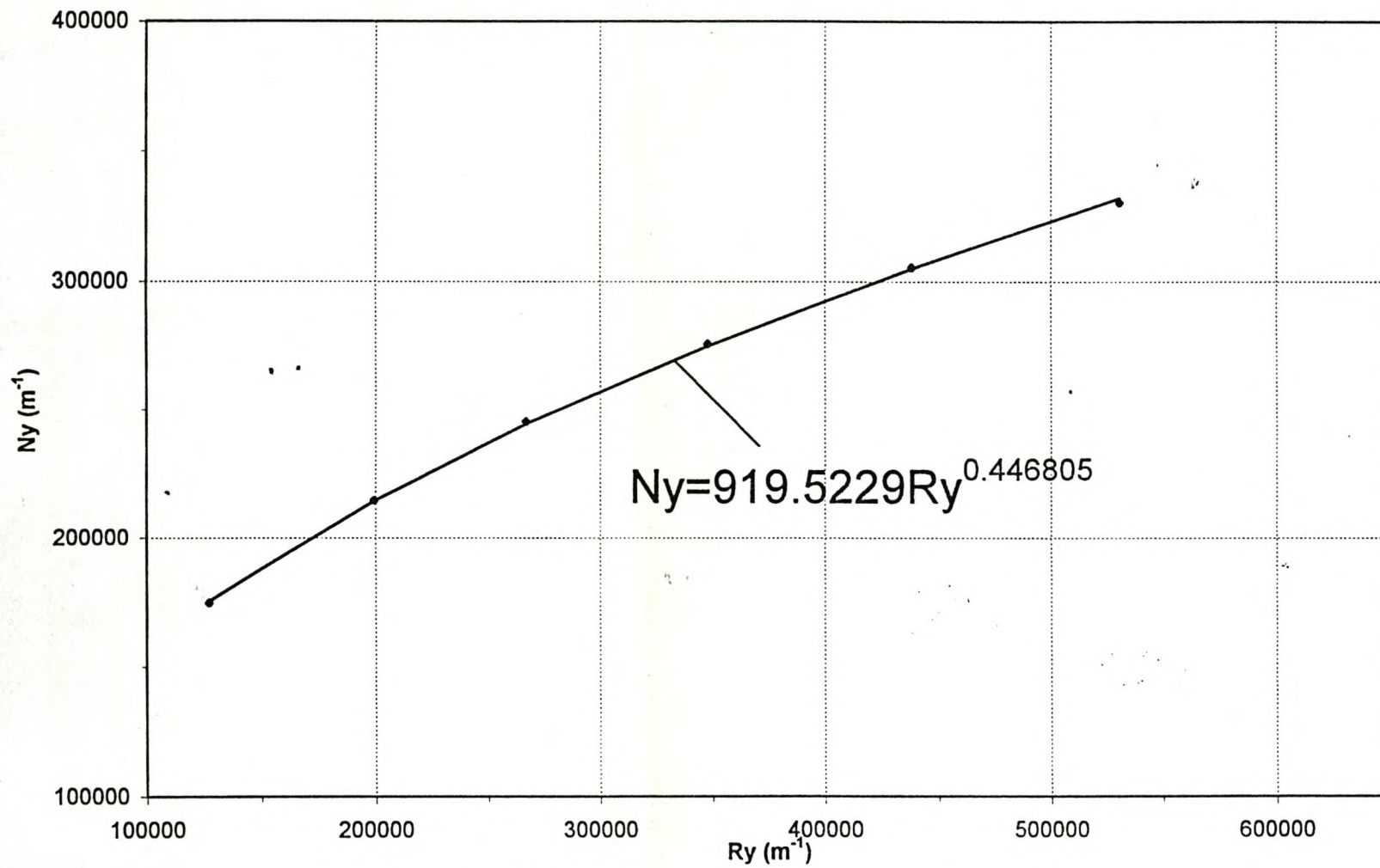


Figure E.3: Heat transfer parameter (ED-2.5S).

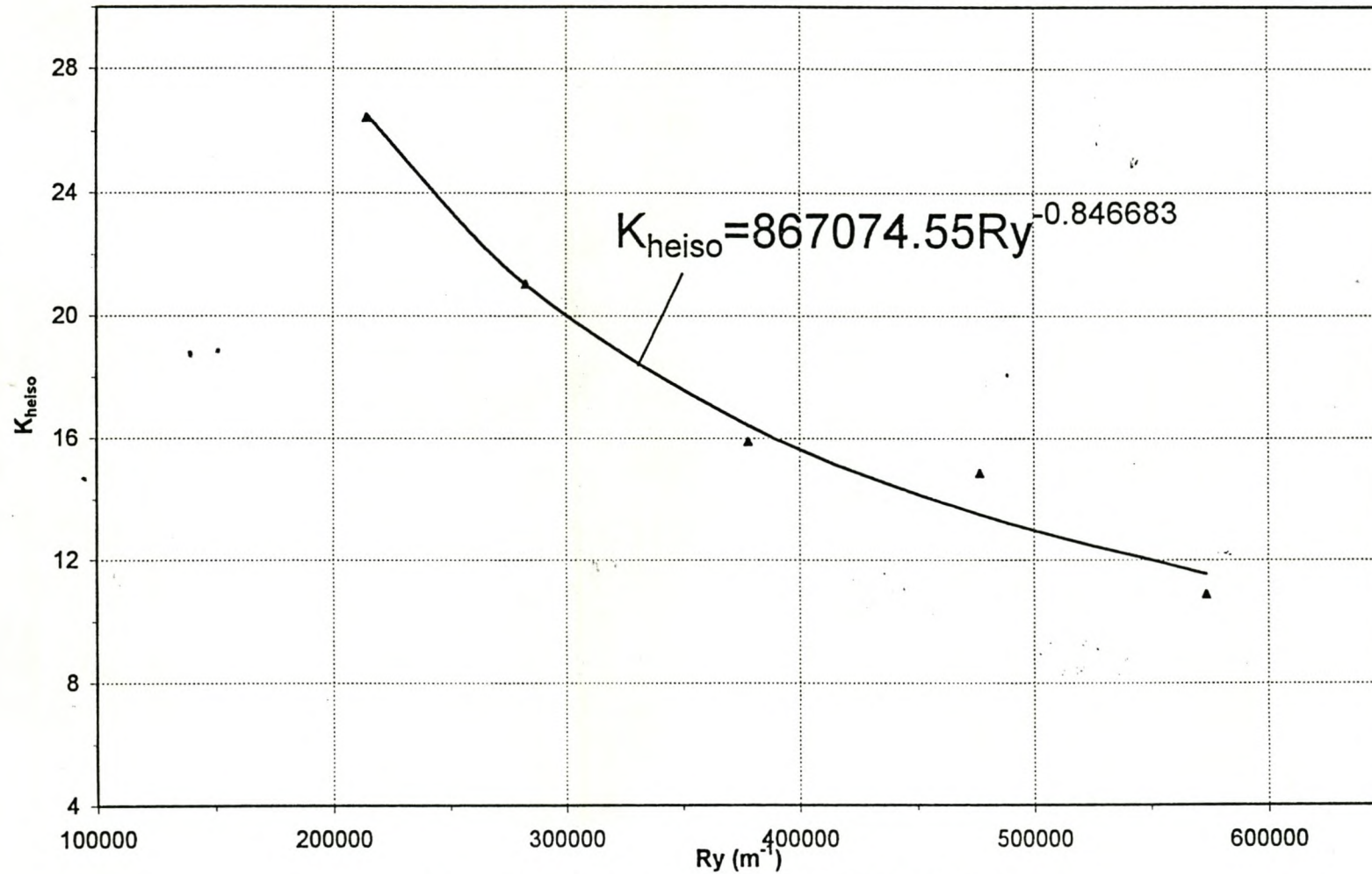


Figure E.4: Pressure drop coefficient (ED-2.5S).

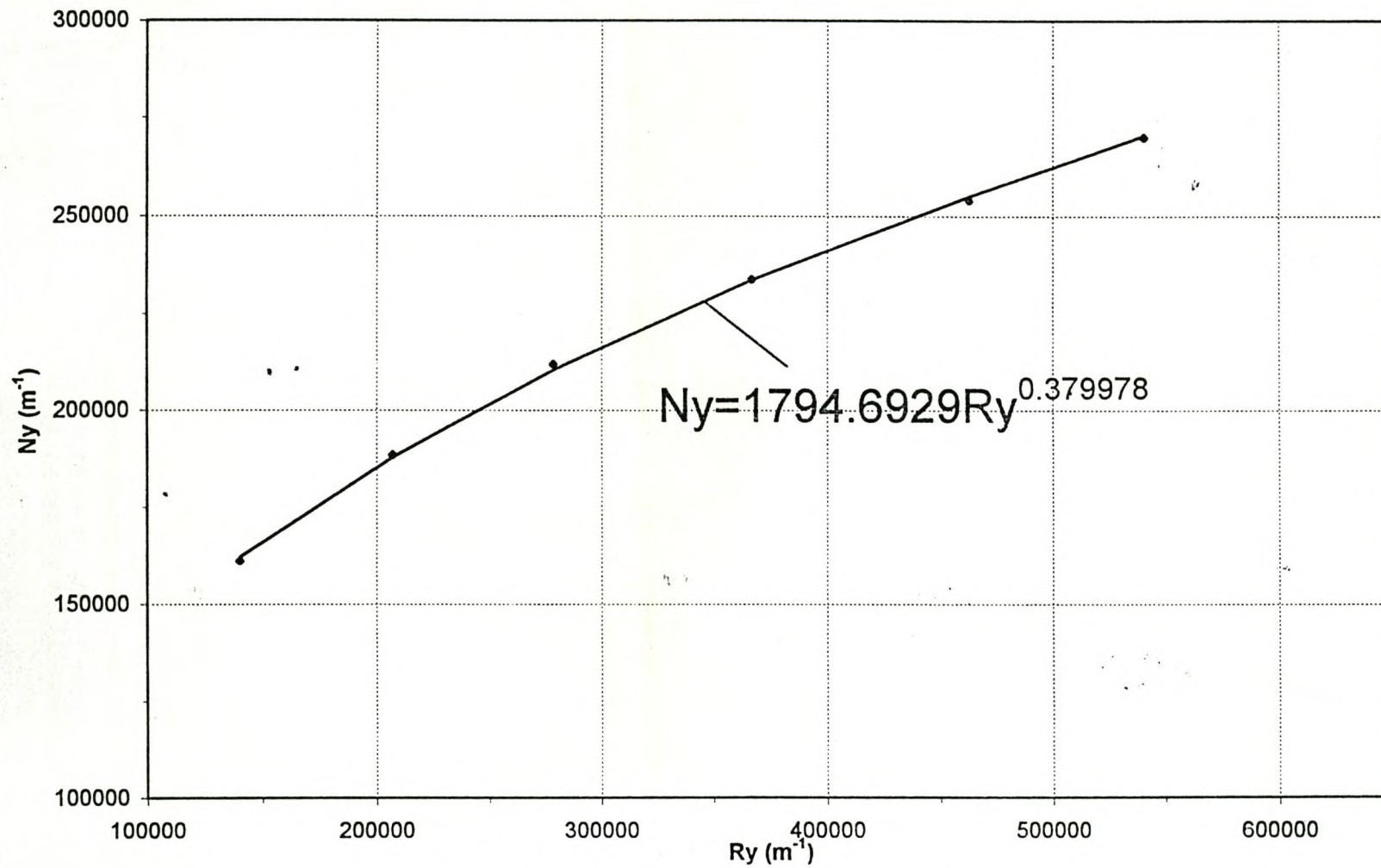


Figure E.5: Heat transfer parameter (F- 3.0).

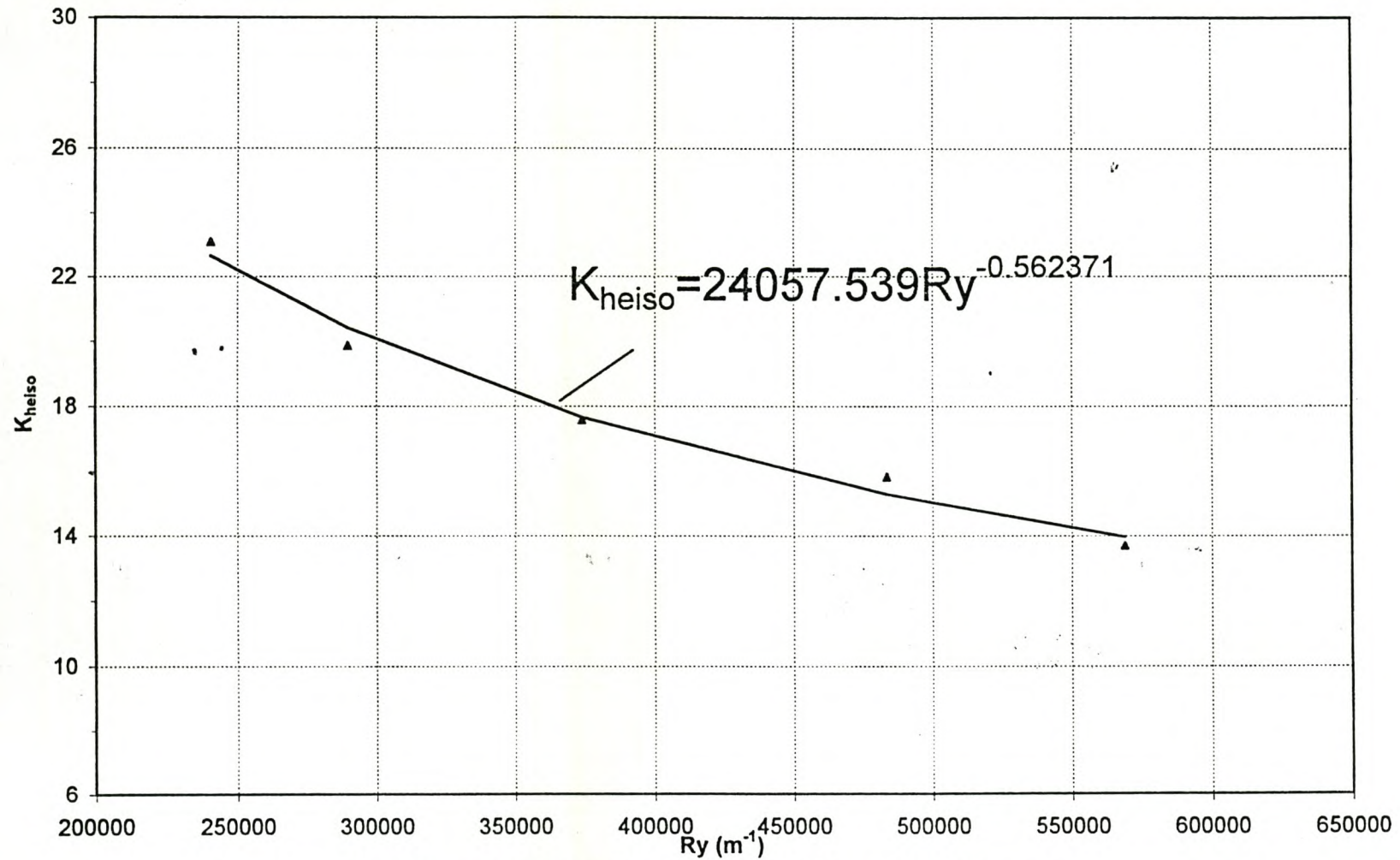


Figure E.6: Pressure drop coefficient (F- 3.0).

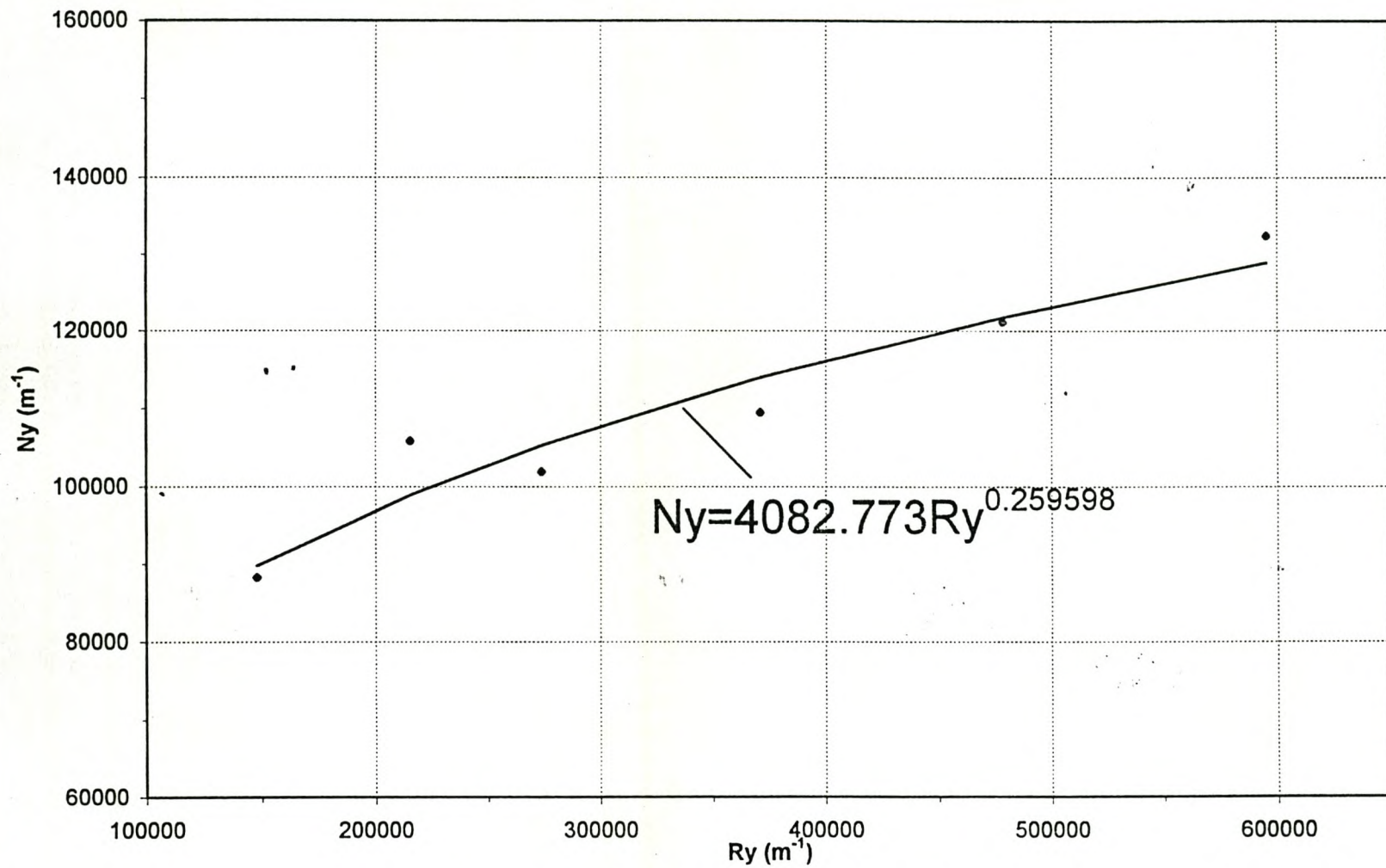


Figure E.7: Heat transfer parameter (R-2.4G).

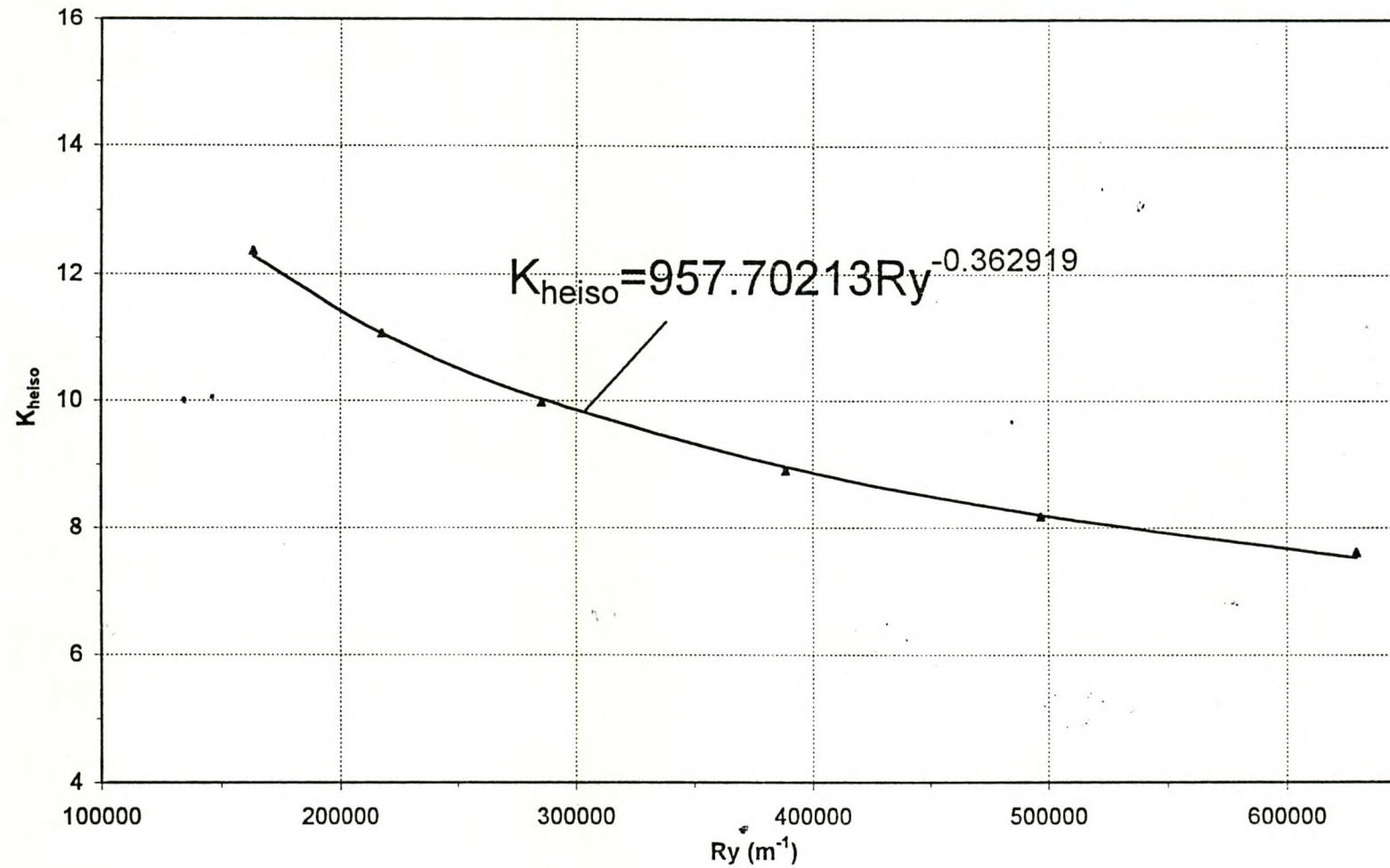


Figure E.8: Pressure drop coefficient (R-2.4G).

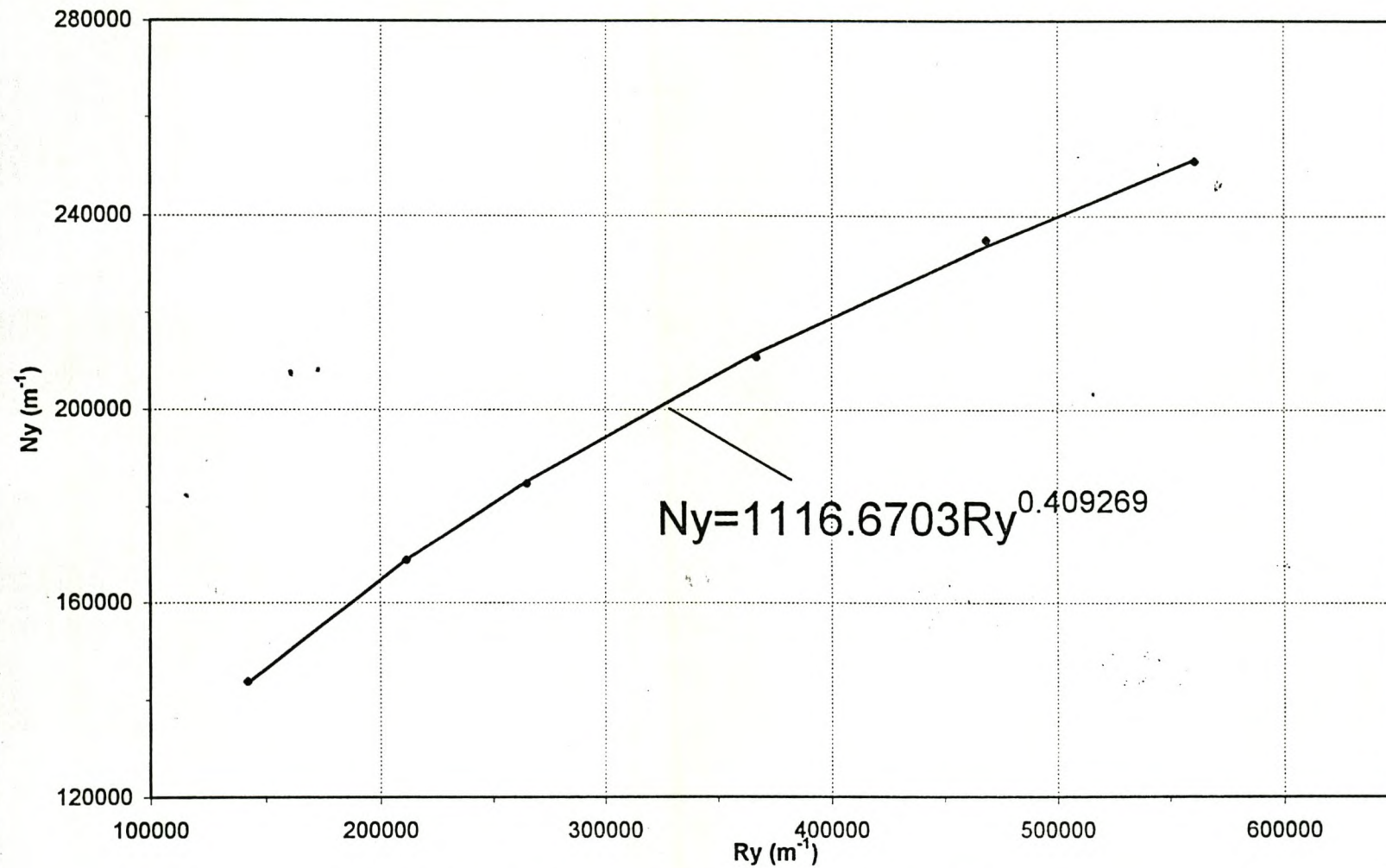


Figure E.9: Heat transfer parameter (R-2.3D).

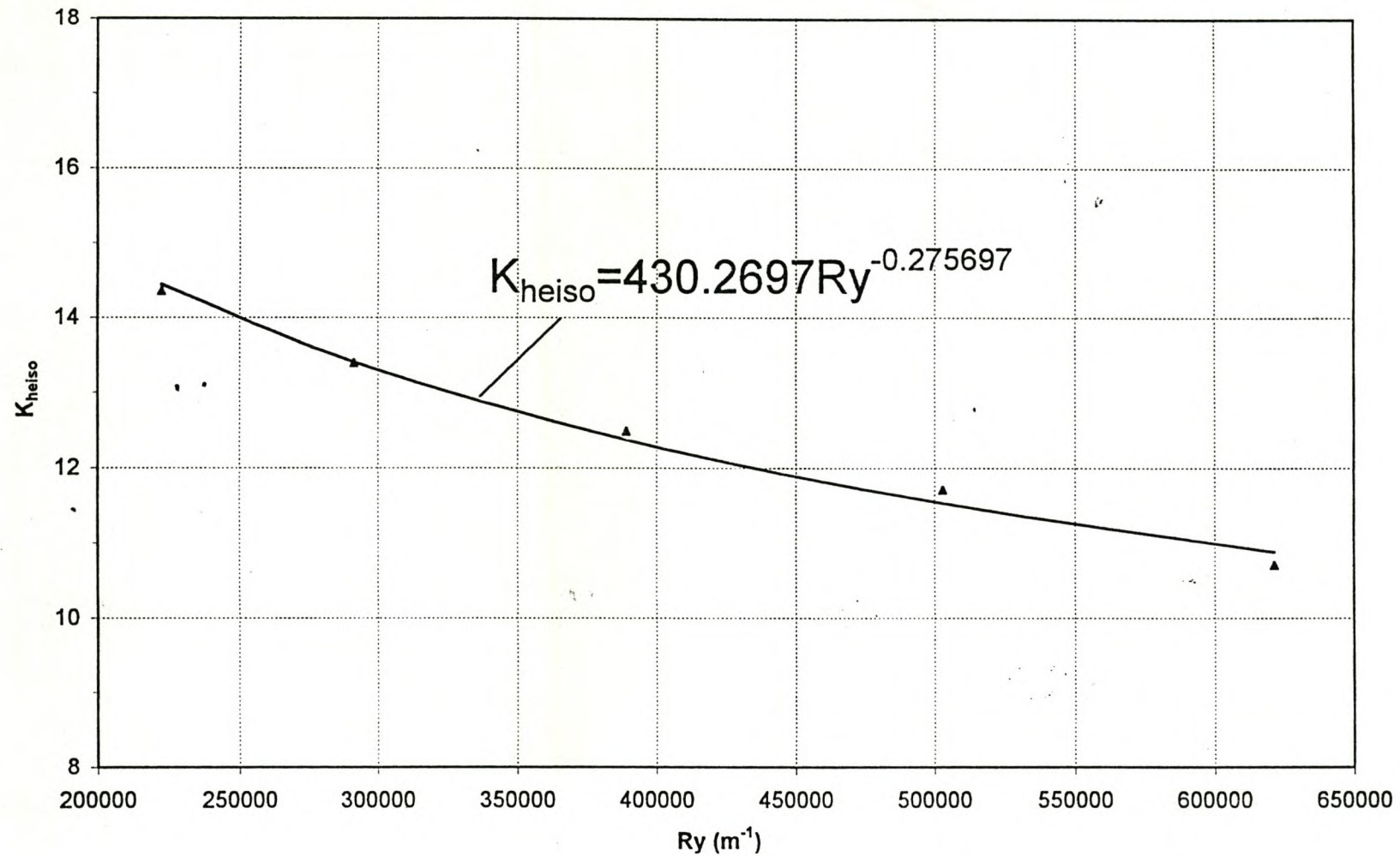


Figure E.10: Pressure drop coefficient (R-2.3D).

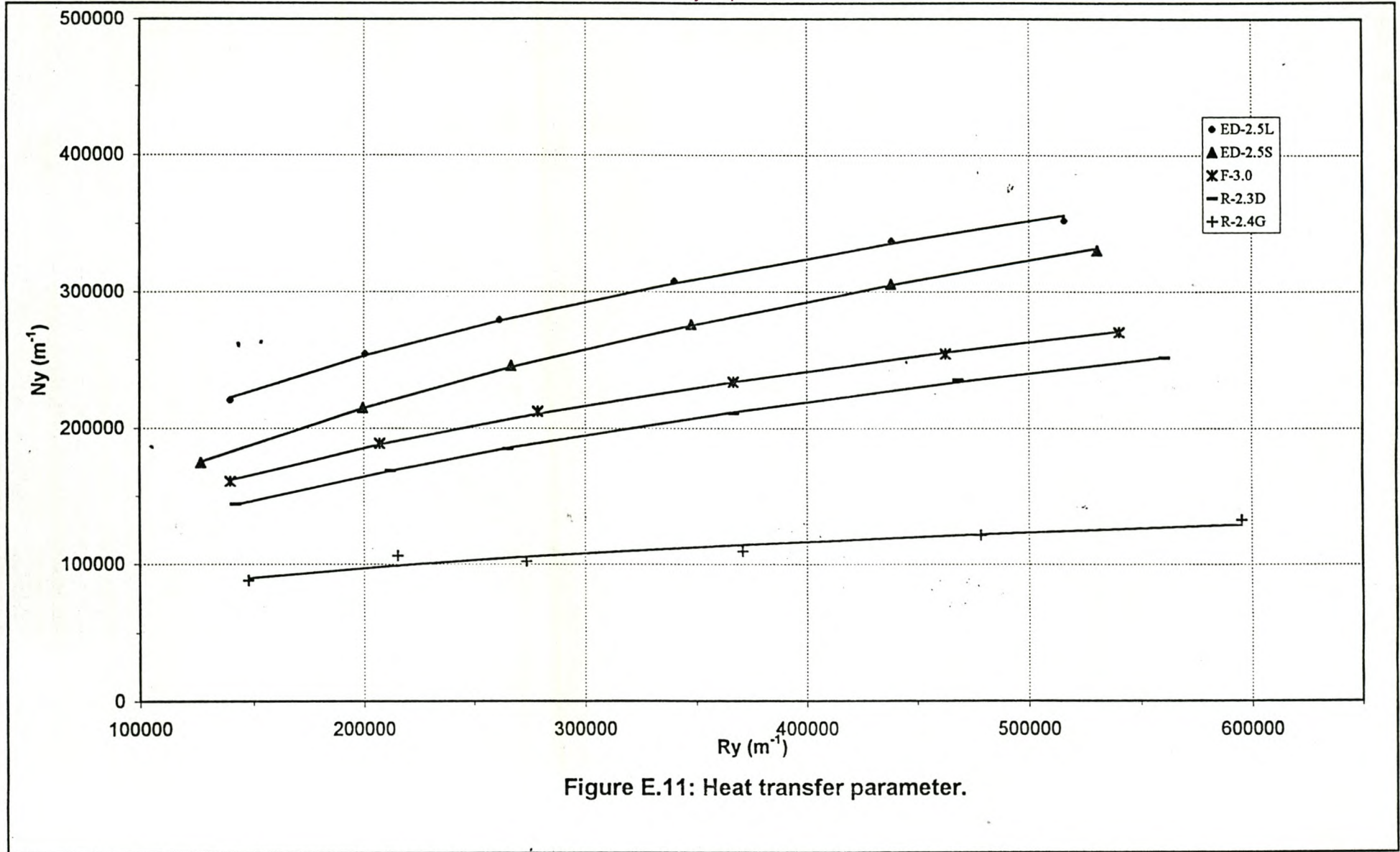


Figure E.11: Heat transfer parameter.

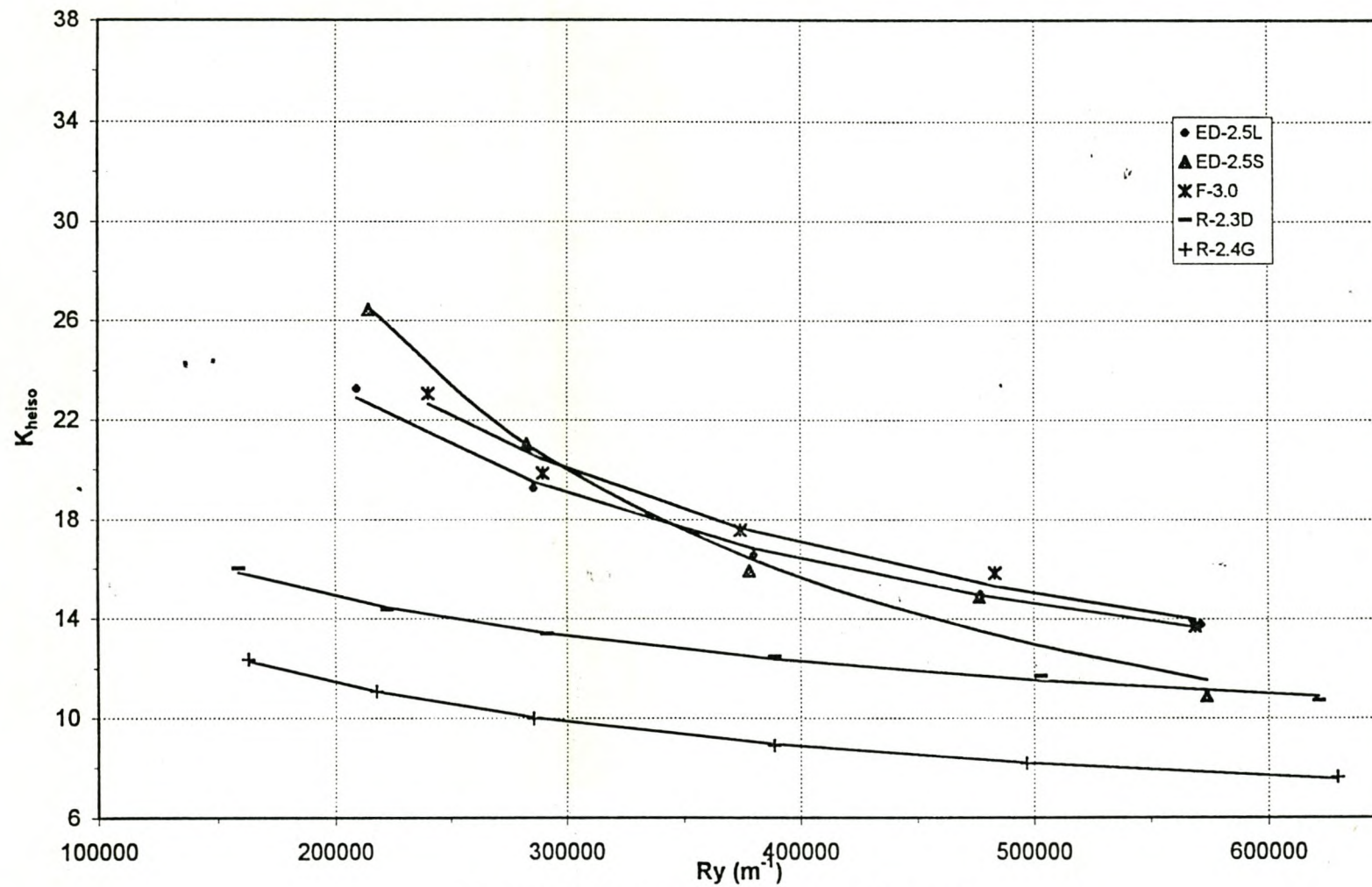


Figure E.12: Pressure drop coefficient.

APPENDIX F

Sample calculation for a forced-draught air-cooled heat exchanger bay

Sample calculation for a forced-draught air-cooled heat exchanger bay.

The difference in power consumption between a forced draught and an induced draught air-cooled heat exchanger having the same heat rejection rate is to be evaluated. The two arrangements are depicted schematically in figures 2.1 and 2.2 respectively. The sample calculation is given only for the forced draught arrangement, since the calculation procedure for the induced draught arrangement is similar.

A forced draught air-cooled heat exchanger bank at a petrochemical plant consists of bays having two fans as shown in figure 2.1. Water enters the heat exchanger at a temperature of $T_{wi} = 60\text{ }^{\circ}\text{C}$ and flows at a rate of $m_w = 100\text{ kg/s}$.

Ambient conditions:

Air temperature at ground level $T_{a1} = 28\text{ }^{\circ}\text{C}$ (301.15K)

Atmospheric pressure at ground level $p_{a1} = 101325\text{ N/m}^2$

The ambient temperature gradient is -0.00975 K/m from ground level and it may be assumed that the air is essentially dry.

Thermophysical properties of water fluid are evaluated at the water inlet temperature of $60\text{ }^{\circ}\text{C}$ (333.15 $^{\circ}\text{C}$).

Specific heat $c_{pw} = 4183\text{ J/kgK}$

Thermal conductivity $k_w = 0.652\text{ W/mK}$

Dynamic viscosity $\mu_w = 0.00047\text{ kg/ms}$

Prandtl number $Pr_w = 3.015$

It may be assumed that these properties do not change significantly with temperature over the cooling range of about $12\text{ }^{\circ}\text{C}$. The process fluid flows inside finned tubes where its heat transfer coefficient, which includes fouling effects, is specified as $h_w = 31500\text{ W/m}^2\text{K}$.

Finned tube bundle specifications:

The heat exchanger consists of R-2.3D finned tubes (see table E.5.1 in appendix E).

Number of bundles	$n_b = 2$
Effective frontal area of one bundle	$A_{fr} = 35.96 \text{ m}^2$
Effective length of finned tube	$L_t = 10.203 \text{ m}$
Hydraulic diameter of tube	$d_e = 0.02086 \text{ m}$
Area ratio (A_c = minimum flow area through finned tube bundle)	$\sigma = A_c/A_{fr} = 0.5384$
Number of tube rows	$n_r = 4$
Number of tubes per row	$n_{tr} = 55$
Number of tube passes (process fluid mixes between passes)	$n_p = 2$

The experimentally determined characteristic heat transfer parameter (appendix E) for a bundle is given by

$$N_y = 1116.6703 \text{ Ry}^{0.409269}$$

This correlation was obtained for very low turbulence intensity in the upstream air.

The isothermal loss coefficient through the bundle is

$$K_{heiso} = 430.2697 \text{ Ry}^{-0.275697}$$

Fan installation:

The bay includes two ($n_F = 2$) 4.265m diameter fans having a conical inlet shrouds. Other details are as follows:

Fan diameter	$d_F = 4.265 \text{ m}$
Fan casing diameter	$d_c = 4.325 \text{ m}$

Fan rotational speed	$N_F = 265 \text{ rpm}$
Fan hub diameter	$d_h = 1.524 \text{ m}$
Plenum height	$H_{pl} = 1.7 \text{ m}$
Height of fan platform above ground level	$H_3 = 12.7 \text{ m}$
Fan upstream loss coefficients (based on A_e)	$K_{up} = 0.1$
Fan downstream loss coefficient (based on A_e)	$K_{do} = 0.15$
Conical shroud inlet loss coefficient	$K_{Fsi} = 0.07$
Heat exchanger support loss coefficient (based on frontal area of heat exchanger)	$K_{ts} = 1.5$

The performance characteristics of the 4.265 m diameter fan mounted in a 4.325 m diameter casing with a bellmouth-type inlet and tested according to BS 848 in a type A installation, are specified at a reference air density of $\rho_r = 1 \text{ kg/m}^3$ and $N_{Fr} = 216 \text{ rpm}$.

Fan static pressure:

$$\Delta p_{Fsr} = 140.2243 + 0.8776 V_{Fr} - 0.014 V_{Fr}^2 + 1.5075 \times 10^{-5} V_{Fr}^3, \text{ N/m}^2$$

Fan shaft power consumption

$$P_{Fr} = 31.6268 - 0.9904 V_{Fr} + 0.019 V_{Fr}^2 - 1.4427 \times 10^{-4} V_{Fr}^3 + 3.7075 \times 10^{-7} V_{Fr}^4, \text{ kW}$$

Losses due to separation at the inlet to the fan platform can be neglected.

Solution

The problem is solved by an iterative procedure. Energy equations (2.2.1) and (2.2.2) as well as the draught equation (2.2.9) must be satisfied simultaneously. It is found that these equations are indeed satisfied for a total air mass flow rate through the bay of $m_a = 317.7933 \text{ kg/s}$. At this flow rate the temperature entering the heat exchanger is $T_{a5} = 301.1098 \text{ K}$ while its outlet temperature is $T_{a6} = 316.7982 \text{ K}$.

Corresponding air densities at these temperatures and a pressure of $p_{a1} = 101325 \text{ N/m}^2$ are according to equation (2.2.6).

$$\rho_{a5} \approx p_{a1} / (RT_{a5}) = 101325 / (287.08 \times 301.1098) = 1.1722 \text{ kg/m}^3$$

and similarly,

$$\rho_{a6} \approx 101325 / (287.08 \times 316.7982) = 1.1141 \text{ kg/m}^3$$

Thermophysical properties of air flowing through the heat exchanger are evaluated at the arithmetic mean temperature i.e. $T_{am} = (T_{a5} + T_{a6}) / 2 = (301.1098 + 316.7982) / 2 = 308.954 \text{ K}$.

Mean density,

$$\rho_{am} \approx 101325 / (287.08 \times 309.954) = 1.1424 \text{ kg/m}^3$$

Specific heat,

$$\begin{aligned} c_{pam} &= 1.045356 \times 10^3 - 3.161783 \times 10^{-1} T_{am} + 7.083814 \times 10^{-4} T_{am}^2 - 2.705209 \times 10^{-7} T_{am}^3 \\ &= 1.045356 \times 10^3 - 3.161783 \times 10^{-1} \times 309.954 + 7.083814 \times 10^{-4} \times 309.954^2 \\ &\quad - 2.705209 \times 10^{-7} \times 309.954^3 = 1007.355 \text{ J/kgK} \end{aligned}$$

Dynamic viscosity,

$$\begin{aligned} \mu_{am} &= 2.287973 \times 10^{-6} + 6.259793 \times 10^{-8} T_{am} - 3.131956 \times 10^{-11} T_{am}^2 + 8.15038 \times 10^{-15} T_{am}^3 \\ &= 2.287973 \times 10^{-6} + 6.259793 \times 10^{-8} \times 309.954 - 3.131956 \times 10^{-11} \times \\ &\quad 309.954^2 + 8.15038 \times 10^{-15} \times 309.954^3 = 1.8924 \times 10^{-5} \text{ kg/m} \end{aligned}$$

Thermal conductivity,

$$k_{am} = -4.937787 \times 10^{-4} + 1.018087 \times 10^{-4} T_{am} - 4.627937 \times 10^{-8} T_{am}^2$$

$$\begin{aligned}
 &+ 1.250603 \times 10^{-11} T_{am}^3 \\
 &= -4.937787 \times 10^{-4} + 1.018087 \times 10^{-4} \times 309.954 - 4.627937 \times 10^{-8} \times 309.954^2 \\
 &+ 1.250603 \times 10^{-11} \times 309.954^3 = 2.6989 \times 10^{-2} \text{ W/mK}
 \end{aligned}$$

Prandtl number,

$$Pr_{am} = \mu_{am} c_{pam} / k_{am} = 1.8924 \times 10^{-5} \times 1007.355 / 2.6989 \times 10^{-2} = 0.70633$$

The total effective frontal area of the heat exchanger in the bay is given by

$$A_{frtot} = n_b A_{fr} = 2 \times 35.96 = 71.92 \text{ m}^2$$

Find the characteristic flow parameter

$$Ry = m_a / (\mu_{am} A_{frtot}) = 317.7933 / (1.8924 \times 10^{-5} \times 71.92) = 233497.437 \text{ m}^{-1}$$

According to the specified relation, the corresponding heat transfer parameter is

$$Ny = 1116.6703 \times 233497.437^{0.409269} = 175790.912 \text{ m}^{-1}$$

It follows from equation (3.4.6) that

$$\begin{aligned}
 h_{ae} A_a &= Ny k_{am} A_{frtot} Pr_{am}^{0.333} = 175790.912 \times 2.6989 \times 10^{-2} \times 71.92 \times 0.70633^{0.333} \\
 &= 303915.213 \text{ W/K}
 \end{aligned}$$

The total inside surface area of the tubes that is exposed to the water stream can be expressed as

$$A_w = n_{tr} n_r L n_b \pi d_e = 55 \times 4 \times 10.203 \times 2 \times \pi \times 0.02086 = 294.201 \text{ m}^2$$

With the above values find the overall heat transfer coefficient.

$$UA = (1/h_{ac}A_a + 1/h_wA_w)^{-1} = (1 / 303915.213 + 1/(31500 \times 294.201))^{-1} = 294265.012 \text{ W/K}$$

To find the number of transfer units, it is noted that $C_{\max} = m_w c_{pw} = 100 \times 4183 = 418300 \text{ W/K}$
 $W/K > C_{\min} = m_a c_{pam} = 317.7933 \times 1007.355 = 320130.6697 \text{ W/K}$ such that

$$NTU = UA/C_{\min} = 294265.012 / 320130.6697 = 0.9192$$

There are two tube-side passes, with each pass having

$$NTU_p = N_p = NTU / 2 = 0.9192 / 2 = 0.4596$$

Furthermore, the heat capacity ratio

$$C = C_{\min} / C_{\max} = 320130.6697 / 418300 = 0.76531$$

If both the air stream and the process fluid are unmixed in each pass, then the effectiveness per pass is given as [84KA1],

$$\begin{aligned} e_p &= 1 - \exp[N_p^{0.22} \{ \exp(-CN_p^{0.78}) - 1 \} / C] \\ &= 1 - \exp[0.4596^{0.22} \{ \exp(-0.76531 \times 0.4596^{0.78}) - 1 \} / 0.76531] = 0.31323 \end{aligned}$$

With this value it follows that the effectiveness of the entire heat exchanger, where mixing of the process fluid occurs between passes, is

$$\begin{aligned} e &= [\{(1 - e_p C) / (1 - e_p)\}^{np} - 1] / [\{(1 - e_p C) / (1 - e_p)\}^{np} - C] \\ &= [\{(1 - 0.31323 \times 0.76531) / (1 - 0.31323)\}^2 - 1] / [\{(1 - 0.31323 \times 0.76531) / \\ &\quad (1 - 0.31323)\}^2 - 0.76531] = 0.49006 \end{aligned}$$

According to equation (2.2.2) the rate of heat transfer is thus

$$Q = e C_{\min} (T_{wi} - T_{as}) = 0.49006 \times 320130.6697 [60 - (301.1098 - 273.15)] = 5.0265 \text{ MW}$$

The heat transfer rate can also be determined from equation (2.2.1) i.e.

$$Q = m_a c_{pam} (T_{a6} - T_{a5}) = 317.7933 \times 1007.355 (316.7982 - 301.1098) = 5.0223 \text{ MW}$$

These two values for the heat transfer rate are in excellent agreement.

To determine whether the draught equation is satisfied, the fan performance has to be evaluated.

The approximate air temperature at the fan inlet is

$$T_{a3} \approx T_{a1} - 0.00975 H_3 = 301.15 - 0.00975 \times 12.7 = 301.026 \text{ K}$$

At this temperature and the specified atmospheric pressure at ground level, the approximate air density is given by equation (2.2.6)

$$\rho_{a3} \approx 101325 / (287.08 \times 301.026) = 1.172 \text{ kg/m}^3$$

and the specific heat is

$$\begin{aligned} c_{pa3} &= 1.045356 \times 10^3 - 3.161783 \times 10^{-1} T_{am} + 7.083814 \times 10^{-4} T_{am}^2 - 2.705209 \times 10^{-7} T_{am}^3 \\ &= 1.045356 \times 10^3 - 3.161783 \times 10^{-1} \times 301.026 + 7.083814 \times 10^{-4} \times 301.026^2 \\ &\quad - 2.705209 \times 10^{-7} \times 301.026^3 = 1006.99 \text{ J/kgK} \end{aligned}$$

Actual air volume flow rate through each fan is

$$V = m_a / (n_F \rho_{a3}) = 317.7933 / (2 \times 1.172) = 135.577 \text{ m}^3/\text{s}$$

Since the actual density and rotational speed of the fan are not the same as the reference conditions for which fan performance characteristics were specified, the relevant fan laws [98KR1] are employed.

The reference air volume flow rate is

$$V_{Fr} = V(N_{Fr}/N_F) = 135.577 \times 216/265 = 110.508 \text{ m}^3/\text{s}$$

At this flow rate the reference fan static pressure rise is given by

$$\Delta p_{Fr} = 140.2243 + 0.8776 \times 110.508 - 0.014 \times 110.508^2 + 1.5075 \times 10^{-5}$$

$$\times 110.508^3 = 86.582 \text{ N/m}^2$$

The actual change in fan static pressure is

$$\Delta p_{Fs} = \Delta p_{Fr}(N_F / N_{Fr})^2(\rho_{a3} / \rho_r) = 86.582(265 / 216)^2(1.172 / 1) = 152.735 \text{ N/m}^2$$

At the reference condition, the fan shaft power is

$$P_{Fr} = 31.6268 - 0.9904 \times 110.508 + 0.019 \times 110.508^2 - 1.4427 \times 10^{-4} \times 110.508^3$$

$$+ 3.7075 \times 10^{-7} \times 110.508^4 = 14.8032 \text{ kW}$$

The actual fan shaft power follows is

$$P_F = P_{Fr}(N_F / N_{Fr})^3(\rho_{a3} / \rho_r) = 14.8032(265 / 216)^3(1.172 / 1) = 32.0375 \text{ kW}$$

With this value it is possible to determine the approximate temperature of the air immediately upstream of the heat exchanger [98KR1]

$$T_{a5} \approx T_{a1} + P_F / (m_a c_{pa3}) - 0.00975(H_3 + H_{pl})$$

$$= 301.15 + 32037.5 / (317.7933 \times 1006.99) - 0.00975 \times (12.7 + 1.7) = 301.1097$$

This value is essentially as given initially.

The fan unit pressure rise coefficient is

$$K_{Fs} = 2\Delta p_{Fs}\rho_{a3} / (m_a / (n_F A_c))^2 = 2 \times 152.735 \times 1.172 / [317.7933 \times 2 / (\pi \times 4.325^2)]^2$$

$$= 3.0605$$

It follows from equation (3.4.17) that for non-isothermal flow the heat exchanger loss coefficient in this case is given by

$$K_{he} = 430.2697 Ry^{0.275697} + 2(\rho_{a5} - \rho_{a6}) / \sigma^2(\rho_{a5} + \rho_{a6})$$

$$= 430.2697(233497.437)^{0.275697} + 2 \times (1.1722 - 1.1141) / \{0.5384^2 \times (1.1722$$

$$+ 1.1141)\} = 14.4222$$

The recommended plenum recovery factor $K_{rec} = 0.3$ for $15 \leq K_{he} \leq 21$. Furthermore, for $H_{pl} / d_c = 1.7 / 4.325 = 0.393 > 0.3$ the corresponding heat exchanger outlet kinetic energy correction factor is

$$\alpha_{e6} = 1.6 - 0.48 A_c / A_{fr} - 0.012 K_{he} = 1.6 - 0.48 \times \pi \times 4.325^2 / (4 \times 35.96) - 0.012$$

$$\times 14.4222 = 1.2308$$

The upstream and downstream loss coefficients, K_{up} and K_{do} , are based on the effective fan area

$$A_e = A_c - A_h = \pi(d_c^2 - d_h^2) / 4 = \pi(4.325^2 - 1.524^2) / 4 = 12.8672 \text{ m}^2$$

Since no windwall is provided, $H_6^* = H_7$ and the left-hand side of the draught equation (2.2.9) is equal to zero. The terms on the right-hand side of the equation give

$$K_{ts} (m_a / A_{frtot})^2 / (2\rho_{a3}) + K_{Fsi} (m_a / (2A_c))^2 / (2\rho_{a3}) + K_{up} (m_a / (2A_e))^2 / (2\rho_{a3})$$

$$- (K_{rec} + K_{Fs}) (m_a / (2A_c))^2 / (2\rho_{a3}) + K_{do} (m_a / (2A_e))^2 / (2\rho_{a3}) + K_{he} (m_a / A_{frtot})^2 / (2\rho_{am})$$

$$\begin{aligned}
 & + \alpha_{e6} (m_a / A_{f\text{tot}})^2 / (2\rho_{a6}) \\
 & = 1.5 \times (317.7933 / 71.92)^2 / (2 \times 1.172) + (0.07 - 3.0605 - 0.3) \times (317.7933 \times 2 / \\
 & (\pi \times 4.325^2))^2 / (2 \times 1.172) + (0.1 + 0.15) \times (317.7933 / (2 \times 12.8672))^2 / (2 \times 1.172) + \\
 & 14.4222 \times (317.7933 / 71.92)^2 / (2 \times 1.1424) + 1.2308(317.7933 / 71.92)^2 / (2 \times 1.1141) \\
 & = -1.4232 \text{ N/m}^2
 \end{aligned}$$

This value is close to zero and therefore the draught equation is satisfied.

Finally, table F.1 below shows comparison in performance between a forced as well as an induced draught air-cooled heat exchanger.

Table F.1: Performance comparison of a forced and an induced draught ACHE.

	Forced draught ACHE	Induced draught ACHE
Heat rejected, Q_{rem} (MW)	5.022	5.022
Fan shaft power, P_F (kW)	32.0583	34.3135
Air mass flow rate, m_a (kg/s)	317.7933	316.799
Fan rotational speed, N_F (rpm)	265	276
Air outlet temperature, °K	316.7982	316.799